

1-14-2016

Climate Change Impact on Agricultural Land Use in West Africa and Its Implication on Regional Climate Projection

Kazi F. Ahmed

University of Connecticut - Storrs, kazi.ahmed@uconn.edu

Follow this and additional works at: <https://opencommons.uconn.edu/dissertations>

Recommended Citation

Ahmed, Kazi F, "Climate Change Impact on Agricultural Land Use in West Africa and Its Implication on Regional Climate Projection" (2016). *Doctoral Dissertations*. 1018.
<https://opencommons.uconn.edu/dissertations/1018>

Climate Change Impact on Agricultural Land Use in West Africa and Its Implication on Regional Climate Projection

Kazi Farzan Ahmed, PhD

University of Connecticut, 2016

Projection of climate change impact on anthropogenic land use and the resulting feedback to the regional climate in West Africa is the core focus of this research. In the first part, we evaluate climate change impact on future crop yield, a key factor affecting agricultural land use in a region. Using a process-based crop model at a regional scale, we project future changes in cereal crop yields as a result of climate change for the West African countries. Without agricultural adaptation, the long-term mean of crop yield is projected to decrease in most of the countries by the middle of the century, while the inter-annual variability of yield increases significantly. This increase of yield variability is attributed to an increase of inter-annual variability of growing season temperature and/or precipitation in future climate.

Using the projected crop yield as an input, we then develop a cropland projection model (LandPro_Crop), based on a balance between food supply and demand, to compare the contributions of climate change and socioeconomic development to potential future changes of agricultural land use in West Africa. The model accounts for the impact of socioeconomic drivers on the demand side and the impact of climate-induced crop yield changes on the supply side. The climate-induced decrease of crop yield together with increase of food demand are found to cause a significant increase in agricultural land use

at the expense of forest and grassland by the mid-century. The increase of agricultural land use is primarily climate-driven in the western part of West Africa and socioeconomically driven in the eastern part. Analysis of multiple “what-if” scenarios suggests that human adaptation characterized by science-informed decision making can potentially minimize land use changes in many parts of the region.

Using the future land use maps projected by LandPro_Crop, we perform multiple future-climate experiments to assess the land use-climate interactions in West Africa. We employ an asynchronous coupling between the land use model and the regional climate model RegCM 4.3.4-CLM 4.5 to capture the transient trends in dynamics of agricultural land use and its implication on the regional climate projections. Projections from the climate experiments indicate that land use feedback could significantly affect the future climate changes in West Africa. Projected change in climate variables caused by the greenhouse gas forcing would be modified in many cases because of the changes in leaf area index and surface albedo resulting from the future crop area expansion replacing natural vegetation.

Climate Change Impact on Agricultural Land Use in West Africa and Its Implication on Regional Climate Projection

Kazi Farzan Ahmed

B.Sc., Bangladesh University of Engineering and Technology (2008)

M.S., University of Connecticut (2011)

A Dissertation

Submitted in Partial Fulfillment of the

Requirements for the Degree of

Doctor of Philosophy

at the

University of Connecticut

2016

Approval Page

Doctor of Philosophy Dissertation

**Climate Change Impact on Agricultural Land Use in West Africa and
Its Implication on Regional Climate Projection**

by

Kazi Farzan Ahmed, B.S., M.S.

Major Advisor_____ Dr. Guiling Wang

Associate Advisor_____ Dr. Chuanrong Zhang

Associate Advisor_____ Dr. Richard Anyah

Associate Advisor_____ Dr. Amy Burnicki.

Associate Advisor_____ Dr. Liangzhi You

University of Connecticut

2016

Acknowledgements

I owe my deepest gratitude to Professor Guiling Wang for her continuous and invaluable guidance throughout this research. Without her motivation and encouragement, this work would not have been possible. Her meticulous skill to identify even the slightest of errors has greatly enhanced the quality of this thesis. While I would always cherish her instrumental support for my professional development, I consider myself extremely fortunate for getting the opportunity of working under her supervision.

I express my gratitude to Dr. Liangzhi You for his continuous enthusiasm and support. His helpful guidance from different perspectives was immensely valuable for this study. I would like to thank Dr. Richard Anyah for his interest in my research work. His supervision throughout my graduate studies was extremely helpful. I am grateful to Dr. Chuanrong Zhang and Dr. Amy Burnicki for their valuable comments and suggestion on my research.

My gratitude extends to Professor Jobair Bin Alam at BUET for giving me the opportunity of working in a research project in Bangladesh. It was a great privilege and life-changing experience working with him.

I take this opportunity to express my heartfelt appreciation to my fellow researchers in Professor Wang's group - Shanshan and Rui - for helping me get familiar with the research tools when I started my research as a graduate student at UConn. They were ready to extend their support at any hour regarding any problem. I express my gratitude to my group members – Miao Yu, Dana Paar, Jeehee Kim, Amir Erfanian, Congsheng Fu, Roop Saini, Zhenming Ji, Huanghe Gu, Di Liu, Bing Gao – for their help and friendship. Thanks to all my past and present colleagues in the Environmental Engineering Program who created an excellent working environment in Bronwell.

Thousands of miles away from home, it was never easy for me getting accustomed to life abroad. I would like to thank the members from the Bangladeshi community who extended their warmth and helped me settle down in a country which was very different from my own in every aspect. My experiences at UConn would have been far less enjoyable without my association with them. My life would have been far less exciting without my friendship with Nayeem who provided invaluable support and relentless encouragement in my different ventures. I can't thank him enough.

I could not have reached this point in my life without the care, support and inspiration from my family. I am grateful to my grandparents for always keeping me in their prayers. I especially remember my late grandfather Kazi Abdul Qader who has been, and always will be, my mentor for personal development. I am the proudest brother in the world to have the two most wonderful sisters, Afia and Fatema. I express my sincere gratitude to them for always being my sunshine. Words are not enough to express my gratitude to my wife, Moushumi, for her unconditional love and care. Her unwavering support and inspiring words kept me motivated to survive many difficult moments.

I am indebted to my parents Kazi Nurul Islam and Farida Begum, the source of strength in my life, for their endless love and sacrifice. I owe what I have achieved today, and what I would in future, to their shrewd vision for my upbringing. With respect and appreciation, I would like to dedicate this thesis to my parents.

Contents

Chapter 1

1.1 Background and Motivation.....	1
1.2 Literature review.....	4
1.2.1 Land use-climate interaction.....	4
1.2.2 Modeling Climate change impact on LULCC.....	5
1.2.3 Climate change impact on crop yield.....	6
1.3 Research Questions.....	8
1.4 Thesis Structure.....	9

Chapter 2

Impact of climate change on cereal crop yield

2.1 Introduction.....	10
2.2 Methods.....	12
2.2.1 Description of the crop model DSSAT.....	12
2.2.2 Modeling approach.....	13
2.2.3 Data.....	15
2.3 Results and Discussions.....	18
2.4 Summary.....	25

Chapter 3

Modeling climate change impact on agricultural land use

3.1 Introduction.....	44
-----------------------	----

3.2 Model, Data, and Methodology.....	45
3.2.1 Algorithm for Cropland Projection.....	45
3.2.2 Projecting Future Crop Yield.....	49
3.2.3 Projecting Future Demand for Local Production.....	50
3.2.4 Present-Day Land Use and Crop Yield Data.....	51
3.3 Results and Discussions.....	52
3.4 Summary.....	59

Chapter 4

Feedback of land use changes to regional climate projection

4.1	
Introduction.....	78
4.2 Models and Methodology.....	81
4.2.1 Modeling approach with asynchronous coupling.....	81
4.2.2 Description of the climate model.....	83
4.3 Results.....	84
4.4 Summary.....	90

Chapter 5

Summary and Conclusion

5.1 Summary of the Study and Concluding Remarks.....	101
5.2 Future Research.....	104

References

Table Captions

Table 2.1: Ranking of crops in West Africa according to 2003-2012 average of total harvested area and value of agricultural production. Source: FAOSTAT database, FAO.

<http://faostat3.fao.org/faostat-gateway/go/to/download/Q/QC/E>

Table 2.2: Genetic coefficients of the maize, sorghum and millet cultivars chosen for this study. Base temperature = 8°C, NA = not applicable

Table 2.3: Changes in mean (%) and changes in standard deviation (kg/ha) between present-day mean (1980-1998) and future mean (2041-2059) country-average yield from DSSAT driven with bias-corrected RegCM-downscaled MIROC-ESM climate for the chosen cultivars. The p-values of tests of significance at $\alpha=0.05$ are shown in parentheses.

Table 2.4: As in Table 2.3, but for DSSAT driven with bias-corrected RegCM-downscaled CESM climate.

Table 3.1: Present-day (SPAM 2005) and the LandPro_Crop-projected future (mid-21st century) average crop area coverage in the West African countries.

Table 3.2: Future average crop area coverage in the West African countries under the MIROC-driven climate as projected by the LandPro_Crop algorithm following three different orders of yield values in selecting the cropping area to optimize agricultural land use. Initial scenario (best case in land use optimization): descending order of yield; alternative scenario 01 (worst case): ascending order; alternative scenario 02 (intermediate case): random order.

Table 3.3: Future average crop area coverage in the West African countries under the MIROC-driven climate as projected by the LandPro_Crop algorithm following four different rankings of crops prioritized by the farmers to optimize agricultural land use. Rank 1: descending order of country-level crop deficit; rank 2: ascending order of country-level crop deficit; rank 3: maize, sorghum, millet, cassava, peanut; rank 4: peanut, cassava, millet, sorghum, maize.

Table 4.1: Present-day (SPAM 2005) and the LandPro_Crop-projected future (mid-21st century) average crop area coverage in the West African countries.

Figure Captions

Figure 2.1: Spatial maps of the present-day (mean over 1980-1999) June-July-August (JJA) average daily temperature (°C), average daily precipitation (mm/day), and the present-day crop area (%) distribution on a spatial scale of 0.5° in West Africa. Crop fraction coverage at 0.5° was aggregated from the Spatial Production Allocation Model (SPAM) (You et al. 2014) data which represents the geographic distribution of crop harvest area across the globe at a spatial scale of 5 min. for the year of 2005.

Figure 2.2: Comparison of time series (1980-1998) of maize yield (kg/ha) in Nigeria from different DSSAT runs. FAO: the grey line represents FAO observed data. DSSAT Run 1: the red line shows DSSAT output for short season cultivar with initial input data used in this study. DSSAT Run 2: the green line shows model output after model calibration by modifying the nitrogen fertilizer input. DSSAT Run 3: the purple line showing lower yield simulated by model because of delaying planting time by one month reflects the effect of growing season on yield. DSSAT Run 4: the cyan line shows the model output for medium season cultivar with initial data. DSSAT Run 5: the orange line represents the medium season cultivar with calibrated fertilizer input and planting time delayed by one month.

Figure 2.3: DSSAT vs FAO scatterplot before (left column) and after (right column) calibration for present-day average (1980-1998) of country-level yield (kg/ha) for maize, sorghum and millet in West Africa. Niger is shown by the red circle. The green line represents 1:1 line.

Figure 2.4: Spatial maps of the present-day (mean over 1980-1999) yield (kg/ha) for maize, millet and millet in West Africa.

Figure 2.5: Correlation coefficient ($p < 0.1$) between present-day mean (1980-1999) yield and growing season temperature (left column) and precipitation (right column). Only grid cells with significant correlation are shown.

Figure 2.6: Side-by-side boxplots of yearly country-average yield (kg/ha) of maize (top row), sorghum (middle row) and millet (bottom row) in 13 West African countries; black: 1980-1998; blue: 2041-2059 under the MIROC climate; red: 2041-2059 under the CESM climate.

Figure 2.7: Side-by-side boxplots of yearly country-average growing season temperature ($^{\circ}\text{C}$) for maize (top row), sorghum (middle row) and millet (bottom row) production (corresponding to yield values shown in Figure 3) in 13 West African countries; black: 1980-1998; blue: 2041-2059 under the bias-corrected RegCM-downscaled MIROC climate; red: 2041-2059 under the bias-corrected RegCM-downscaled CESM climate.

Figure 2.8: Side-by-side boxplots of yearly country-average growing season precipitation (mm) for maize (top row), sorghum (middle row) and millet (bottom row) production (corresponding to yield values shown in Figure 3) in 13 West African countries; black: 1980-1998; blue: 2041-2059 under the bias-corrected RegCM-downscaled MIROC climate; red: 2041-2059 under the bias-corrected RegCM-downscaled CESM climate.

Figure 2.9: Side-by-side boxplots of yearly country-average maximum temperature ($^{\circ}\text{C}$) during panicle initiation and anthesis of sorghum in 13 West African countries; black:

1980-1998; blue: 2041-2059 under the bias-corrected RegCM-downscaled MIROC climate; red: 2041-2059 under the bias-corrected RegCM-downscaled CESM climate.

Figure 2.10: Spatial maps of the future changes (%) in yield (future mean minus present-day mean) for maize, sorghum and millet in West Africa.

Figure 2.11: Contour plots of changes in yield against changes in growing season precipitation (ordinate) and changes in average growing season temperature (abscissa) as projected by DSSAT driven with MIROC (top row) and CESM climate (bottom row). Contours were plotted using the grid-level data from 13 countries of West Africa.

Figure 2.12: Spatial maps of the future (mean over 2041-2059) maize yield (kg/ha) at two different levels of atmospheric CO₂ concentration (left: 571 ppm, middle: 380 ppm) and the difference in yield values.

Figure 3.1: Time-series (2005-2050) of total demand and local production of maize in Nigeria according to future projection by the IMPACT model.

Figure 3.2: Spatial distribution of crop, forest and grass coverage (%) in 14 West African countries from present-day (year 2005) observation (top row) and future projection by the LandPro_Crop algorithm for mid-21-st century under two GCM climate - MIROC (middle row) and CESM (bottom row).

Figure 3.3: Spatial distribution of crop, forest and grass coverage (%) in 14 West African countries from present-day (year 2005) observation (top row) and future projection by the LandPro_Crop algorithm for mid-21-st century under two GCM climate - MIROC (middle row) and CESM (bottom row).

Figure 3.4: Sensitivity of land use change pattern to the demand values used as input to LandPro_Crop under the MIROC-driven climate. 1st row: absolute magnitude of total change for three future scenarios of demand; 2nd row: change due to socioeconomic factors; 3rd row: change due to climatic factors; 4th row: fraction of climate-induced change to total change.

Figure 3.5: As in Figure 3.4, but for CESM-driven climate. (Note that the SE-induced changes in both Figure 3 and Figure 4 are same).

Figure 3.6: Country-average values of total change in crop area (top) and fraction of climate-induced changes to total change (bottom) according to three future scenarios of demand under the MIROC- and the CESM-driven climate.

Figure 3.7: Spatial maps of future crop area percentage (1st and 3rd rows) in the West Africa (under the MIROC- and the CESM-driven climate) projected by the LandPro_Crop algorithm following two alternative scenarios with respect to selecting the remaining grid cells for conversion to agricultural land based on the order of yield and their respective differences (2nd and 4th rows) with the initial run which follows descending order of yield (best scenario). Alternative scenario 01: ascending order of yield; alternative scenario 2: random order.

Figure 3.8: Sensitivity of land use change pattern to the demand values used as input to LandPro_Crop with the alternative cropping scenario following ascending order of yield under the MIROC-driven climate. 1st row: absolute magnitude of total change for three future scenarios of demand; 2nd row: change due to socioeconomic factors; 3rd row:

change due to climatic factors; 4th row: fraction of climate-induced change to total change.

Figure 3.9: Spatial maps of future crop area coverage (%) in the West Africa under the MIROC-driven climate as projected by the LandPro_Crop algorithm following four different rankings of crops prioritized by the farmers to optimize agricultural land use. Rank 1: descending order of country-level crop deficit (initial run); rank 2: ascending order of country-level crop deficit; rank 3: maize, sorghum, millet, cassava, peanut; rank 4: peanut, cassava, millet, sorghum, maize.

Figure 3.10: Future changes in crop area distribution according to the LandPro_Crop projections accounting for only socioeconomic changes (LandPro_Crop-SE) and Hurtt et al. (2011) data (top row). Comparison of the SPAM present-day (2005) crop area with respective Hurtt et al. (2011) data (bottom row).

Figure 4.1: Present-day (mean over 1981-2000) average summer (JJA) precipitation and temperature (left column) simulated by the CESM-driven RegCM 4.3.4-CLM 4.5 and its comparison (right column) with the University of Delaware observed datasets.

Figure 4.2: Spatial distribution of crop, forest and grass coverage (%) in 14 West African countries from present-day (year 2005) observation (top row) and future projection by the LandPro_Crop algorithm driven in the transient mode for mid-21-st century under two GCM climate - MIROC (middle row) and CESM (bottom row).

Figure 4.3: Time-series (2005-2050) of changes in fraction of crop area in each of the West African countries.

Figure 4.4: Time-series (2005-2050) of the IMPACT-projected food demand and the DSSAT-Projected yield for five major crops in Ghana

Figure 4.5: Future changes in average summer (JJA) precipitation (mm/day), ET and temperature projected by future-climate runs using three different land use scenarios in West Africa.

Figure 4.6: Future changes in average summer (JJA) daily incident and absorbed solar radiation (W/m^2) projected by future-climate runs using three different land use scenarios West Africa.

Figure 4.7: Future changes in LAI and surface albedo averaged over summer (JJA) projected by future-climate runs using three different land use scenarios West Africa.

Chapter 1

1.1 Background and Motivation

Land use and land cover change (LULCC) is an important factor responsible for observed global environmental changes (Foley 2005, Pongtraz 2010, Ellis 2011). Although the terms - land use and land cover - are often exchangeable, they suggest different implications in climate change studies. Land use refers to utilization of land resource by human for various socio-economic purposes, while land cover indicates the type of physical material at Earth's surface. Land cover type plays a critical role in land-atmosphere interaction and anthropogenic land use patterns have direct impact on land cover type. In addition to increasing the atmospheric concentration of greenhouse gases and therefore influencing global climate, LULCC also affects the regional or local climate by altering the water and energy budget at Earth's surface via changing albedo and Bowen ratio. Therefore, both land use and land cover can be strongly linked with local and regional climate (Lambin 2003, Kalnay and Cai 2004, Mahmood 2010, Mei and Wang, 2010).

Although there is a strong link between climate and LULCC, the dynamics of land use change is not explicitly represented in regional and global climate models, partly due to the difficulties in formulating the human decision-making processes influencing anthropogenic land use (Pielke 2011, Rounsevell 2014). Instead, anthropogenic land use is usually included as an external driver in climate models, which does not incorporate the potential adaptive measures. Using the Integrated Assessment Models (IAMs) is another approach to combine the socioeconomic aspects and the climatic systems into the

same analytical framework. Projections from IAMs on future land use changes are often at the continental or regional scale and need to be downscaled to derive spatially distributed future land use scenario (Hurtt et al. 2011, West et al. 2014). Also because of their rather complex modeling framework with different sources of uncertainties involved, it is difficult to engage IAMs in assessing relative roles played by climate and socioeconomic changes in projected LULCC (Ackerman 2009, Rounsevell 2014). However, in projecting the future land use map on a spatial scale, no previous studies have explicitly integrated the physical impact of climate change on agricultural productivity with human decision-making processes regarding socio-economic adaptation.

While agricultural land use is directly responsible for the human-induced land cover change, impact of regional climate change on future crop productivity can play an important role in crop area expansion influencing local and regional agricultural practices. Therefore, assessment of climate change impact on crop yield and the consequent changes in the distribution of crop area in a region is of great importance in evaluating the land-atmosphere interaction on a local or regional scale. Many agricultural regions across the globe have already observed significant changes in crop yield variability over the past few decades (Osborne and Wheeler 2013). Nevertheless, previous studies projecting the climate change impact on agriculture have overwhelmingly focused on the mean yield of various crops, with little attention paid to how the inter-annual variability of crop yield might change in future climate.

Sub-Saharan Africa is extremely vulnerable to climate change impact because of its large dependence on natural resources, fragile economic infrastructure and limited capacity for

mitigation and adaptation. Although local crop production provides the majority supply of staple foods, mostly rainfed agricultural system in Sub-Saharan Africa is not prepared to adapt to projected future climate. Various studies predicted significant reduction in productivity of the major crops in the region under the changed climate scenario unless new technology and adaptation policy can counteract the adverse effect of climate variability (Schlenker and Lobell 2010, Knox 2012, Ahmed et al. 2015). Also in Sub-Saharan Africa, more than 80% of the agricultural growth since 1980 was attributed to crop area expansion instead of increase of productivity over already existing agricultural land (The World Bank, 2008). Considering the vulnerability of agricultural infrastructures in the region, despite the potential scope of improving yield to minimize land use change, addition of new crop area is likely to be a prevailing strategy for agricultural growth in the near future. Therefore, comprehensive analysis of crop response to regional climate changes should be included in investigating future land use changes, and the resulting feedback to regional climate. However, to our knowledge, no previous studies projecting regional climate change in West Africa directly addressed the climate change impact on crop yield and crop area distribution in evaluating land use-climate interaction in West Africa.

The motivation of this study stems from the several gaps of knowledge identified above which need to be filled for comprehensive assessment and quantification of land use-climate feedback in the context of potential climate-induced changes in future crop yield and agricultural land use in West Africa.

1.2 Literature Review

1.2.1 Land use-climate interaction

Anthropogenic land use and land cover changes (LULCC) affect regional climate through alterations of both biogeophysical and biogeochemical processes involved in land-atmosphere interactions. Human-induced modifications of the physical land surface properties lead to changes in surface albedo and roughness length, partitioning between sensible and latent heat fluxes, compositions of atmospheric greenhouse gases, and other key components of water, energy and carbon cycles, which in turn alter the existing climatic patterns (Claussen et al. 2001, Pitman et al. 2009, Pongratz et al. 2010, Sylla et al. 2015). While assessments of the effect of anthropogenic land use are critically important in climate change impact studies, uncertainties are rife in quantifying the response of climate variables to land cover changes (Pitman et al. 2009, Brovkin et al. 2013, Frieler et al. 2015). Because of the counteracting effects of various underlying processes with large regional variability, it is difficult to determine the magnitudes and signals of changes in climatic variables in response to LULCC. For example, while conversion of forests into croplands tend to induce warmer condition in the tropics and the subtropics because of potential reduction in evapotranspiration (Brovkin et al. 2009, Sylla et al. 2015), the similar land cover type conversion results in an increase in surface albedo which usually leads to cooling in high and mid-latitudes (Clausen et al. 2001, Lee et al. 2011). Therefore, the interaction between climate and LULCC needs to be evaluated comprehensively in regional climate projection.

1.2.2 Modeling Climate change impact on LULCC

There are different approaches to modeling LULCC with a wide range of modeling perspectives (Agarwal et al. 2002, Parker et al. 2003, Verburg et al. 2006). Agarwal et al. (2002) reviewed and evaluated a set of 19 land use models with respect to spatial and temporal resolutions as well as human decision-making processes. They concluded that models involving more complex human decision-making are limited to lower resolution and extension in both space and time. In reviewing a number of methodologies of modeling LULCC, Parker et al (2003) suggested to combine cellular model, which focuses on transitions in landscapes, with agent-based model, which represents human decision-making process, to incorporate anthropogenic elements in a spatially explicit modeling scheme. In projecting future agricultural land use, human decision-making is crucially important as farmers can adapt to a changing climate especially if there is national policy or strategies in place to incentivize or guide adaptation. Moreover, different crops may have different responses to the same climate change scenario. Agent-based modeling approach, which considers the interaction between agents representing decision-makers with certain optimization schemes, has been used to represent the complex anthropogenic behaviors regarding land use changes (Parker et al. 2003, Verburg 2006, Valbuena et al. 2010). However, application of agent-based approach in modeling land use change at a regional scale is limited because of its inherent complexity and larger data requirements (Valbuena et al. 2010).

Computable general equilibrium (CGE) and partial equilibrium (PE) models are often used to analyze land use patterns on a regional or global scale accounting for multiple natural and socioeconomic factors in an integrated modeling scheme. Schmitz et al.

(2014) compared performances of ten global agro-economic models (six CGE and four PE models) in projecting future agricultural land use scenarios. Among these models, two PE models, the Model of Agricultural Production and its Impact on the Environment (MAGPIE) (Lotze-Campen et al. 2008) and the Global Biosphere Management Model (GLOBIOM) (Havlik et al. 2011), are applicable for modeling land use and land cover changes on a spatially explicit scheme. MAGPIE simulates land use patterns at a spatial resolution of 0.5° based on an objective function to minimize the production cost for specific demand values. Input data to MAGPIE include grid-level crop yield data and regional demand for agricultural commodities. GLOBIOM simulates land use change scenario accounting for competition among agriculture, forestry and bioenergy on a spatially explicit scheme. In the integrated modeling approach, crop-specific yield information is supplied to GLOBIOM by the Environmental Policy Integrated Climate (EPIC) model (Valin et al. 2013, Leclère et al. 2014).

1.2.3 Climate change impact on crop yield

The physiological processes of crop growth can be affected by changes in both mean and variability of temperature and precipitation through different mechanisms. Both photosynthesis and respiration are nonlinear functions of temperature, whereas the relation between the crop development rate and temperature is approximately linear (Monteith and Moss, 1977 and Porter and Semenov, 2005). The rates of physiological processes increase with temperature before reaching the optima and then decrease. Therefore, although crops develop more quickly in warmer condition, the yield

essentially declines as a result of temperature increase (Schlenker and Lobell, 2010 and Lobell et al., 2011). High temperature tends to increase the vapor pressure deficit between the leaf and its surrounding air, forcing plants to reduce their stomatal opening. In arid and semi-arid regions/seasons, water is a limiting factor for crop growth. Decrease in growing season precipitation reduces soil moisture available to rainfed crops, and the resulting water stress can also trigger stomatal closure. Both high temperature and increased water stress can lead to elevated level of abscisic acid in plants, which induces stomatal closure (Barnabás et al., 2008). The reduced stomatal opening hinders carbon assimilation and crop growth affecting the overall crop yield.

Numerous studies implementing different approaches project detrimental impact of climate change on cereal crop yield in Sub-Saharan Africa (Schlenker and Lobell 2010; Lobell et al. 2013; Ruane et al. 2013; Waha et al. 2013). Schlenker and Lobell (2010) predicted more than 15% decrease by mid-century in the average production of maize, sorghum and millet because of future changes in temperature and precipitation. According to Lobell et al. (2011), 1°C of warming would reduce yield in approximately 65% of present-day area for maize harvest in the region. Waha et al. (2013) projected that the average decline in maize yield because of reduction in growing season precipitation in many parts of Sub-Saharan Africa would be as high as 30% surpassing the average yield loss (3% to 20%) induced by warming in future decades. Roudier et al. (2011), in a review of 16 published studies analyzing climate change impact on crop productivity, estimated the median values of country-average yield loss of cereal crops to be 13% and 18% in the northern and the southern part of West Africa, respectively.

1.3 Research Questions

This dissertation aims to model the land use-climate interaction and feedback in West Africa accounting for the climate-induced changes in future crop yield and agricultural land use. The specific questions we aim to address in this study are –

1. What is the trend of future change in both the mean and the inter-annual variability of cereal crop yields, as projected by the calibrated DSSAT model, under changed climate scenario?
2. What climate variables are primarily responsible for future changes in the yield of cereal crops?
3. What will likely be the future distribution of crop areas in West Africa to satisfy the future country-level demand for foods with current agricultural practice?
4. What are the relative roles of socioeconomic factors and climate changes in driving future land use changes and how this may vary spatially?
5. Could land use optimization through human decision-making have considerable impact on the overall LULCC?
6. How may the feedback from projected land use change impact the future climate in the region?

1.4 Thesis Structure

This thesis is organized in five chapters. Chapter 2 evaluates potential impact of climate change on crop productivity in West Africa using a process-based crop model. Chapter 3 focuses on developing a prototype cropland projection model which simulates future scenarios of agricultural land use patterns in the region accounting for climate-induced changes in crop yield as projected in Chapter 2. In Chapter 4, an asynchronous coupling is employed between the cropland projection model and a regional climate model to investigate how the feedback from the projected land use change in Chapter 2 may impact the future climate in the region. Chapter 5 summarizes the core findings of this study and outlines the scope of future research.

Chapter 2

Impact of climate change on cereal crop yield

2.1 Introduction

The impact of climate change on crop yield has been extensively investigated from different perspectives. There are two basic approaches to modeling the crop response to climate variability – statistical and process-based. Statistical models are developed based on the statistical relationships between yield and climatic factors, such as temperature and precipitation, which affect crop growth. The main caveat to a statistical model is the fact that it does not simulate actual physiological processes that govern crop growth and development. Although a statistical model usually reproduces the desired yield response for the location it is trained for, it may not be transferable to other locations. Therefore, statistical models either suffer from their rigid applicability or compromise the spatial variability by compelling the entire region to follow the same statistical relationship (Lobell and Burke, 2010). Yet, statistical approaches are often useful because of their relative simplicity and minimal data requirement. Process-based crop models solve the equations pertaining to plant physiology, soil moisture budget and other aspects of crop production. Compared to the statistical methods, they tend to possess higher fidelity in capturing the spatial and temporal heterogeneity of crop response to environmental changes. However, to reproduce the observed yield over a large spatial scale using a process-based crop model is somewhat difficult because of the uncertainties resulting from a large number of parameters (both physical and socio-economic) associated with the model (Lobel and Burke, 2008 and Thornton et al., 2009). Nevertheless, spatial

variability in crop productivity is a key factor to better understand the climate change impact on regional agriculture. Different responses from different crops will demand a diverse crop management and adaptation strategies based on a wide range of socio-economic policies within a country. Crop yield in future climate, coupled with rapidly increasing global food demand, will be a critical factor influencing land use and land cover change (LULCC), a key component of the earth's radiative budget (Lambin et al., 2003, Ewers et al., 2009). Comprehensive regional analysis of the variability of crop sensitivity to climate change is, therefore, a prerequisite to predict the future LULLC.

In the present study, using the process-based crop model Decision Support System for Agrotechnology Transfer (DSSAT) (Jones et al., 2003) , we aim to capture the present-day country-level yield for maize, sorghum and millet for the West African countries and project the future yield respectively. We employ the model to address three questions: how can DSSAT be calibrated to reproduce the observed country-level yield of the cereal crops?; what is the trend of future change in both the mean and the inter-annual variability of cereal crop yields, as projected by the calibrated DSSAT model, under changed climate scenario?; what climate variables are primarily responsible for future changes in the yield of cereal crops? We also examine the potential sources of uncertainties, which may result from a number of human decision-making processes inherited in local agricultural practices, associated with DSSAT in the case of a spatially explicit regional study.

2.2 Methods

2.2.1 Description of the crop model DSSAT

The process-based crop model DSSAT integrates crop physiology and phenotype, weather and soil data, and crop management strategies. It has different modules to perform simulation for different crop types. The module responsible for simulation of the cereal crops in DSSAT is originally based on the crop model CERES developed for maize and wheat modeling (Ritchie and Otter 1985; Jones and Kiniry 1986). DSSAT models crop growth by simulating the processes involved in the plant-soil-atmosphere interactions at a daily or hourly time step. As of version 4.5, which was used in this study, the CERES module of DSSAT can perform the simulation for six cereal crops – barley, maize, millet, rice, sorghum and wheat. For the CERES module in DSSAT, the plant life cycle is divided into several stages – germination, emergence, end of juvenile, floral induction, flowering, beginning of grain fill and physiological maturity. The rate of development in cereal crops is governed by the growing degree days (GDD) expressed as a function of daily maximum and minimum temperature. The required GDD for the transition between two successive growth stages depends on the genetic coefficients of a cultivar. The CERES module calculates the daily plant growth rate using crop-specific ecotype coefficient derived from Radiation Use Efficiency (RUE) which converts the daily intercepted photosynthetically active radiation into plant dry matter. In CERES, grain filling in plants is regulated by the cultivar's genetic potential, rate of carbohydrate accumulation during flowering, temperature, water stress and available nitrogen.

2.2.2 Modeling approach

Cereal crops analyzed in this study were maize, millet and sorghum which are important sources of calories and nutrition in West Africa. According to FAO data, they are among the major crops based on total area harvested and value of agricultural production in the region (Table 2.1). These three crops are also mostly rainfed in the West African planting areas. Rice, another important cereal crop, was not included in this study because rice production involves substantial irrigation. For maize, we selected the Obatampa cultivar which has a growing season of approximately 90 days. The CSM 335 cultivar was selected for sorghum and the CIVT cultivar was chosen for millet because these cultivars are commonly cultivated in the region and the information of their genetic coefficients (as required by DSSAT) was available to us (Table 2.2 presents more details about genetic coefficients of the selected cultivars). Growing season lengths of the CSM 335 and the CIVT cultivar span approximately 110 days and 85 days, respectively. The study area includes 13 countries in the Sahel and the Guinea Coast region - Benin, Burkina Faso, Gambia, Ghana, Guinea, Guinea-Bissau, Ivory Coast, Mali, Niger, Nigeria, Senegal, Sierra Leone and Togo. Liberia was excluded since the country's agricultural sector is still recovering from damage because of the civil war and there is little information available to calibrate DSSAT at the country level. West Africa, which lies between 15°E-16°W and 4°N-26°N, is considered to be one of the most vulnerable regions to climate change. Diverse climate in the region is characterized by hot desert climate of the Sahara Desert, hot semi-arid climate of the Sahel and tropical climate of Central and Western Africa (Fig. 2.1). Agricultural land use is more dominant generally in the eastern part of West Africa as indicated by the present-day cropland distribution in

the region. We ran DSSAT at a spatial scale of 0.5° for the West African region. The country-average yield values represent the arithmetic mean of yield values across all of the 0.5° grid cells within a country. As the primary concern here is with crop yield as opposed to the total agricultural output, DSSAT was run for every grid cell within a country with no regard to the current fraction of agricultural land use or whether land use in each specific grid cell will increase or decrease in the future.

The FAO country-average yearly yield data (FAOSTAT database) were used to evaluate the time-series of DSSAT outputs and to calibrate the model. In order to perform the model calibration, for each country separately, the grid-level fertilizer input and planting time data within a country were adjusted in order to match the DSSAT country-average yield with the FAO data for present-day (1980-1998) mean. In the case of point-based simulation, calibration of the model can be performed by adjusting different model input parameters. However, for spatially explicit regional study, grid-level data is absent or sparse for many input parameters required by DSSAT since they are determined by local agricultural practice. Moreover, the grid-level time series data for the present-day yield was not available. The large degree of uncertainty involved in crop yield simulation results from the dependence of the crop production system on human decision-making. Factors such as fertilizer use, irrigation, choice of cultivar, and planting date selection greatly vary from one location to another and cannot be modeled explicitly as input parameters. However, any shift in one of the parameters can noticeably influence the model output and eventually lead to deviation between simulated and observed yield (Fig. 2.2). Time series of country-average crop yields (as shown in Fig. S2) indicate a variable response in the yields among years implying an interaction between the seasonal

climate and the variation in input. The uncertainties in model input parameters, which mainly result from heterogeneity of agricultural practice across a region or a country, implies the difficulties in applying a process-based crop model on a regional scale. Given the large uncertainties with input parameters, which can considerably vary from place to place, DSSAT was calibrated by adjusting the fertilizer input and planting time for this study. Calibration was done for each crop and each country separately. Yield of cereal crops is sensitive to the amount of nitrogen fertilizer applied since optimum nitrogen level can effectively increase the yield. Results from the sensitivity analysis of DSSAT yields and its input parameters also conform to the positive correlation between simulated yield and nitrogen input. Changes in planting time affect the yield by altering the growing season length.

2.2.3 Data

For grid-level soil data, the reanalyzed ISRIC-WISE 1.1 soil profile dataset were used. The original World Inventory of Soil Emission Potentials (WISE) soil database (Batjes 2002) version 1.1 developed by the International Soil Reference and Information Center (ISRIC) includes 4382 soil profiles, which were released by FAO, ISRIC and the United States Department of Agriculture (USDA), across the globe. The reanalysis of ISRIC-WISE 1.1 was performed to identify and correct the discrepancies or replace the missing values in physical and chemical properties of the soil profiles (Romero 2012). For example, drained upper limit (DUL) of a soil profile should be less than the saturated soil water content (SAT) and greater than the lower limit (LL) of plant extractable water. In the case of any inconsistency detected among the hydraulic coefficients (LL, DUL and SAT) in ISRIC-WISE 1.1, the corrected values were estimated based on soil texture

(Saxton et al. 1985). The reanalysis detected a total of 1945 soil profiles suffering from discrepancy or missing values and corrected 967 of them. The remaining 978 profiles could not be corrected, and therefore, 3404 valid soil profiles were available in the final reanalyzed dataset.

The geographically explicit fertilizer application dataset (Potter et al. 2010) used in the study was derived by merging a number of datasets. The International fertilizer Association (IFA) national-level fertilizer data and grid-level maps of harvested area (Monfreda et al. 2008), which represents the geographic distribution of crop areas and yields of 175 different crops, were combined to produce the data at a spatial scale of 5 min. for the year of 2000. The spatial pattern of harvested area dataset was used to disaggregate the national-level fertilizer data to produce spatially explicit N and P fertilizer input at 0.5° spatial resolution. The global manure distribution data at 0.5° was developed using the global grid-level dataset on livestock distribution from FAO GLW project (Wint 2007) which was converted into the equivalent OECD (Organization for Economic Co-operation and Development) livestock unit and combined with the OECD nutrient excretion data (OECD 2008). For the planting time data, we followed the FAO crop calendar (FAO 2012) that selects the local onset of monsoon rainfall as the planting period for rain-fed crops.

For the model calibration, the Potter et al. (2010) grid-level fertilizer data was manipulated to reduce the disagreements among FAO and DSSAT yield. Since cereal crop yield are positively correlated to nitrogen fertilizer input, the initial fertilizer value was decreased (increased) in the case of an overestimation (underestimation) by DSSAT. However, in some cases, only the perturbation of fertilizer data was not enough to

produce satisfactory results from the calibrated model. Therefore, in addition to adjusting fertilizer input, growing season length was also somewhat altered by means of modifying the initial FAO-prescribed planting time by delaying it by one month.

For the present-data daily climate data, we used a gridded global climate dataset at 0.5 degree resolution (Sheffield et al. 2006), which was developed by combining the observation and the National Centers for Environmental Prediction–National Center for Atmospheric Research (NCEP–NCAR) reanalysis data. The future climate data (2041–2060) used in this study were derived from the outputs of the regional climate model RegCM 4.3.4 (Giorgi et al. 2012) coupled with the Community Land Model version 4.5 (CLM 4.5) (Oleson et al. 2010). The performance of this coupled model in West Africa is documented in Wang et al. (2015). To run RegCM, the initial and boundary conditions (ICBC) was generated from the Representative Concentration Pathways (RCP) 8.5 runs of two General Circulation Models (GCMs): the Model for Interdisciplinary Research On Climate – Earth System Model (MIROC-ESM) and the Community Earth System Model (CESM) version 1.0 which is the updated version of the Community Climate System Model version 4.0 (CCSM4). In capturing the present-day vegetation distribution in West Africa, the MIROC-ESM-driven and the CCSM4-driven CLM-CN-DV model performed better than other GCM-driven runs (Yu and Wang, 2014). The outputs from RegCM, at a native resolution of 50km and interpolated to a 0.5° resolution, were first bias-corrected using the Statistical Downscaling and Bias Correction (SDBC) method (Ahmed et al. 2013). The SDBC bias correction algorithm mapped the month-specific probability distributions of daily climate data from the present-day RegCM outputs and observational data (Sheffield et al. 2006) for 1980–1999, and assumes that the statistical relationship

between the distributions of model outputs and observations established for the present-day climate will remain unchanged in future climate (Wilby 1998; Boé et al. 2006).

2.3 Results and discussions

The scatterplot of country-level yield values from the DSSAT and the Food and Agriculture Organization (FAO) data averaged over 1980-1998 before and after calibration shows that the calibration reduced the difference between the model output and FAO data (Fig. 2.3). However, in Niger, the observed yields of all three cereal crops are substantially lower than the DSSAT simulations despite assuming zero fertilization. Therefore, Niger is excluded from the calculation of correlation coefficient but presented in the plots for completeness. For most countries, the DSSAT model without calibration underestimates the maize yield, but overestimates sorghum and millet yields. Calibration brings the model output into a better agreement with the FAO data. In calculating the country-level yield, grid-level yield values within a country were averaged, although some grid points with extremely low (less than 100 kg/ha) yield values because of unfavorable climatic conditions were excluded from calculating the average yield (Fig. 2.4). The yield values of cereal crops from calibrated DSSAT over the period of 1980-1998 show generally negative correlation with growing season temperature for most part of the West African region. The negative correlation between yield and temperature is significant ($p\text{-value} < 0.1$) for 17.4%, 25% and 68.8% of the grid points for maize, sorghum and millet respectively for the cultivars used in the study (Fig. 2.5). For many parts of the region, since average growing season temperature during the study period

(1980-1998) did not exceed the optimum temperature (30-32°C) for the growth and grain development of cereal crops, high temperature in the past did not reduce the yield. Similar to previous studies, (Berg et al. 2010; Rowhani et al. 2011), yields of the cereal crops in the region show mostly positive correlation with growing season precipitation. For the cultivars chosen, the positive correlation between yield and precipitation is significant for 30.3% and 20.6% of the grid points for maize and sorghum respectively, while it is 77.3% in the case of millet (Fig. 2). Since crop growth and development can be simultaneously affected by growing season temperature and precipitation in opposite directions, their individual impacts can offset each other.

The side-by-side boxplots of present-day (1980-1998) and future (2041-2059) country-average yield indicate an overall decrease in future cereal crop yield as a result of projected changes in temperature and precipitation (Fig. 2.6). Since no adaptation, except sowing date, was considered in the future crop modeling, the projected changes in yield are driven by climatic factors as reflected by the changes in average temperature and total precipitation between present-day and future growing season (Figs. 2.7 and 2.8). There are noticeable disagreements among two scenarios of future country-average yield as projected by DSSAT driven with two different climate forcing data. The decrease in country-average maize yield is larger when DSSAT is driven with the RegCM-downscaled CESM climate. Future yield from the DSSAT runs driven with RegCM-downscaled MIROC-ESM climate indicate that the countries in the Sudano-Sahelian region, in general, are expected to experience greater yield loss compared to the countries along the Guinea Coast. This is consistent with previous studies (Roudier et al. 2011; Sultan et al. 2013) that also projected larger yield loss induced by higher degree of future

warming and drought in the northern part of West Africa. As shown in Table 2.3, the difference between the present-day mean and the future mean of cereal crop yield (average for maize, sorghum and millet) in Senegal, Gambia and Mali (>25%) is substantially higher than that in Ivory Coast, Togo, Ghana and Sierra Leone (<15%). Apart from Guinea-Bissau, which would experience a 8.9% increase, all the countries in the region would suffer a loss in maize yield, which ranges from 0.4% to 40.1%. This result is consistent with the study of Jones and Thornton (2003) that projected a yield loss ranging from 1.5% to 29.7% by 2055 across the West African countries except for an increase of maize yield by 1.6% in Ivory Coast. The RegCM(CESM)-driven DSSAT outputs do not indicate any clear spatial pattern in the future yield changes, with all the countries across the region experiencing larger decrease in yield ranging from 14.7% to 53.8% (Table 2.4). For sorghum and millet, the RegCM(MIROC)-driven DSSAT projected a decrease in country-level productivity varying from 4% to 45.5%. Although exact comparison cannot be made because of the different methodologies, our results are broadly consistent with the climate-change-induced yield loss (0% to 40%) for sorghum and millet in West Africa as projected by Sultan et al (2013). However, driven with the RegCM(CESM) future climate, DSSAT projects a considerable increase in sorghum and millet yield for many countries although future changes in climatic variables are similar to what is projected by RegCM(MIROC). Particularly for sorghum, the yield is projected to increase significantly in 9 countries. This inconsistency highlights the uncertainty in future projections of crop yield resulting from the climate input data. Also using only the growing season temperature and precipitation may not be enough to assess the crop response to climate change since the average over the whole growing season cannot fully

represent the impact of hydrometeorological conditions on crop yield. A specific crop may be more sensitive to warming and water stress during a certain part of the growing season. Therefore, the distribution of temperature and precipitation over different growth stages should be examined more specifically for the comprehensive understanding of crop response to climate variables. For example, future sorghum yield in Mali is projected to decrease (by 7.6%) under the MIROC-driven climate and conversely increasing (30.7%) under the CESM-driven climate, although changes in growing season average temperature and precipitation for the two future climate scenarios are somewhat similar. To understand this seeming inconsistency, we examined the distribution of average daily maximum temperature in Mali during a critical growth stage of sorghum spanning from panicle initiation to anthesis (approximately from 25 to 65 days after emergence) (Fig. 2.9). Yield of sorghum is largely influenced by heat and water stress during this growth stage. The country-average future mean of daily maximum temperature during this particular growth period tends to be higher under the MIROC-driven climate (36.8° C) compared to the CESM-driven climate (35.3° C), which negatively impacts the sorghum yield. However, distribution of maximum temperature alone may not fully explain the changes in sorghum yield. Although the average daily maximum temperature under the CESM-driven future climate in Mali is higher than the present-day average (34.6° C), the yield is projected to increase because of the increased precipitation during panicle initiation and anthesis in future climate (4.35 mm/day) compared to the present-day climate (3.93 mm/day). Therefore, to explain the response of a specific crop in a particular country, more comprehensive analysis, which can significantly differ from one case to another, is required.

The larger distance between quantiles in the boxplots for future yield values indicates that the general decline in mean yield is accompanied by increased inter-annual variability (Fig 2.6). According to the RegCM(MIROC)-driven results, out of a total of 39 cases (3 crops and 13 countries), the inter-annual variability of yield would significantly increase in 28 cases. The increase in standard deviation is projected to be the largest for maize ranging from 66.6 kg/ha to 242.2 kg/ha among the countries. The RegCM(CESM)-driven results project significant increases in 29 cases with the standard deviation of sorghum yield increasing the most ranging from 56.8 kg/ha to 291.0 kg/ha (Tables 2.2 and 2.3). The increased year-to-year variation in cereal crop yield generally coincides with the larger inter-annual variability of growing season temperature and/or precipitation in the future climate, which illustrates the potential impact of changes in climatic pattern on the year-to-year variation of cereal crop yield in West Africa (Figs. 2.7 and 2.8). There are a few exceptions where the yield inter-annual variability can significantly increase despite the rather small increase of temperature and precipitation variability (e.g., maize in Senegal for the RegCM(MIROC)-driven projection). This apparent disparity might be also due to possibly higher sensitivity of a specific crop to temperature and precipitation during certain growth stages, which gets smoothed out when averaged over the whole growing season.

The comparison between present-day mean and future mean according to the RegCM(MIROC)-driven results shows significant ($p < 0.05$) decrease in the country-average maize yield for 9 countries, while the increase in inter-annual variability of maize yield is significant ($p < 0.05$) for all the countries (Table 2.3). The decrease in sorghum yield is significant only for 5 countries, although the variability is projected to increase

significantly for 9 countries. It implies that many countries may experience significantly larger fluctuations in annual average yield although the change in mean is not significant. For millet, the country-average yield is projected to decrease significantly for 12 countries, whereas the increase in variability is not significant for 6 countries since most of them are projected to experience larger decrease in annual yield (compared to maize and sorghum) in all the future years.

It is also noteworthy that, for a specific crop, the largest decrease in mean yield may or may not be associated with the largest increase in variability. According to our model projection, Gambia would suffer both the highest decrease in mean (40.1%) and the highest increase (242.2 kg/ha) in inter-annual variability of maize yield. For sorghum, the highest decrease in mean would occur in Senegal (25.3%) although variability would increase most in Guinea-Bissau (132.6 kg/ha). The yearly millet yield in future decades would vary most in Togo (170.0 kg/ha) while Gambia would experience the largest yield loss (45.3%). For the RegCM(CESM)-driven DSSAT projection, the mean maize yield would decrease significantly in 12 countries while, in some of the cases, the increase in inter-annual variability would not be significant (Table 2.4). Although mean sorghum and millet yield is projected to increase in many countries, most of them would experience significantly larger year-to-year variation in yield in future climate. The projections from DSSAT, driven with both climate change scenarios, emphasize the importance of assessing the changes in inter-annual variability of crop yield in addition to the changes in mean in devising a strategic framework for food security in West Africa. Moreover, in some counties, both the magnitude and the direction of projected crop yield changes

show strong spatial variability (Fig. 2.10), which adds another dimension of complexity to the development of country-level adaptation strategies.

Different crops respond differently to warming and drought, as evident from the contours of yield changes against changes in precipitation and growing season temperature (Fig. 2.11). Under the RegCM(MIROC) climate, Maize is generally sensitive to both warming and drought. Maize yield is projected to decrease as a result of warming combined with a decrease or a small increase of precipitation. However, a larger increase in precipitation would lead to an increase in yield. Sorghum and millet tend to be mostly sensitive to warming. Although warming of a small magnitude would lead to an increase in sorghum yield in the region, a general decrease is projected for millet yield. Under the RegCM(CESM) climate, however, the same crop cultivars respond differently to the similar range of changes in growing season average of temperature and precipitation. Sorghum tends to be more sensitive to precipitation, while the positive effect of increase in growing season precipitation on maize and millet yield is offset by future warming. There can be two possible explanations for some parts of the contour plots showing increased yield related to increased temperature. First, increase in both temperature and yield in the plots is usually associated with increase in precipitation. Increased growing season precipitation can moderate the negative effect of warming on crop yield. Second, depending on the present-day temperature, warming may not necessarily cause the growing season temperature to exceed the optimum temperature of a particular crop. As a result, some parts in the contour plots for sorghum yield indicate an increase in yield under future scenarios associated with both warming and a smaller decrease in precipitation. The heterogeneity of crop response to climate change reflects the

uncertainties in determining the most critical climatic factor for future yield loss and represents the challenge farmers would face to devise the adaptation strategies.

2.4 Summary

Under the future climate scenario, change in temperature and precipitation might impact the yield of different crops to different magnitudes. Future warming will be responsible for an overall decrease in cereal crop yield across the region. Furthermore, productivity of some crops will be decreased by drought resulting from the reduction in growing season precipitation in future years. Future projection of the country-average yield by the calibrated model indicates significant reduction in mean yield and increase in the year-to-year variation of yield because of future climate change in the region. Note that, for the cereal crops, as most of them follow the C4 pathway for photosynthesis, the effect of CO₂ fertilization is projected to be minimal in future years. Photosynthesis efficiency of C4 crops tends to reach saturation at about 400 ppmv of atmospheric concentration of CO₂. Previous studies based on experimental and modeling approaches concluded that CO₂ fertilization will not significantly affect the future yield of cereal crops (Allen et al. 1996; Leakey et al. 2006). Nevertheless, we tested the sensitivity of the DSSAT yield for cereal crops to the changes in atmospheric CO₂ level. According to the RCP 8.5, the mid-century level of atmospheric CO₂ is projected to be 571 ppm. To project the future yield, we ran DSSAT for both 380 ppm (equivalent to mean CO₂ level over 1980-1999) and 571 ppm, and the difference between simulated yield values for two CO₂ scenarios were negligible (Fig. 2.12).

While the decrease in mean can be intrinsically linked to increased temperature and changed precipitation pattern, the analysis of climate change impact on variability of yield involves a greater degree of uncertainties. More importantly, the temperature and precipitation pattern during certain growth stage of cereal crops, in addition to their distributions over the entire growing season, can also be critical in affecting both mean and variability of yield. The disparity between the MIROC-driven and the CESM-driven DSSAT projection highlights the caveat in projecting the climate change impact on crop yield resulting from the uncertainties in input climate variables. Therefore, more rigorous crop-specific analyses, in addition to using multiple future climate projections (based on climate models and emission scenarios) to force the crop model, are required to appropriately evaluate the change in crop yield because of future climate change in the region.

The first limitation of using a process-based crop model without incorporating information on possible adaptation is that it ignores the adaptive potential of the farmers to address environmental and socio-economic changes (Mendelsohn et al. 1994). While we included the change in planting time as one of the adaptation strategies, it is not sufficient because it is hard to predict what the future farming system would look like under usually long term climate change scenarios. Even for the present-day farming, availability of datasets providing comprehensive information on different adaptation techniques, which can be suitable included in modeling crop yield over a region, is extremely limited. Especially in West Africa, where small-scale agriculture is predominant, farmers' adaptive potential tends to be more diverse, and therefore, it is more difficult to incorporate adaptation information into a systematic modeling framework.

While farmers would naturally adopt diverse adaptation strategies to counteract potential yield losses resulting from future changes in climatic patterns, better data availability and more rigorous modeling approaches would be required to effectively account for the potential agricultural adaptation.

Table 2.1: Ranking of crops in West Africa according to 2003-2012 average of total harvested area and value of agricultural production. Source: FAOSTAT database, FAO.

<http://faostat3.fao.org/faostat-gateway/go/to/download/Q/QC/E>

Crops	Area Harvested (1000 ha)	Crops	Gross Production Value (1000 USD)
Millet	15,364.8	Yams	12,050,708
Sorghum	12,975.8	Cassava	6,878,989
Cow peas, dry	9,447.5	Rice, paddy	2,759,410
Maize	8,296.4	Cocoa, beans	2,675,029
Cassava	5,752.3	Groundnuts, with shell	2,673,586
Groundnuts, with shell	5,474.1	Millet	2,328,343
Rice, paddy	5,431.6	Sorghum	1,944,946
Cocoa, beans	5,330.7	Maize	1,925,730
Yams	4,265.8	Cow peas, dry	1,456,323
Oil, palm fruit	4,176.0	Taro	1,271,036

Table 2.2: Genetic coefficients of the maize, sorghum and millet cultivars chosen for this study. Base temperature = 8°C, NA = not applicable

Cultivar (Crop)	Obatampa (Maize)	CSM335 (Sorghum)	CIVT (Millet)
Thermal time from seedling emergence to the end of the juvenile phase during which the plant is not responsive to changes in photoperiod (degree days)	280	413	100
Thermal time from silking to physiological maturity (degree days)	700	640	390
Maximum possible number of kernels per plant	550	NA	NA
Kernel filling rate during the linear grain filling stage and under optimum conditions (mg/day)	7.74	NA	NA
Scaler for relative leaf size	NA	3	1
Scaler for partitioning of assimilates to the panicle	NA	4	0.6
Phylochron interval: the interval in thermal time between successive leaf tip appearances (degree days)	40	49	43

Table 2.3: Changes in mean (%) and changes in standard deviation (kg/ha) between present-day mean (1980-1998) and future mean (2041-2059) country-average yield from DSSAT driven with bias-corrected RegCM-downscaled MIROC-ESM climate for the chosen cultivars. The p-values of tests of significance at $\alpha=0.05$ are shown in parentheses.

	Maize		Sorghum		Millet	
Country	Percentage of change in mean (p-value)	Change in standard deviation (p-value)	Percentage of change in mean (p-value)	Change in standard deviation (p-value)	Percentage of change in mean (p-value)	Change in standard deviation (p-value)
Benin	-16.9 (0.001)	66.6 (0.001)	-15.3 (<0.001)	67.9 (0.027)	-28.3 (<0.001)	51.6 (0.343)
Burkina Faso	-17.5 (0.001)	108.1 (0.004)	-4.7 (0.166)	55.8 (0.036)	-34.0 (<0.001)	44.1 (0.008)
Gambia	-40.1 (<0.001)	242.2 (0.001)	-8.8 (0.113)	74.1 (0.198)	-45.3 (<0.001)	65.2 (0.014)
Ghana	-10.2 (0.012)	75.2 (0.006)	-7.0 (0.002)	34.9 (<0.001)	-24.8 (<0.001)	10.8 (0.036)
Guinea	-17.1 (<0.001)	90.9 (0.005)	-6.4 (0.059)	101.8 (0.015)	-39.2 (<0.001)	87.5 (<0.001)
Guinea Bissau	8.9 (0.086)	122.9 (<0.001)	4.5 (0.472)	132.6 (0.011)	-35.0 (<0.001)	82.4 (0.002)
Ivory Coast	-9.9 (0.031)	91 (0.003)	-4.0 (0.114)	46.1 (0.010)	-25.6 (<0.001)	24.4 (0.001)
Mali	-30.4 (<0.001)	109.2 (0.012)	-7.6 (0.184)	61.7 (0.058)	-39.3 (<0.001)	52.9 (0.184)
Niger	-2.0 (0.780)	151.5 (0.006)	-5.1 (0.427)	41.4 (0.475)	-15.5 (0.010)	16.8 (0.561)
Nigeria	-11.0 (0.006)	128.3 (<0.001)	-11.8 (0.001)	87.0 (0.003)	-29.3 (<0.001)	47.60 (0.115)
Senegal	-39.5 (<0.001)	105.8 (0.006)	-25.3 (<0.001)	90.3 (0.011)	-45.5 (<0.001)	30.8 (0.315)
Sierra Leone	-5.4 (0.243)	95.1 (0.004)	-5.4 (0.199)	88.2 (0.015)	-29.6 (<0.001)	101.5 (0.004)
Togo	-0.4 (0.962)	176.8 (0.045)	-7.6 (0.022)	25.7 (0.082)	-13.7 (0.137)	170.0 (0.295)

Table 2.4: As in Table 2.3, but for DSSAT driven with bias-corrected RegCM-downscaled CESM climate.

	Maize		Sorghum		Millet	
Country	Percentage of change in mean (p-value)	Change in standard deviation (p-value)	Percentage of change in mean (p-value)	Change in standard deviation (p-value)	Percentage of change in mean (p-value)	Change in standard deviation (p-value)
Benin	-50.4 (<0.001)	29.1 (0.11)	30.3 (<0.001)	128.2 (<0.001)	-13.6 (0.014)	83.4 (<0.001)
Burkina Faso	-39.8 (<0.001)	47.7 (0.182)	53.9 (<0.001)	88.3 (0.012)	3.43 (0.329)	36.2 (0.17)
Gambia	-44.7 (<0.001)	118.7 (<0.001)	11.2 (0.373)	291.0 (<0.001)	-38.6 (<0.001)	126.1 (0.004)
Ghana	-55.8 (<0.001)	56.9 (0.043)	13.6 (0.004)	104.5 (<0.001)	-4.8 (0.364)	86.1 (0.001)
Guinea	-32.2 (<0.001)	85.5 (0.005)	-15.1 (<0.001)	74.0 (0.013)	-36.2 (<0.001)	89.9 (<0.001)
Guinea Bissau	-24.3 (<0.001)	125.4 (<0.001)	50.2 (<0.001)	223.1 (0.004)	-11.1 (0.097)	150.9 (0.002)
Ivory Coast	-47.4 (<0.001)	49.1 (0.016)	18.9 (<0.001)	61.2 (<0.001)	0.3 (0.941)	80.5 (<0.001)
Mali	-52.1 (<0.001)	9.5 (0.893)	30.7 (<0.001)	107.4 (0.006)	-19.9 (<0.001)	74.4 (0.043)
Niger	-14.7 (0.068)	176.1 (<0.001)	19.6 (0.005)	56.8 (0.362)	-4.4 (0.405)	-8.7 (0.839)
Nigeria	-20.2 (<0.001)	178.1 (<0.001)	28.2 (<0.001)	168.6 (<0.001)	-32.1 (<0.001)	57.8 (0.038)
Senegal	-53.8 (<0.001)	13.6 (0.353)	-15.4 (<0.013)	142.2 (0.016)	-31.3 (<0.001)	56.6 (0.075)
Sierra Leone	-40.1 (<0.001)	103.2 (0.011)	-36.0 (<0.001)	68.6 (0.065)	-48.8 (<0.001)	71.0 (0.01)
Togo	-49.3 (<0.001)	19.0 (0.408)	30.1 (<0.001)	107.6 (0.003)	2.6 (0.682)	77.9 (<0.001)

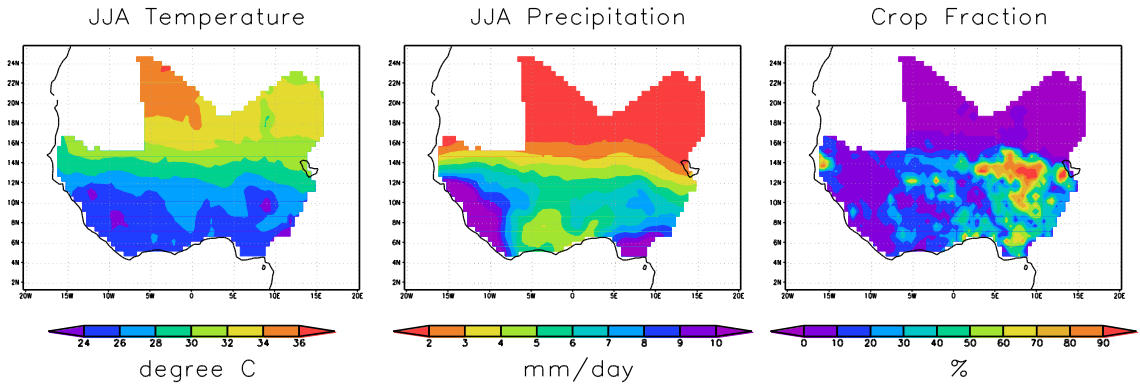


Fig. 2.1: Spatial maps of the present-day (mean over 1980-1999) June-July-August (JJA) average daily temperature ($^{\circ}\text{C}$), average daily precipitation (mm/day), and the present-day crop area (%) distribution on a spatial scale of 0.5° in West Africa. Crop fraction coverage at 0.5° was aggregated from the Spatial Production Allocation Model (SPAM) (You et al. 2014) data which represents the geographic distribution of crop harvest area across the globe at a spatial scale of 5 min. for the year of 2005.

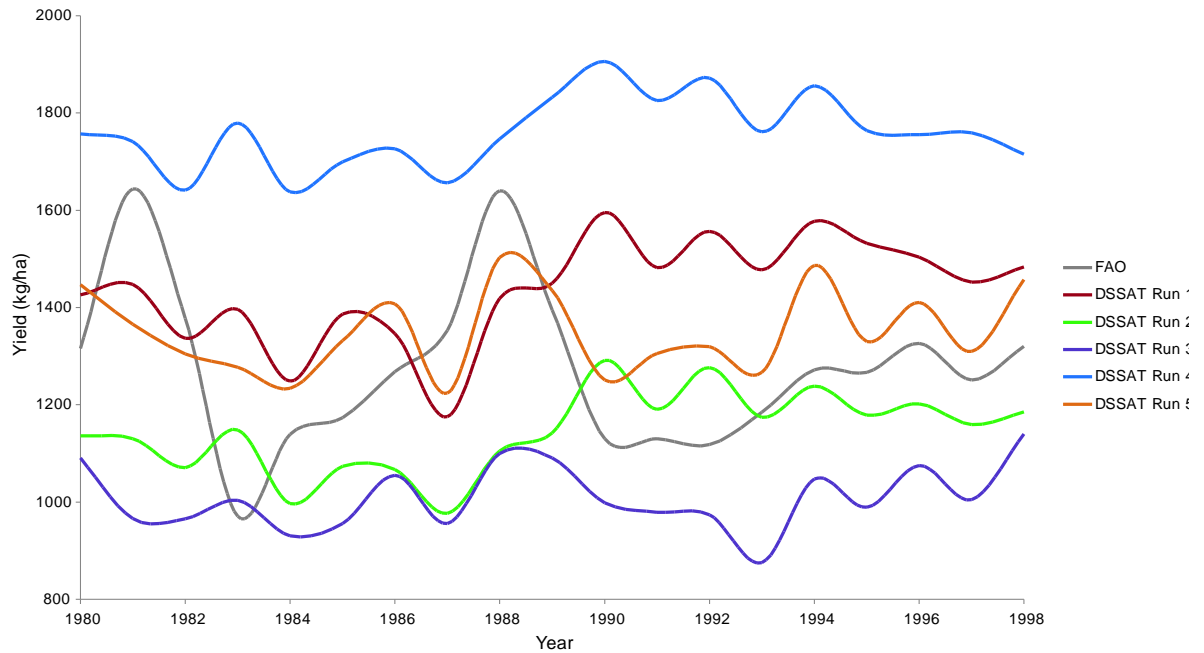


Fig. 2.2: Comparison of time series (1980-1998) of maize yield (kg/ha) in Nigeria from different DSSAT runs. FAO: the grey line represents FAO observed data. DSSAT Run 1: the red line shows DSSAT output for short season cultivar with initial input data used in this study. DSSAT Run 2: the green line shows model output after model calibration by modifying the nitrogen fertilizer input. DSSAT Run 3: the purple line showing lower yield simulated by model because of delaying planting time by one month reflects the effect of growing season on yield. DSSAT Run 4: the cyan line shows the model output for medium season cultivar with initial data. DSSAT Run 5: the orange line represents the medium season cultivar with calibrated fertilizer input and planting time delayed by one month.

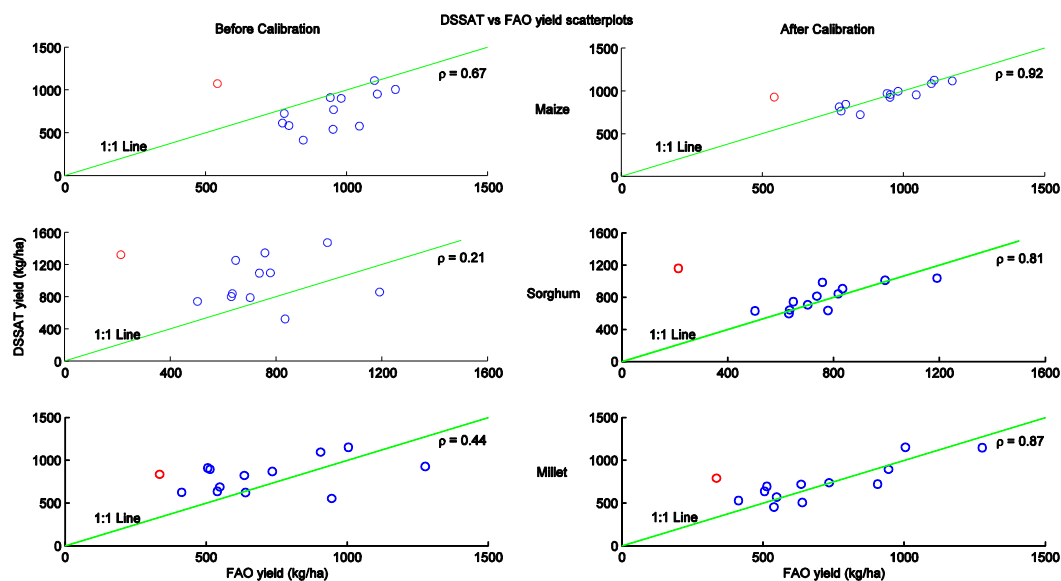


Fig. 2.3: DSSAT vs FAO scatterplot before (left column) and after (right column) calibration for present-day average (1980-1998) of country-level yield (kg/ha) for maize, sorghum and millet in West Africa. Niger is shown by the red circle. The green line represents 1:1 line.

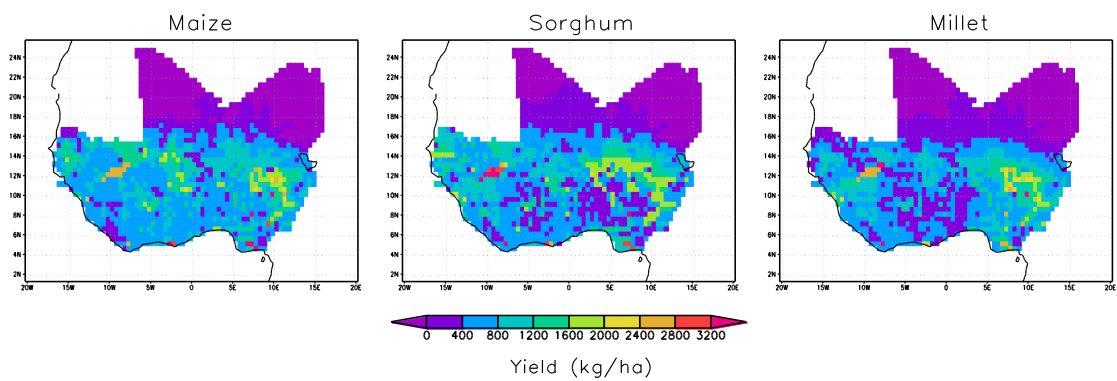


Fig. 2.4: Spatial maps of the present-day (mean over 1980-1999) yield (kg/ha) for maize, millet and millet in West Africa.

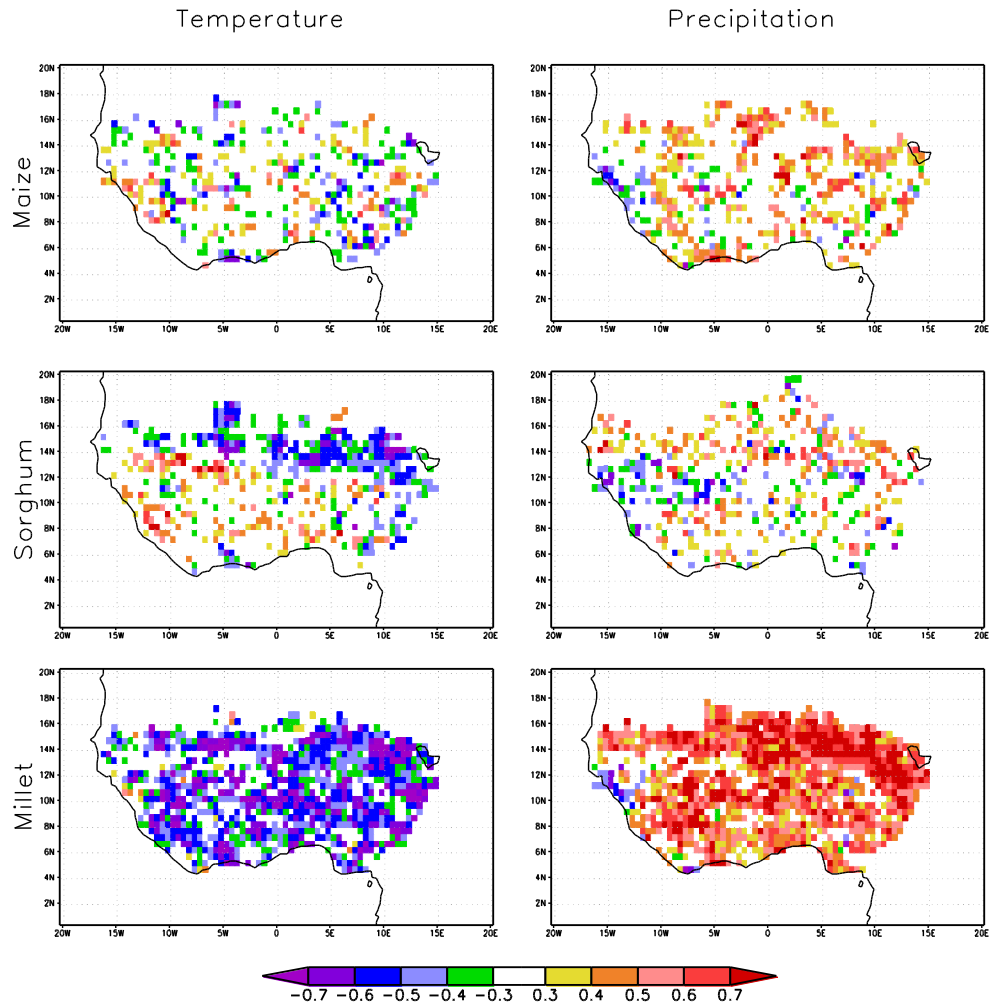


Fig. 2.5: Correlation coefficient ($p < 0.1$) between present-day mean (1980-1999) yield and growing season temperature (left column) and precipitation (right column). Only grid cells with significant correlation are shown.

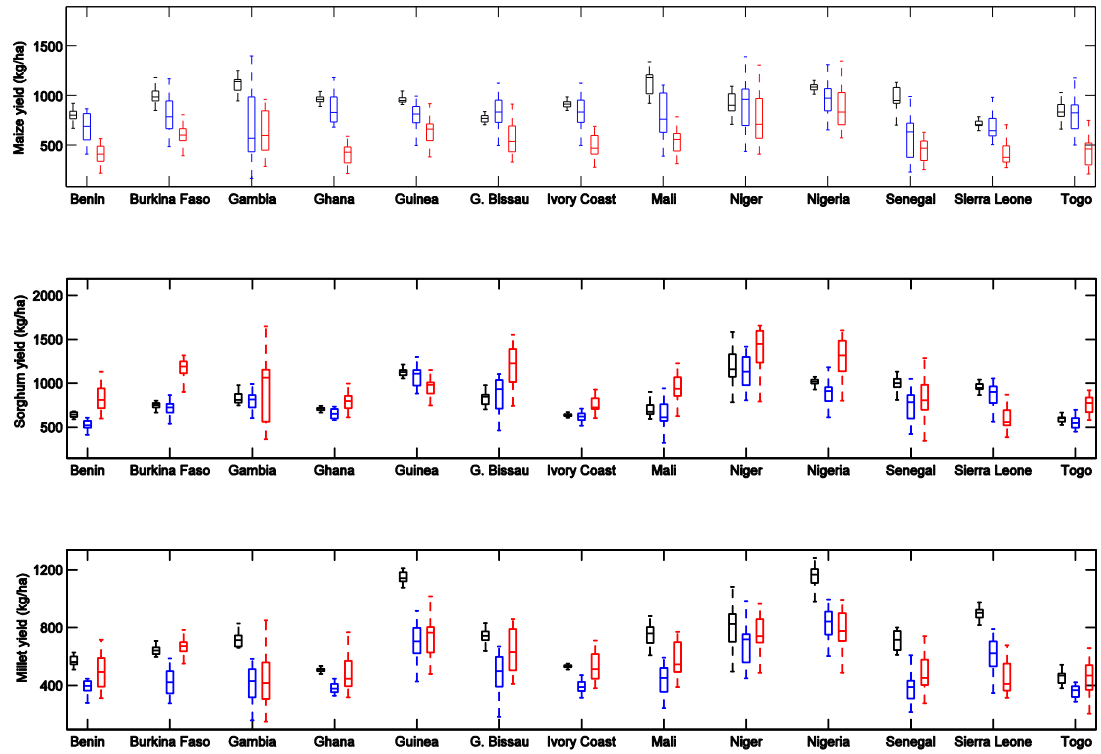


Fig. 2.6: Side-by-side boxplots of yearly country-average yield (kg/ha) of maize (top row), sorghum (middle row) and millet (bottom row) in 13 West African countries; black: 1980-1998; blue: 2041-2059 under the MIROC climate; red: 2041-2059 under the CESM climate.

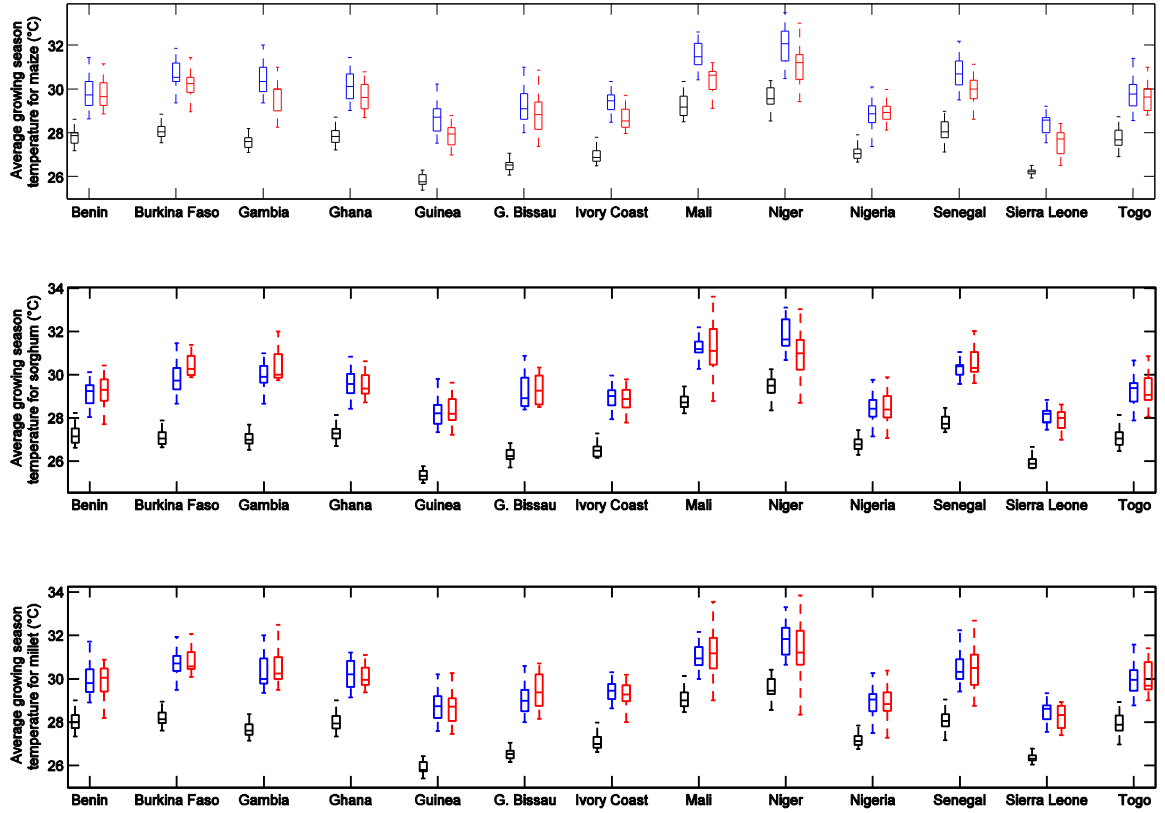


Fig. 2.7: Side-by-side boxplots of yearly country-average growing season temperature (°C) for maize (top row), sorghum (middle row) and millet (bottom row) production (corresponding to yield values shown in Fig. 3) in 13 West African countries; black: 1980-1998; blue: 2041-2059 under the bias-corrected RegCM-downscaled MIROC climate; red: 2041-2059 under the bias-corrected RegCM-downscaled CESM climate.

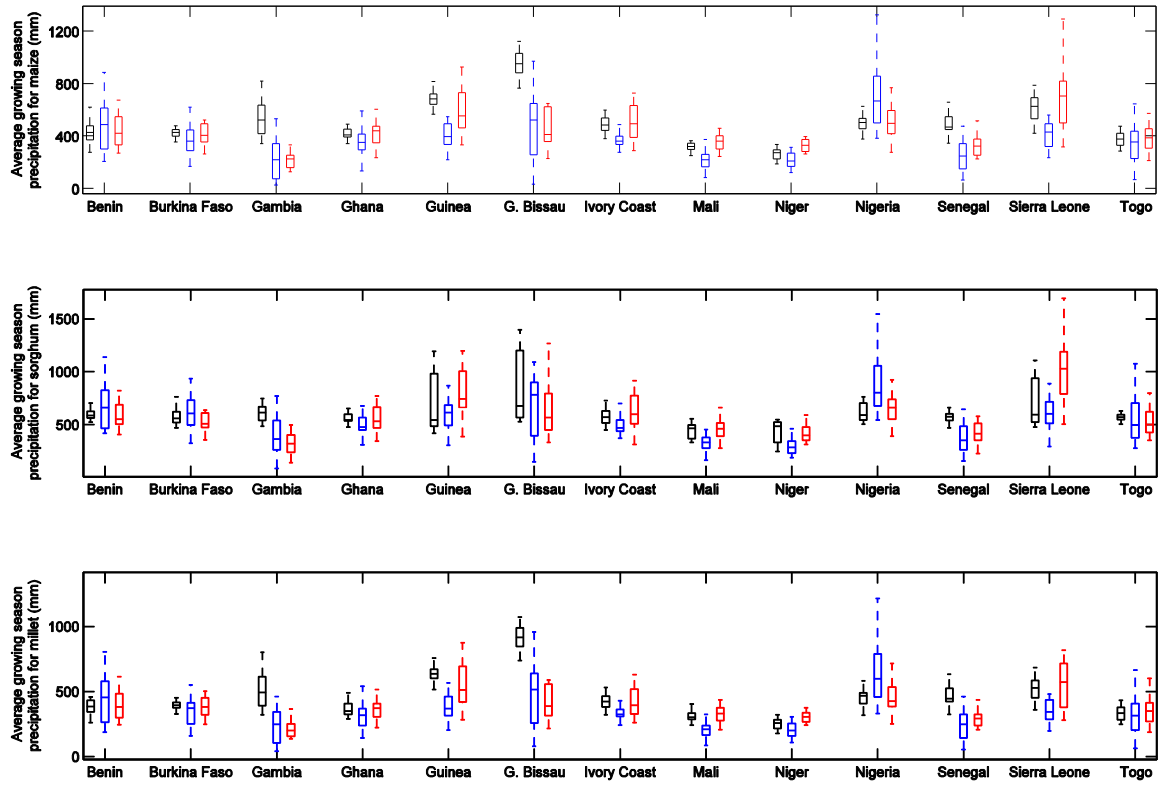


Fig. 2.8: Side-by-side boxplots of yearly country-average growing season precipitation (mm) for maize (top row), sorghum (middle row) and millet (bottom row) production (corresponding to yield values shown in Fig. 3) in 13 West African countries; black: 1980-1998; blue: 2041-2059 under the bias-corrected RegCM-downscaled MIROC climate; red: 2041-2059 under the bias-corrected RegCM-downscaled CESM climate.

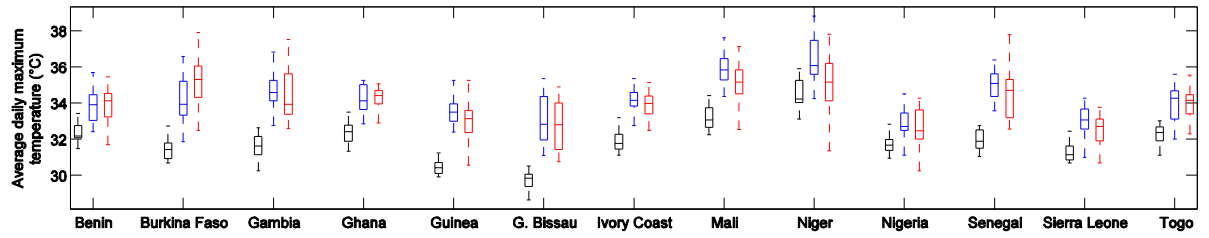


Fig. 2.9: Side-by-side boxplots of yearly country-average maximum temperature (°C) during panicle initiation and anthesis of sorghum in 13 West African countries; black: 1980-1998; blue: 2041-2059 under the bias-corrected RegCM-downscaled MIROC climate; red: 2041-2059 under the bias-corrected RegCM-downscaled CESM climate.

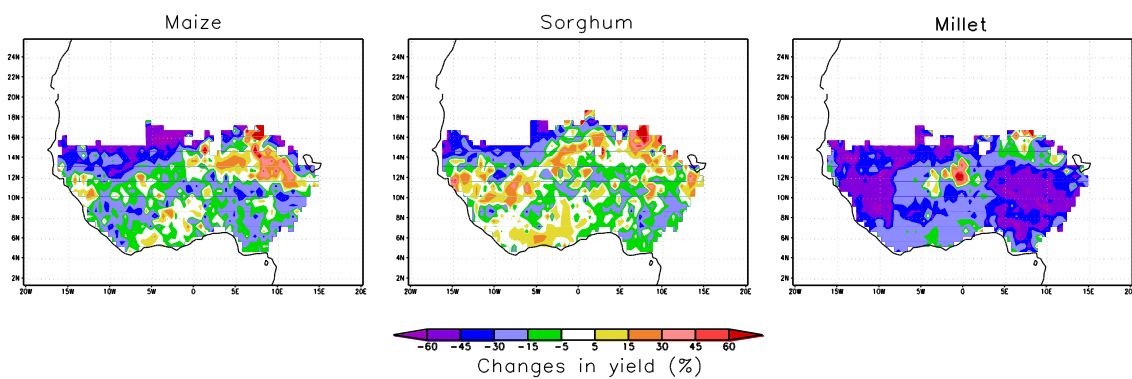


Fig 2.10: Spatial maps of the future changes (%) in yield (future mean minus present-day mean) for maize, sorghum and millet in West Africa.

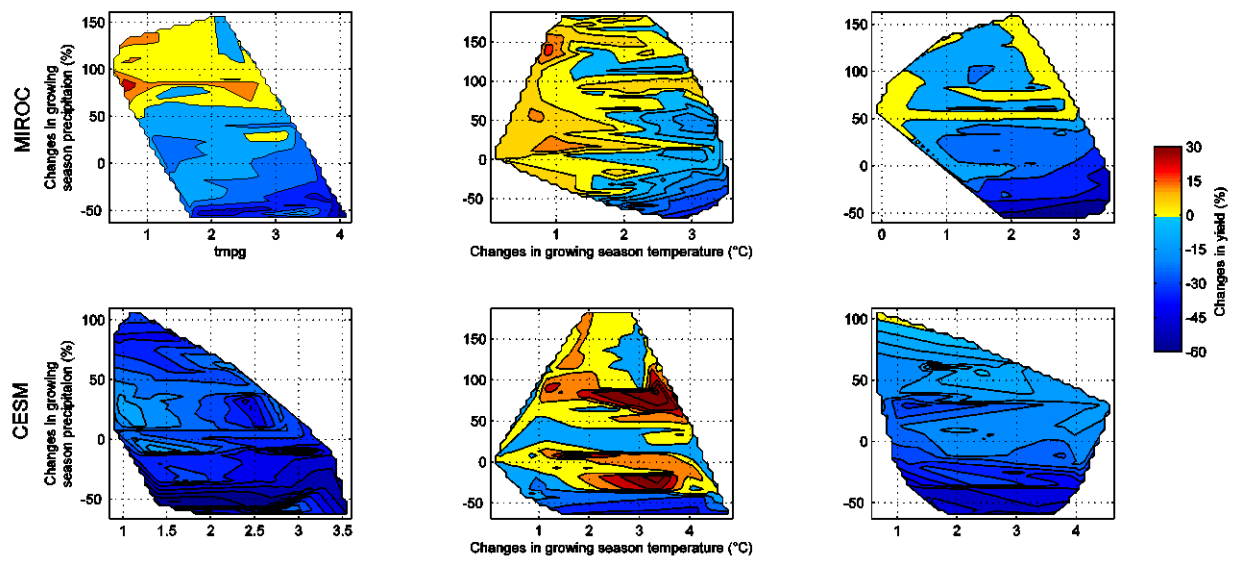


Fig. 2.11: Contour plots of changes in yield against changes in growing season precipitation (ordinate) and changes in average growing season temperature (abscissa) as projected by DSSAT driven with MIROC (top row) and CESM climate (bottom row). Contours were plotted using the grid-level data from 13 countries of West Africa.

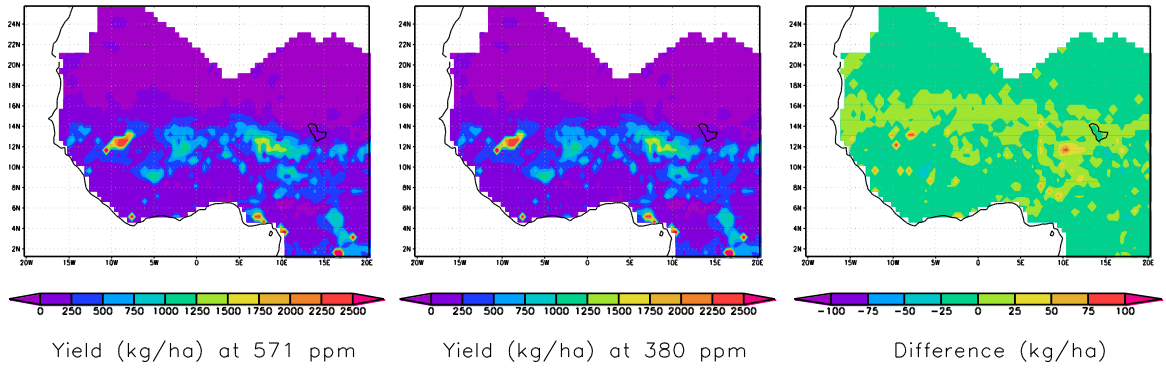


Fig. 2.12: Spatial maps of the future (mean over 2041-2059) maize yield (kg/ha) at two different levels of atmospheric CO₂ concentration (left: 571 ppm, middle: 380 ppm) and the difference in yield values.

Chapter 3

Modeling climate change impact on agricultural land use

3.1 Introduction

Agricultural activity is one of the most important processes driving LULCC in a region. During the pre-industrial period, addition of croplands was the primary response to increasing demand for food and other agricultural products. With the advent of modern agricultural technology, farmers adopted intensive crop farming to minimize the use of land area and slow down the rate of land cover changes (Burney 2010). Nevertheless, globally the fraction of farmland, which comprises cropland and pasture, has been steadily increasing at the expense of forest (Burney 2010, Hurtt 2011). The average global GHG emission from agriculture was reported to increase by 1.6% per year during 1961-2010 (Tubiello 2013).

Many previous studies with different modeling approaches integrated the climate-induced changes in agricultural productivity with socioeconomic changes to project future land use scenarios. However, most of them assessed the land use change on national/sub-national levels, and therefore, do not provided gridded land use map needed by climate projection models (Schmitz et al., 2014). Moreover, most existing models and studies focus only on aggregated land use changes without providing information on individual crops. However, land use policymaking and strategic managements to ensure national or regional food security often require information for production of individual crops. Land use modeling at the individual crop level may help guiding policy making and long-term planning. In this study, we develop a cropland projection (LandPro_Crop) algorithm that

operates on a spatially explicit grid system with the capacity of quantifying land use changes at individual crop level to address the need of climate models for grid-based land use information. In the current application of LandPro_Crop to West Africa in evaluating the impact of future increase of food demand and the climate-induced crop yield changes on agricultural land use changes in the region, the mid-21st century projection is analyzed as an example. Here we engage LandPro_Crop to address three questions: what would be the future distribution of crop areas in West Africa to satisfy the future country-level demand for foods with current agricultural practice? what are the relative roles of socioeconomic factors and climate changes in driving future land use changes? could land use optimization through human decision-making have considerable impact on the overall LULCC? Considering the fact that future crop yield is an input to LandPro_Crop algorithm, we also examine the sensitivity of our results to the selection of future climate data source used in projecting the future yield.

3.2 Model, Data, and Methodology

3.2.1 Algorithm for Cropland Projection

The LandPro_Crop algorithm is developed based on the equilibrium between future demand and supply of food at the country level. In the application to the West African Sahel and Guinea Coast regions, 14 countries are included: Benin, Burkina Faso, Gambia, Ghana, Guinea, Guinea-Bissau, Ivory Coast, Liberia Mali, Niger, Nigeria, Senegal, Sierra Leone and Togo. The spatially explicit model, at a resolution of 0.5°, treats each country separately to calculate the gap between future demand of a particular

crop and its supply from the local production based on future yield of the crop and the respective present-day crop area at each pixel within the country.

$$D_{ij} = G_{ij} - \sum_{k=1}^n y_{ijk} a_{ijk} \quad (1)$$

where, D_{ij} is the future deficit for crop j in country i , G_{ij} is the future demand, y_{ijk} is future yield of crop j at pixel k and a_{ijk} is present-day area allotted for crop j at pixel k in country i with n number of 0.5° pixels.

The model is developed based on the assumption that agricultural land use will be prioritized over natural land use/land cover types to satisfy increased food demand in future decades. Therefore, the deficit will be overcome by means of increasing local production through the expansion of cropland at the expense of existing natural vegetation. Several rules are set to govern the conversion from naturally vegetated land to cropland, and multiple scenarios of decision making are considered. For example, in the best scenario of future land use with science-informed decision-making:

- 1) Forest is preferred over grassland in making new land for crops, due to its generally more fertile soil and the need to preserve grassland for pasture use.
- 2) If the forest area within a country is completely exhausted and crop deficit still remains, the grass area will be used for conversion to cropland.
- 3) For multiple grid cells having the same type of natural vegetation, areas in grid cells with higher yield in future climate for a given crop will be used up to cultivate that particular crop before acquiring land from the next most productive grid cell, i.e., the order of land conversion follows the descending order of crop yield across grid cells within a particular country.

- 4) Naturally vegetated land is converted and allocated to crops following the descending order of crop deficit in a particular country. That is, the crop with the largest remaining gap between demand and production will be prioritized first.

The best scenario implies the minimum crop area expansion at the expense of natural vegetation. Several alternative scenarios are constructed to test the sensitivity of the land use projection results by altering one or multiple rules listed above. For example, a worst scenario implying the maximum crop area expansion involves reversing the order mentioned in rule 3 and rule 4, and several intermediate scenarios represent different degrees of randomness in the decision making related to the rules.

The y_{ijk} in equation 1 is derived using the process-based crop model Decision Support System for Agrotechnology Transfer (DSSAT) (Jones et al. 2003). Future yield projected by the DSSAT are scaled by three factors. First, like any process-based model, outputs from the DSSAT associate with some bias. The ratio of the DSSAT-simulated present-day yield to a reference present-day yield dataset is used to correct the bias in the DSSAT-simulated future crop yield. Second, although the land use allocation model can account for any number of crops, sometimes due to data limitation or other reasons, only a subset of crops are considered. For example, instead of exhausting all crops existing, for simplicity, we consider in this study only five major crops in West Africa - maize, sorghum, millet, cassava and peanut. These crops were chosen for their large present-day harvest area and high economic value in the region (Ahmed et al. 2015). To indirectly account for the existence of other crops (“minor crops”), the DSSAT-simulated future yield for major crops were scaled down using the ratio between major-crop harvesting area and all-crop harvesting area. In addition, mixed cropping systems commonly seen in

West Africa are difficult to model explicitly. To indirectly account for the impact of mixed crops, a third factor, the ratio of total harvest area to the total area of physical land for crops, is used to scale up the DSSAT-simulated future crop yield. These can be summarized as follows:

$$y_{ijk} = y'_{DSSAT,ijk} * \frac{y_{SPAM,ijk}}{y_{DSSAT,ijk}} * \frac{A_{M,ik}}{A_{H,ik}} * \frac{A_{H,ik}}{A_{P,ik}} \quad (2)$$

where, y_{ijk} is the factored future yield, $y'_{DSSAT,ijk}$ is the DSSAT future yield, $y_{DSSAT,ijk}$ is the DSSAT present-day yield, $y_{SPAM,ijk}$ is the present-day yield according to the Spatial Production Allocation Model (SPAM) (You and Wood, 2006, You et al. 2014), $A_{H,ijk}$ is the total harvest area (summation of area allocated to all the individual crops) at pixel k in country i , $A_{P,ik}$ is the total physical area (excluding water body) and $A_{M,ik}$ is the total area allocated to the five major crops chosen for this study. The mixed cropping practice, as well as the ratio of harvest area occupied by the “major” and the “minor” crops in a particular region, is largely influenced by dietary habits, and is likely to stay stable in the absence of any major shift in dietary habits. In the application to the mid-century in West Africa, we assume that the scaling factors in the future will be at the same level as in the present. Harvest area used here was aggregated from the SPAM data which represents the geographic distribution of crop harvest area across the globe at a spatial scale of 5 min. for the year of 2000 and 2005. SPAM was generated combining the Food and Agriculture Organization (FAO) national crop-specific data, population density, satellite imagery and other datasets. Also note that brief descriptions of the reference present-day yield data and the land use land cover data are provided later in section 2.4.

3.2.2 Projecting Future Crop Yield

Agricultural land use in a region depends to a large degree on crop yield which is one of the essential inputs to the LandPro_Crop algorithm. In the application to West Africa, spatially distributed future yields of five major crops were used as the inputs that were simulated using the DSSAT version 4.5 at a spatial resolution of 0.5° across the region. The DSSAT was calibrated and run to simulate future yield for the period of 2041-2059 following the methodology of Ahmed et al. (2015) for cereal crops. For cassava and peanut, however, the DSSAT could not be calibrated satisfactorily following the same approach. Therefore, instead of calibrating the model, yield values of those two crops for the future DSSAT runs were adjusted by the ratio of country-level mean observed yield to the corresponding present-day mean of DSSAT-simulated yield. The mean observed yield values were calculated using the FAO country-level yearly yield data for 1980-1998 (FAOSTAT database). Simulated yield values from 2041 to 2059 were averaged to provide the inputs to the LandPro_Crop algorithm to project the agricultural land use in 2050.

The future climate data required to drive the crop model was derived by dynamically downscaling the RCP8.5 climate of two general circulation models (GCMs) participating in the Coupled Model Intercomparison Project phase 5 (CMIP5) (Taylor et al. 2012), the Model for Interdisciplinary Research On Climate – Earth System Model (MIROC-ESM) and the National Center for Atmospheric Research (NCAR) Community Earth System Model (CESM). The regional climate model RegCM 4.3.4 (Giorgi et al. 2012) coupled with the Community Land Model version 4.5 (CLM 4.5) (Oleson et al. 2010) (Wang et al. 2015) was used to downscale the MIROC and CESM outputs to 50km, which is then

resampled to a 0.5° grid system. The dynamically downscaled climates were then bias-corrected using the Statistical Downscaling and Bias Correction (SDBC) method (Ahmed et al. 2013), and the Sheffield et al. (2006) data was used as present-day climate reference in the bias-correction algorithm.

3.2.3 Projecting Future Demand for Local Production

Future demand for local crop supply is one of the main inputs to the LandPro_Crop. Demand of crops in the West African countries in future years (from 2005 to 2050) was projected using the International Model for Policy Analysis of Agricultural Commodities and Trade (IMPACT) model (Rosegrant et al. 2012). The IMPACT was developed at the International Food Policy Research Institute (IFPRI) to investigate the supply-demand chain in the context of national food security in future decades. It can be used to project the future scenarios of supply, demand and price for more than 40 food commodities globally or regionally. For this study, IMPACT was run under the Shared Socioeconomic Pathway-2 (SSP2), a moderate pathway characterized by historical trends of economic development and medium population growth, according to IPCC AR5. The future climate data used to drive IMPACT were derived from the RCP8.5 output of four GCMs, including GFDL-ESM2M, HadGEM2-ES, IPSL-CM5A-LR, and MIROC-ESM. The average of the output from the four IMPACT runs was used as the input to the LandPro_Crop algorithm. Also, to project the mid-century land use scenario, future average of the demand during 2041-2050 was used. Note that the IMPACT projections include future scenarios for both the total demand (i.e., demand assuming no international trade) and effective demand (i.e., net demand for local production after considering international trade) for a specific commodity in a country. Local production may satisfy

the total demand partially or fully. The deficit or surplus between the total demand and local production reflects the effect of international trading. For example, comparison of the time-series of total demand and local production of maize in Nigeria as projected by the IMPACT for 2005-2050 indicates an increasing trend for the portion of total demand to be met by international trading during the period (Figure 3.1).

3.2.4 Present-Day Land Use and Crop Yield Data

To quantify the bias in crop yield simulated by DSSAT (equation 2), the grid-level dataset of present-day yield from SPAM for the year of 2005 were used as the reference data. The present-day harvest area for five major crops and total physical land area at each 0.5° pixel in West Africa used as inputs to LandPro_Crop were also obtained from the SPAM 2005 dataset. In addition to crop area, the present-day fractions of forest area and grassland at each grid cell are also needed to provide the initial condition for the LandPro_Crop algorithm for projecting future land use. The fractional coverage of each of these three land cover types at each grid cell was obtained from the global land surface data developed by Lawrence and Chase (2007) which combined various satellite products and other datasets to derive the present-day global distribution of plant functional types at a 0.05° resolution. However, crop fraction in the Lawrence and Chase (2007) dataset was estimated according to historical crop area data generated by Ramankutty and Foley (1999) and it shows a considerable deviation from the SPAM crop fraction. Since crop area information for this study were prescribed according to SPAM, crop fraction in Lawrence and Chase (2007) was updated accordingly and the fractional coverage for forest and grassland were adjusted proportionally.

3.3 Results and discussions

The reduction in crop yield as a result of climate change and the increasing demand for food in future years are expected to cause an increase in the agricultural land use, leading to a substantial shift in land cover in West Africa as projected by the LandPro_Crop algorithm (Figure 3.2). The present-day land use distribution shows majority of the agricultural activity occurring in the eastern part of West Africa and the extensive presence of forest area in the southwest, especially along the coast. Although grassland exists almost over the entire region, they are more dominant further inland in the north. The LandPro_Crop algorithm projects further increase in crop areas in the eastern part of West Africa which would result in a complete depletion of forest and grassland in future decades. The western and central parts of West Africa would also experience noticeable increase in cropland. However, most of the increment would occur at the expense of forest area, with generally a lower degree of grassland depletion. In Nigeria, the country-average crop area percentage is projected to increase from 39.4% to 84.5% under MIROC-driven climate and to 80.9% under CESM-driven climate (Table 3.1). In the western part of the region along the coast, the largest increase in cropland is projected to occur in Gambia (45% and 39.2% under the MIROC- and CESM-driven climates respectively). Along the Gulf of Guinea, west of Nigeria, Benin would also experience a large increase of crop area by 37.3% (MIROC) and 40.9% (CESM). In Niger, crop production is clustered only to the south since the vast northern part of the country is mostly covered by desert. Therefore, although the model projects a small change in the fractional coverage of cropland averaged over the entire country, the magnitude of the projected increase of agricultural land use in the south is much larger. For most countries,

the LandPro_Crop projections for aggregated land use change driven by the dynamically downscaled climates from the two GCMs are very similar. The inter-model difference is much smaller than the inter-country difference of land use changes. Several factors contribute to this remarkable similarity in the LandPro_Crop-produced land use changes driven by future climate changes from the two GCMs. First, climate from MIROC and CESM are dynamically downscaled by the regional climate model and statistically corrected for model bias, which eliminates part of the inter-model differences related to model bias; as the bias-corrected future climate data were used to force the crop model DSSAT, a better agreement results between the DSSAT-produced crop yields corresponding to the two climate models. Second, as shown later, results of our study indicate that the future land use changes in this region would mostly be dominated by socioeconomic factors in the region.

To assess the relative importance of climate and socioeconomic factors in driving the future land use changes, we also conducted LandPro_Crop simulations considering only the socioeconomic changes in the region and excluding the impact of climate-induced crop yield changes. In order to do so, the LandPro_Crop was run with the future demand and present-day crop yield (as opposed to the future yield used for the initial run) as inputs. Since the crop yield values remain unchanged, outputs from this run, namely LandPro_Crop-SE, reflect the impact of socioeconomic changes on agricultural land use ignoring the climate-induced changes in yield (Figure 3.3). The difference between the future changes in crop area from the LandPro_Crop-Total run (considering both climate and socioeconomic factors) and the LandPro_Crop-SE run indicate the changes in crop area projected by LandPro_Crop considering only climate change (LandPro_Crop-CC).

Under both the MIROC-driven and CESM-driven regional climates, the socioeconomic changes tend to have a stronger impact on future land use transition than the changes in crop yield in the eastern part of the region. In the western part near the coast, however, the impact of crop yield changes is more dominant, which can be attributed to the larger yield loss resulting from a larger future warming in that part of the region (Ahmed et al. 2015). In the central part of the region, the climate-induced expansion in crop area tends to be somewhat more evident under the CESM-driven climate.

Food demand determined by socioeconomic factors is the most important driver for land use. The land use changes shown in Figure 3.3 were predicted using LandPro_Crop driven by changes in the net demand for local production projected by IMPACT (referred to as “Effective Demand” experiment). To test the sensitivity of LandPro_Crop to the production demand, future changes in agricultural land were also predicted using the total demand projected by IMPACT (as if there would be no international trading) as the driver (referred to as the “Total Demand” experiment), and using a demand that features a future increase half as fast as the projection by IMPACT (referred to as the “50% Change” experiment). Spatial patterns of absolute changes in crop area percentage are essentially similar for both the net demand and total demand experiments (Figures 3.4 and 3.5, for the MIROC- and CESM-driven climates respectively). The magnitude of changes is generally larger in the case of total demand since most of the countries in the region depend on import to satisfy the demands which exceed local production. The land use changes are expectedly smaller for the “50% Change” experiment. However, spatial patterns of the relative importance of climate change and socioeconomic changes can noticeably vary according to demand scenarios. For example, under the MIROC-driven

climate, in the northeast part of Nigeria (East of 10°E and North of 8°N), changes in crop are projected to be dominated by socioeconomic changes to satisfy total demand (Figure 3.4). In contrast, in satisfying either the net demand or 50% future changes of total demand, changes in crop area would be controlled by climate-induced changes in crop yield while the impact of socioeconomic changes would be negligible. Thus, fraction of future land use change attributed to climate change tends to vary spatially within a country depending on the future demand values. However, magnitudes and spatial patterns of the fraction of climate-induced crop area expansion across the regions for all three demand scenarios are generally similar under both of the GCM-driven climate scenarios.

The dependence of future land use patterns on the magnitude of demand can be attributed to two factors which govern LandPro_Crop algorithm – the present-day distribution of forest and grass, and the differences between present-day and future ranking of grid cells according to their respective yield values. Since the LandPro_Crop scenario experimented on uses up forest area over the entire country before it starts to consume grassland, grid cells with grass in the present-day are not converted to crop area until the demand reaches a threshold value. Therefore, with present-day yield, although many grid cells dominated by grass do not experience any change in land use in satisfying lower demand, they are converted to crop area when demand is higher. However, with generally lower yield in future climate, those grid cells need to be converted to cropland even to satisfy a lower level of demand. Furthermore, a grid cell with a lower rank for present-day yield may become higher-ranked for future yield values and vice versa, leading to a difference in spatial variability of climate-induced land use

changes for different demand values. The comparison among country-average values of climate-induced land use changes for different demand scenarios also highlights the uncertainty in LandPro_Crop in determining the fraction of changes attributable to climatic factors (Figure 3.6). For a particular country, the total demand would usually necessitate a larger increase in total crop area than the net demand for local production, whereas the magnitude of the increase would be the lowest in the case of 50% changes of the total demand. Exception can be found for export countries. The relative importance of climate and socioeconomics changes as drivers of land use change and how it varies spatially are relatively stable across the three simulations, with the exception of several countries. For example, under the MIROC-driven climate changes, in Gambia, Senegal and Togo, the fraction of climate-induced changes to total crop area changes projected by LandPro_Crop to satisfy the 50% increase in total demand is larger than the projected changes for other two demand scenarios. Under the CESM-driven climate, the climate-induced change in agricultural land use is the largest for the “50% change” experiment in the case of Burkina Faso as well.

The LandPro_Crop algorithm explicitly considers multiple scenarios of human decision-making (as reflected by the order of land conversion in rule 3 and rule 4 mentioned in section 3.2.1), which is a major source of uncertainty in projected future land use changes. To assess such uncertainties, we evaluated whether human decision regarding agricultural land use optimization can influence the future land use change in West Africa based on alternative decision scenarios. In agricultural expansion, the selection of areas to cultivate from naturally vegetated land is one major uncertainty in human decision-making for land use. Therefore, apart from the best scenario simulated

by the initial run, two alternative projections of future land use distribution, including the worst scenario and an intermediate scenario, were conducted by altering the order of crop area selection based on future crop yield in rule 3 in LandPro_Crop. The worst scenario assumes that the conversion from natural vegetation to cropland by farmers follows the ascending order of crop yield, while the selection is random for the intermediate scenario. Comparison of these alternative scenarios with the best scenario reveals noticeable differences, with both alternative scenarios generally involving more cropland (Figure 3.7). The cropland expansion is minimized if farmers utilize the areas with higher future yield first before engaging the less productive land, whereas the opposite approach would maximize the amount of cropland usage (Table 3.2, using MIROC as example). The difference among multiple future scenarios of agricultural land use, which depends on the farmers' decision regarding the selection of crop area, implies an adaptive potential to minimize the conversion of naturally vegetated land based on appropriate knowledge of future crop yield. We also performed sensitivity analysis of LandPro_Crop projections to input demand (as shown in Figures 3.4 and 3.5) in the case of worst scenario of agricultural land use regarding the order of crop area selection. With the alternative cropping order, the relative importance of climate and socioeconomic factors in driving the future land use change considerably changes in many parts of the region for all the demand scenarios (Figure 3.8, using MIROC as example). This implies that land use decision-making can play a significant role in determining future agricultural land use changes.

Prioritization of the crops by farmers with respect to the sequence of land allocation in a particular country reflects another uncertainty related to human decision-

making. For the best scenario run, the land was allocated to the crops according to the descending order of future crop deficits as stated in rule 4. Several alternative scenarios were examined with LandPro_Crop. In alternative 1, the prioritization in rule 4 follows the ascending order of deficits in a specific country; in alternative 2, in all of the countries, the priority for land allocation was given to the cereal crops first (maize, sorghum and millet) followed by cassava and peanut; in alternative 3, the reverse order of alternative 2 is used. Under the MIROC-driven climate, spatial maps of crop area distribution from the multiple alternative runs indicate that prioritization of the crops as a land use optimization technique would have little impact on the projected future land use land cover changes (Figure 3.9). The difference in country-average future crop area percentage from different runs is negligible as compared to the absolute magnitude in a particular country (Table 3.3). The results are qualitatively similar for the projections based on the CESM-driven climate changes.

To test the performance of LandPro_Crop, we compared the LandPro_Crop projections with the crop area distribution in 2050 projected by Hurtt et al. (2011, henceforth H11) data. H11 projected future (2005-2100) land use scenarios following four Representative Concentration Pathways (RCPs) according to the Fifth Assessment Report (AR5) of the Intergovernmental panel on Climate Change (IPCC), and created a unique grid-level dataset for both the historical land use and the future carbon-climate scenarios. However, the impact of future climate changes on land use and land cover changes was not explicitly accounted for. Therefore, the future change in crop area according to the H11 data is conceptually comparable to our LandPro_Crop-SE projection. The comparison shows that the increase in croplands projected by LandPro_Crop-SE is substantially

higher, especially in the agriculture-dominated eastern part of the region (Figure 3.10). Although noticeable differences exist also in the spatial patterns projected by the two data sets, both projections show consensus with larger increase in the southeastern part of the region. The challenges and uncertainty in quantifying land use are also reflected by the difference in the present-day crop areas between SPAM and H11. For the present-day land use distribution in 2005, the two data sets exhibit noticeable discrepancy over the region dominated by agriculture. This highlights the typical inconsistency between land use maps generated by different methodologies (You et al. 2014).

3.4 Summary

Without accounting for the farmers' adaptive potential to address the negative impact of future warming and changes in precipitation pattern on crop productivity (such as use of irrigation, fertilizer and other crop management techniques), the model projects a large increase in agricultural land use under the future climate scenario. The increase in cropland would occur at the expense of natural vegetation cover, both of which could further modify the regional climate. Multiple possible adaptive measures by the farmers to minimize the harvest area were also analyzed addressing the uncertainties involved in human decision-making process. Although prioritization among the crops in allocating the available land for their cultivation might have no or minimal impact in optimizing the land use, a specific order of selecting cultivation area based on future crop yield might potentially reduce the total loss of naturally vegetated land. The effect of farmers' adaptive actions characterized by their decision-making based on scientific information

suggests the significance of farmers' adaptive potential on future land use change dynamics in the region, and emphasizes the need for more effective adaptation strategies to slow down the regional agricultural land use expansion under future climate scenarios.

Although the LandPro algorithm is based on the equilibrium between supply and demand of food, it is not a strict equilibrium land use model that solves the supply-demand equations endogenously. The main implication of LandPro is to project scenarios of agricultural land use at a spatial scale under future climate accounting for changes in both climate and socio-economic variables. Majority of the existing land use models following different approaches with more sophisticated modeling schemes operate on national/sub-national scale. Moreover, most of them evaluate aggregated agricultural land use instead of crop area specific to individual crops. The relatively complex modeling framework of the existing land use models is one the reasons for such limitations. The simple modeling algorithm of LandPro suitably allows circumventing those difficulties in projecting multiple scenarios of pixel-wise future land use information needed by climate models while providing useful information on crop-specific land use.

We would like to point out that the spatial scale of 0.5 degree, which LandPro_Crop was run in this study, is too coarse to simulate the cropping pattern in each individual farm. It is extremely difficult, if not impossible, to capture the farmers' decision-making at individual farm level for a large region. While many existing land use models, applicable at much smaller scale, are capable of simulating the farm-level changes, they do not address the need of climate models for land use change information at the regional scale. This study attempts to address the climate model needs and simulate the land use-climate interaction at the regional scale, and to facilitate national-level policymaking in devising

strategic framework to address the potential impact of climate and socioeconomic factors on future agricultural land use. The focus therefore is not on developing a land use model capable of analyzing and projecting cropping pattern in each individual farm. Instead, we are interested in the long-term aggregated outcome, assuming that all farmers will eventually adapt to the climate-induced changes in crop yields by adjusting the agricultural land use practice. Therefore, the algorithm assumes similar science-informed decision-making by all the farmers under a particular pixel.

Table 3.1: Present-day (SPAM 2005) and the LandPro_Crop-projected future (mid-21st century) average crop area coverage in the West African countries.

Country	Present-day coverage (%)	Future coverage (%)	
		<i>MIROC-driven climate</i>	<i>CESM-driven climate</i>
Benin	19.2	56.5	60.1
Burkina Faso	20.4	43.0	37.1
Gambia	31.3	76.3	70.6
Ghana	19.1	41.4	52.0
Guinea	6.8	40.3	42.9
Guinea-Bissau	9.4	38.5	41.3
Ivory Coast	13.3	27.7	37.6
Mali	5.0	12.0	10.9
Niger	13.1	17.8	17.6
Nigeria	39.4	84.5	80.9
Senegal	14.6	45.8	42.3
Sierra Leone	8.7	36.0	39.4
Togo	31.6	51.5	60.9

Table 3.2: Future average crop area coverage in the West African countries under the MIROC-driven climate as projected by the LandPro_Crop algorithm following three different orders of yield values in selecting the cropping area to optimize agricultural land use. Initial scenario (best case in land use optimization): descending order of yield; alternative scenario 01 (worst case): ascending order; alternative scenario 02 (intermediate case): random order.

Country	Future coverage (%)		
	<i>Best case</i>	<i>Worst case</i>	<i>Intermediate case</i>
Benin	56.5	75.0	57.2
Burkina Faso	43.0	57.7	52.4
Gambia	76.3	91.5	84.3
Ghana	41.4	56.8	45.9
Guinea	40.3	70.4	47.3
Guinea-Bissau	38.5	80.0	39.4
Ivory Coast	27.7	50.1	29.2
Mali	12.0	22.0	16.4
Niger	17.8	17.8	17.8
Nigeria	84.5	90.4	89.2
Senegal	45.8	81.3	67.9
Sierra Leone	36.0	71.8	39.0
Togo	51.5	73.2	60.1

Table 3.3: Future average crop area coverage in the West African countries under the MIROC-driven climate as projected by the LandPro_Crop algorithm following four different rankings of crops prioritized by the farmers to optimize agricultural land use. Rank 1: descending order of country-level crop deficit; rank 2: ascending order of country-level crop deficit; rank 3: maize, sorghum, millet, cassava, peanut; rank 4: peanut, cassava, millet, sorghum, maize.

Country	Future Coverage (%)			
	<i>Rank 1</i>	<i>Rank 2</i>	<i>Rank 3</i>	<i>Rank 4</i>
Benin	56.5	61.2	59.7	58.4
Burkina Faso	43.0	42.5	41.8	43.1
Gambia	76.3	73.1	73.1	79.0
Ghana	41.4	41.8	41.7	42.3
Guinea	40.3	40.3	40.3	39.5
Guinea-Bissau	38.5	38.0	38.0	38.0
Ivory Coast	27.7	27.5	28.4	27.7
Mali	12.0	11.2	11.0	12.0
Niger	17.8	17.8	17.8	17.8
Nigeria	84.5	83.7	83.3	85.9
Senegal	45.8	51.7	49.8	46.6
Sierra Leone	36.0	36.3	36.3	36.0
Togo	51.5	50.9	52.7	53.2

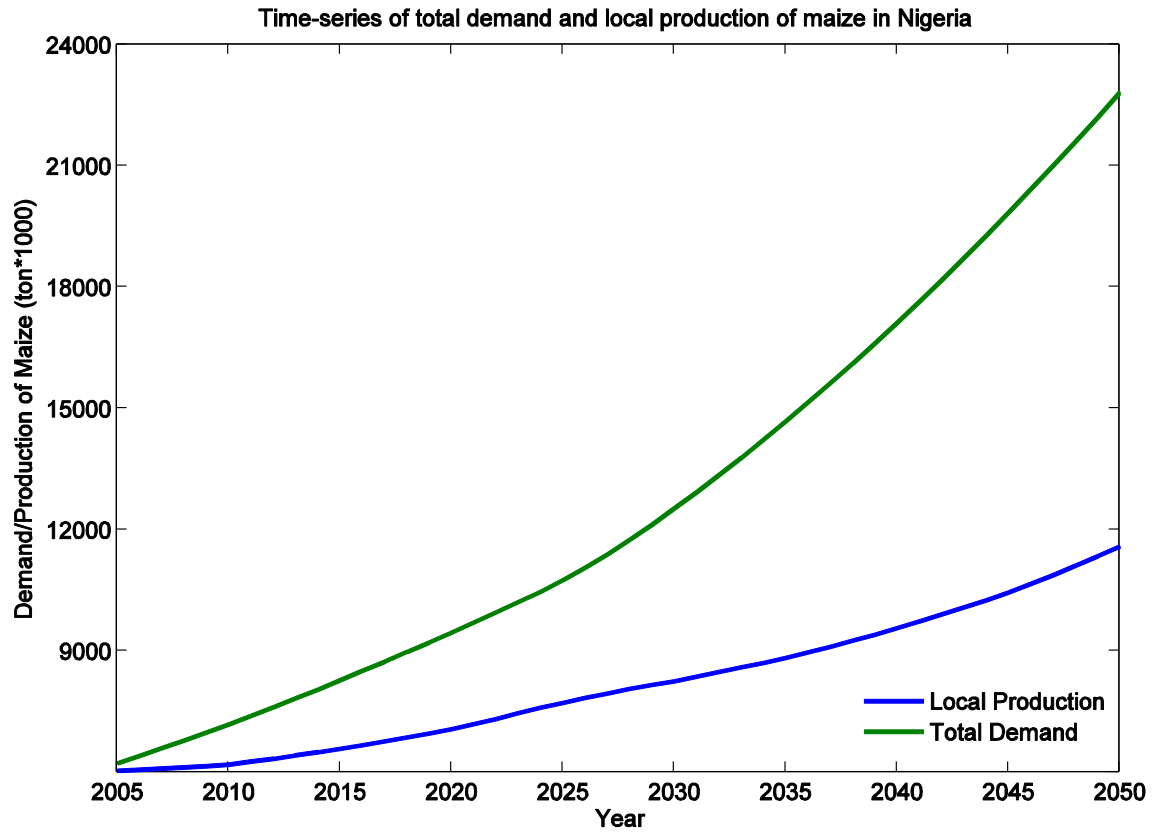


Figure 3.1: Time-series (2005-2050) of total demand and local production of maize in Nigeria according to future projection by the IMPACT model.

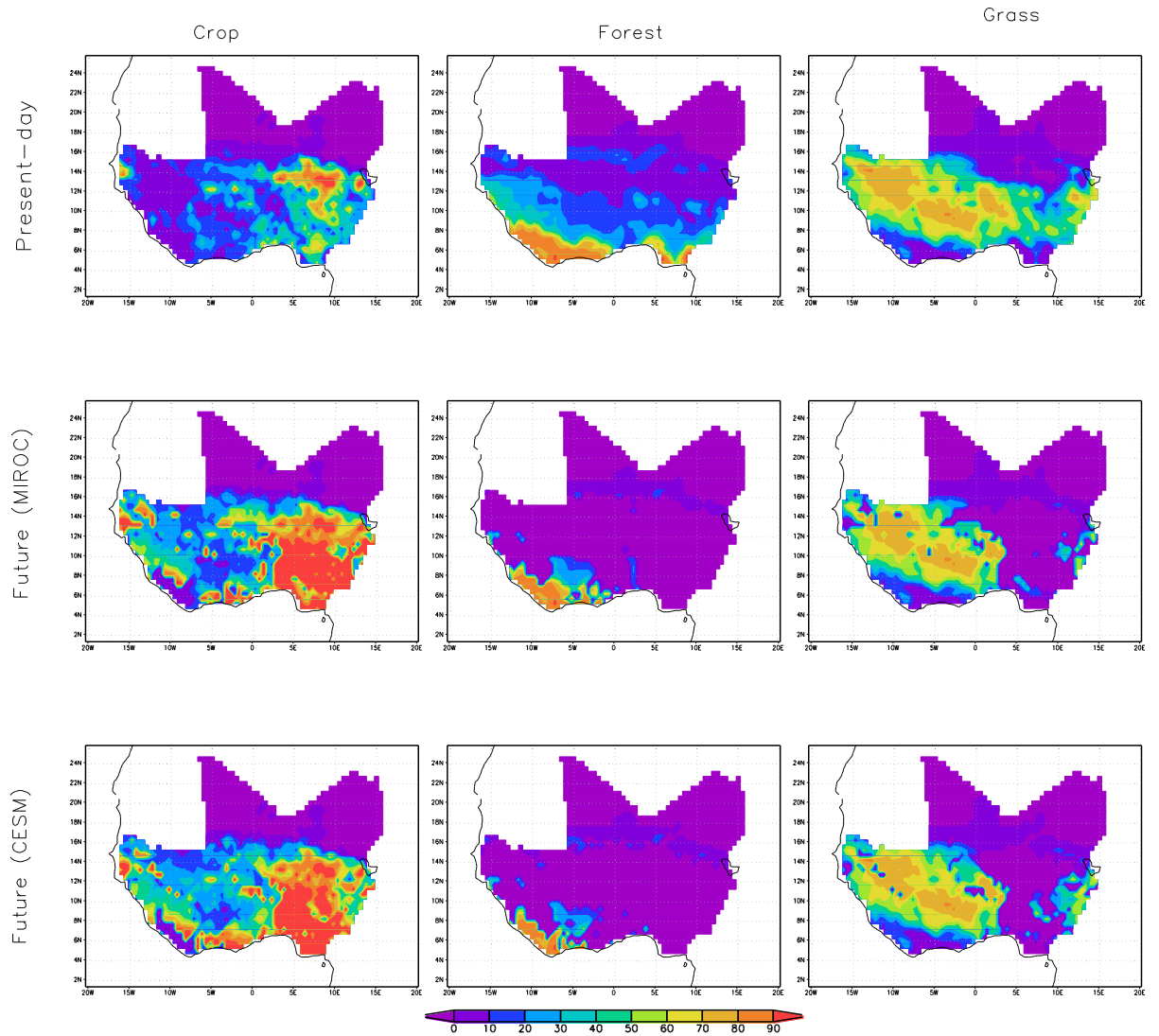


Figure 3.2: Spatial distribution of crop, forest and grass coverage (%) in 14 West African countries from present-day (year 2005) observation (top row) and future projection by the LandPro_Crop algorithm for mid-21-st century under two GCM climate - MIROC (middle row) and CESM (bottom row).

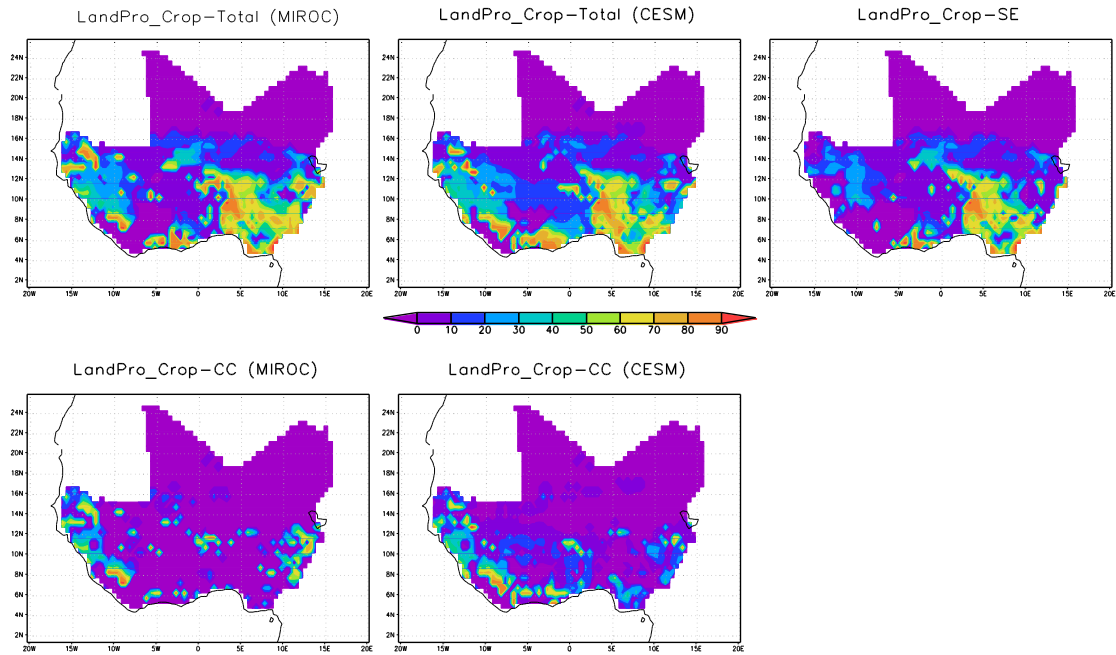


Figure 3.3: Spatial distribution of crop, forest and grass coverage (%) in 14 West African countries from present-day (year 2005) observation (top row) and future projection by the LandPro_Crop algorithm for mid-21-st century under two GCM climate - MIROC (middle row) and CESM (bottom row).

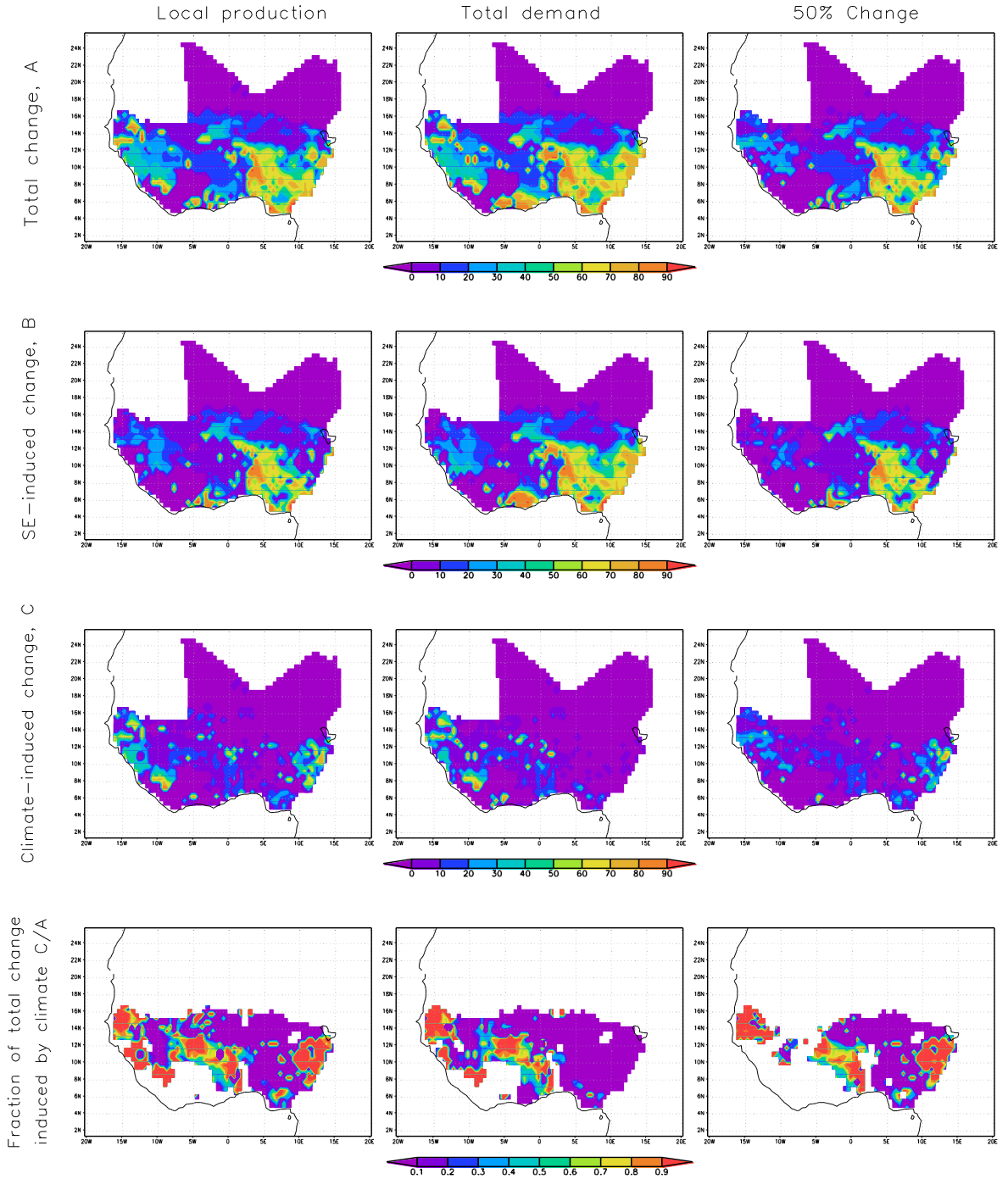


Figure 3.4: Sensitivity of land use change pattern to the demand values used as input to LandPro_Crop under the MIROC-driven climate. 1st row: absolute magnitude of total change for three future scenarios of demand; 2nd row: change due to socioeconomic

factors; 3rd row: change due to climatic factors; 4th row: fraction of climate-induced change to total change.

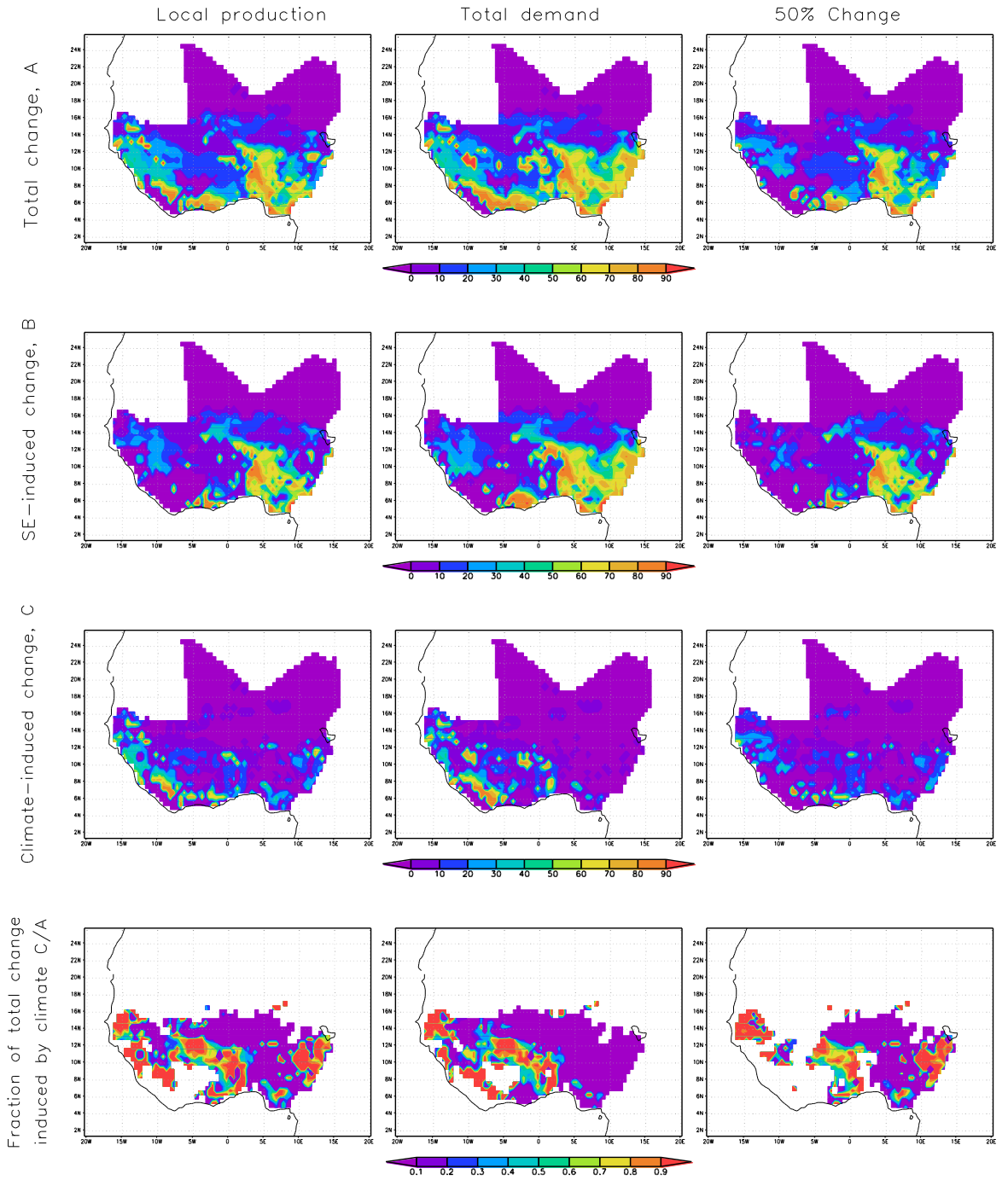


Figure 3.5: As in Figure 3.4, but for CESM-driven climate. (Note that the SE-induced changes in both Figure 3 and Figure 4 are same).

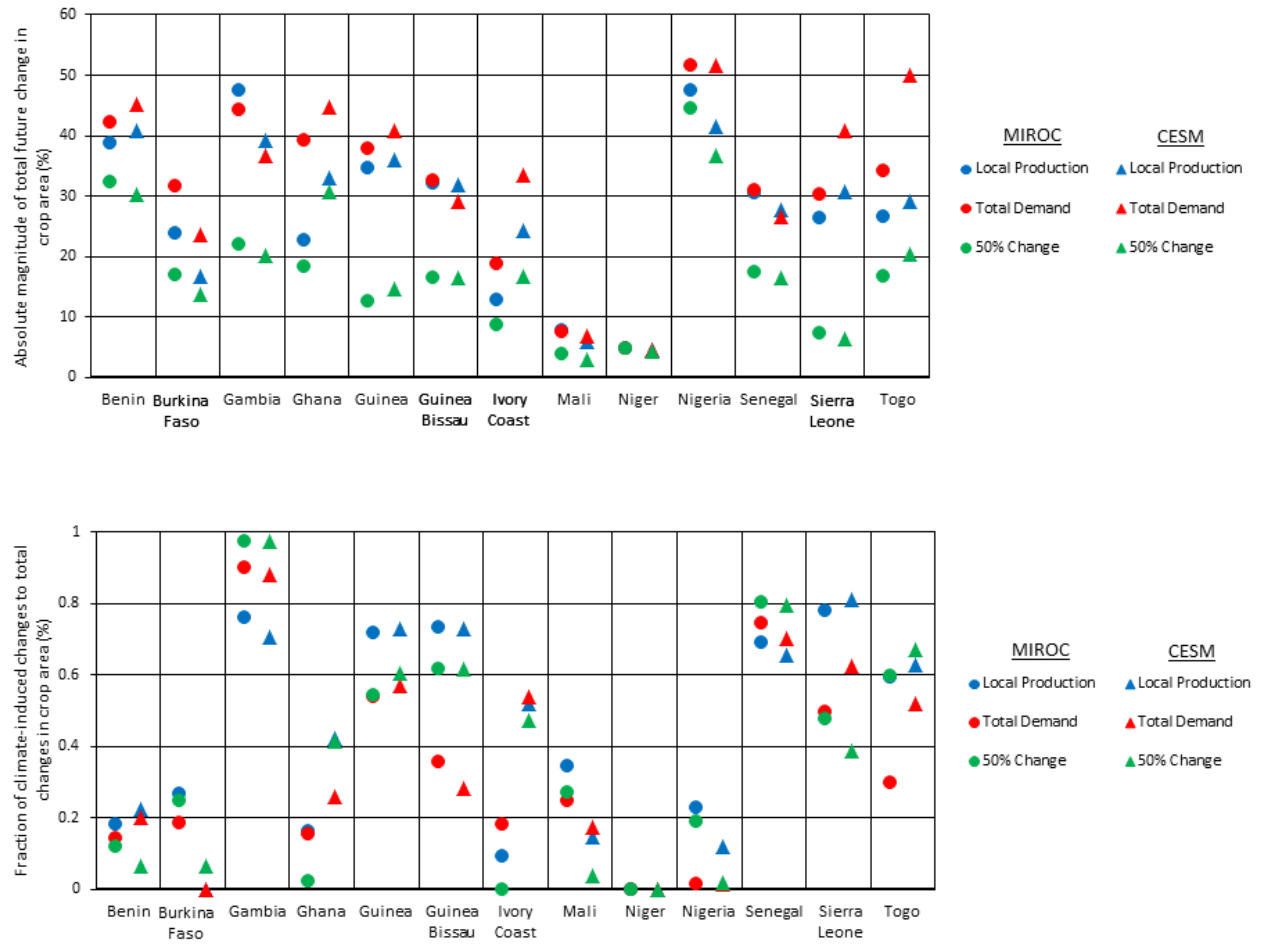


Figure 3.6: Country-average values of total change in crop area (top) and fraction of climate-induced changes to total change (bottom) according to three future scenarios of demand under the MIROC- and the CESM-driven climate.

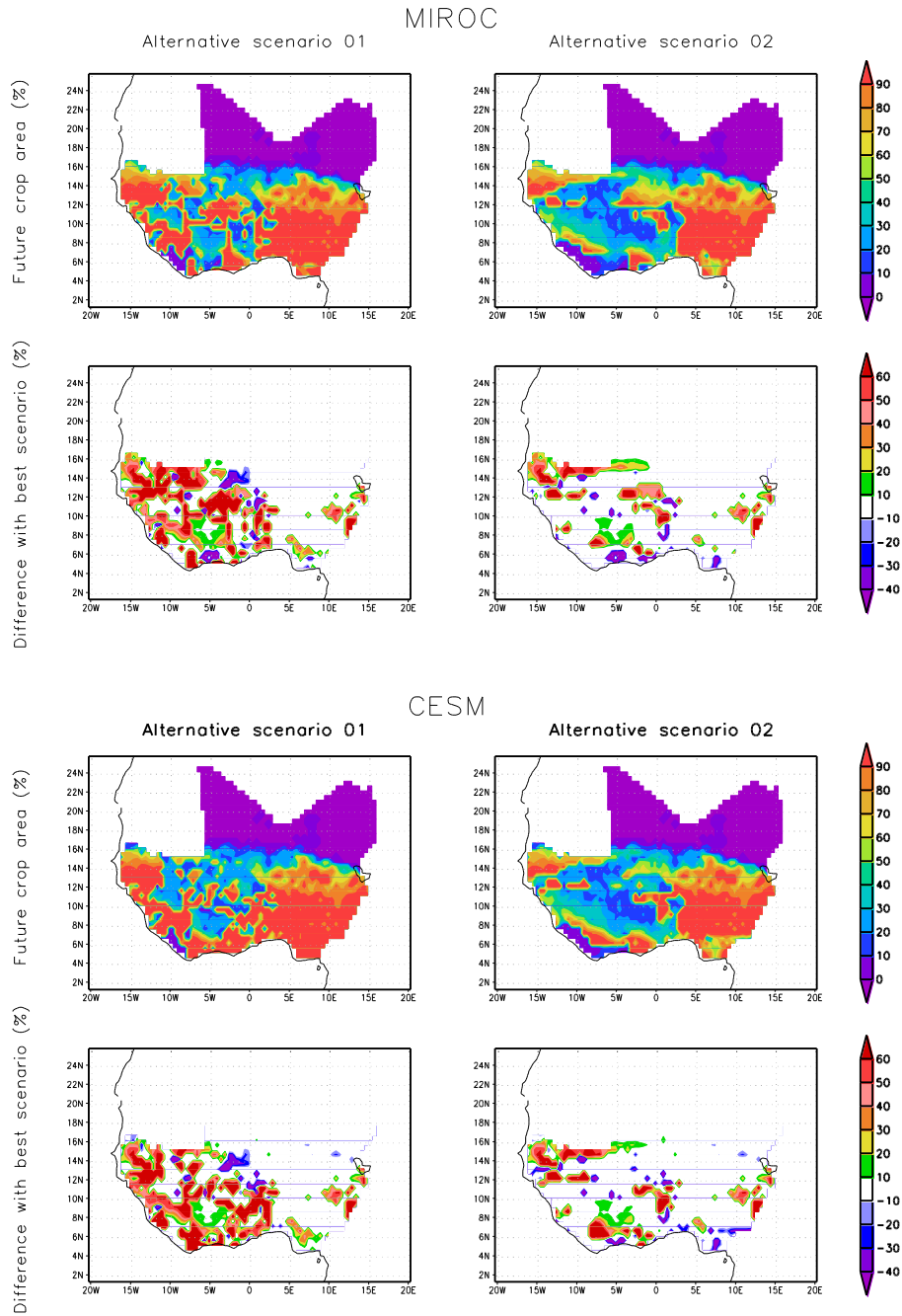


Figure 3.7: Spatial maps of future crop area percentage (1st and 3rd rows) in the West Africa (under the MIROC- and the CESM-driven climate) projected by the LandPro_Crop algorithm following two alternative scenarios with respect to selecting the

remaining grid cells for conversion to agricultural land based on the order of yield and their respective differences (2nd and 4th rows) with the initial run which follows descending order of yield (best scenario). Alternative scenario 01: ascending order of yield; alternative scenario 2: random order.

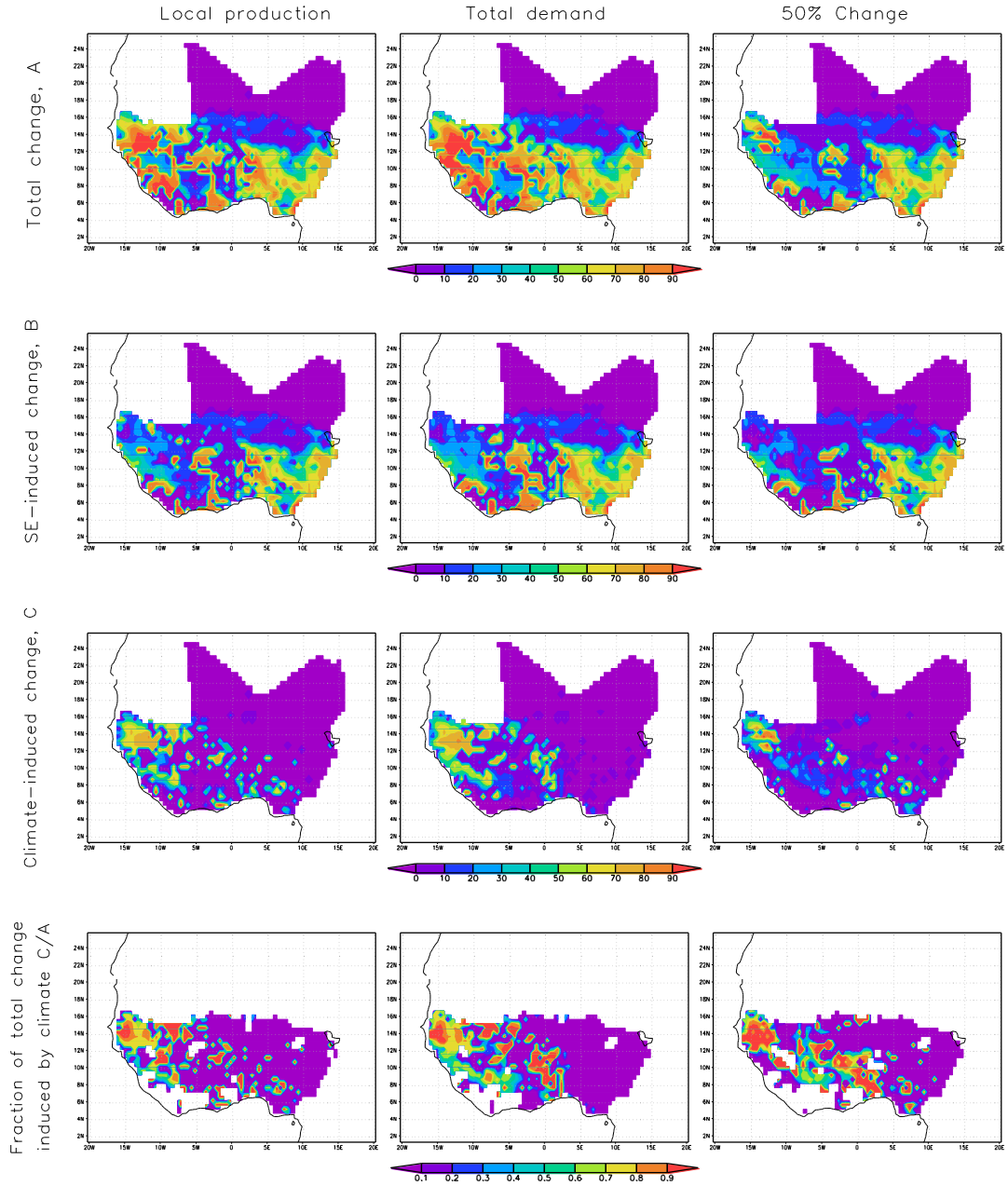


Figure 3.8: Sensitivity of land use change pattern to the demand values used as input to LandPro_Crop with the alternative cropping scenario following ascending order of yield under the MIROC-driven climate. 1st row: absolute magnitude of total change for three future scenarios of demand; 2nd row: change due to socioeconomic factors; 3rd row:

change due to climatic factors; 4th row: fraction of climate-induced change to total change.

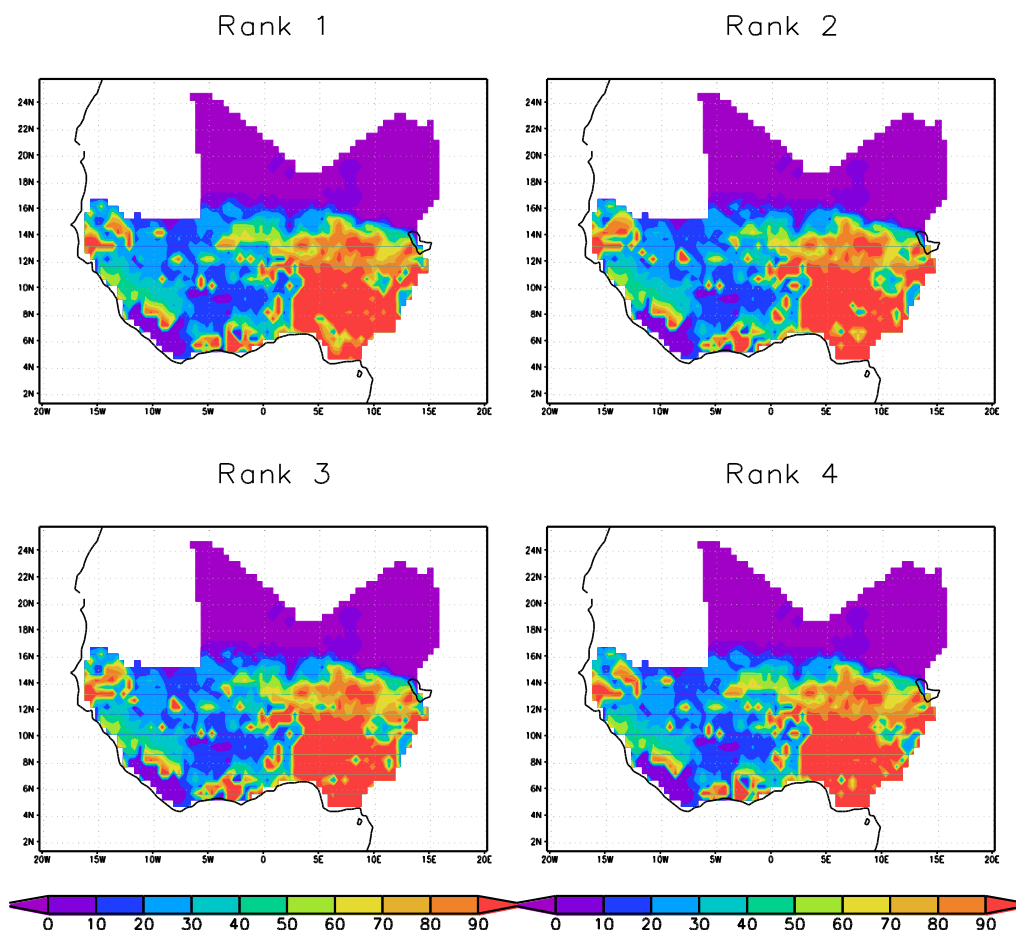


Figure 3.9: Spatial maps of future crop area coverage (%) in the West Africa under the MIROC-driven climate as projected by the LandPro_Crop algorithm following four different rankings of crops prioritized by the farmers to optimize agricultural land use. Rank 1: descending order of country-level crop deficit (initial run); rank 2: ascending order of country-level crop deficit; rank 3: maize, sorghum, millet, cassava, peanut; rank 4: peanut, cassava, millet, sorghum, maize.

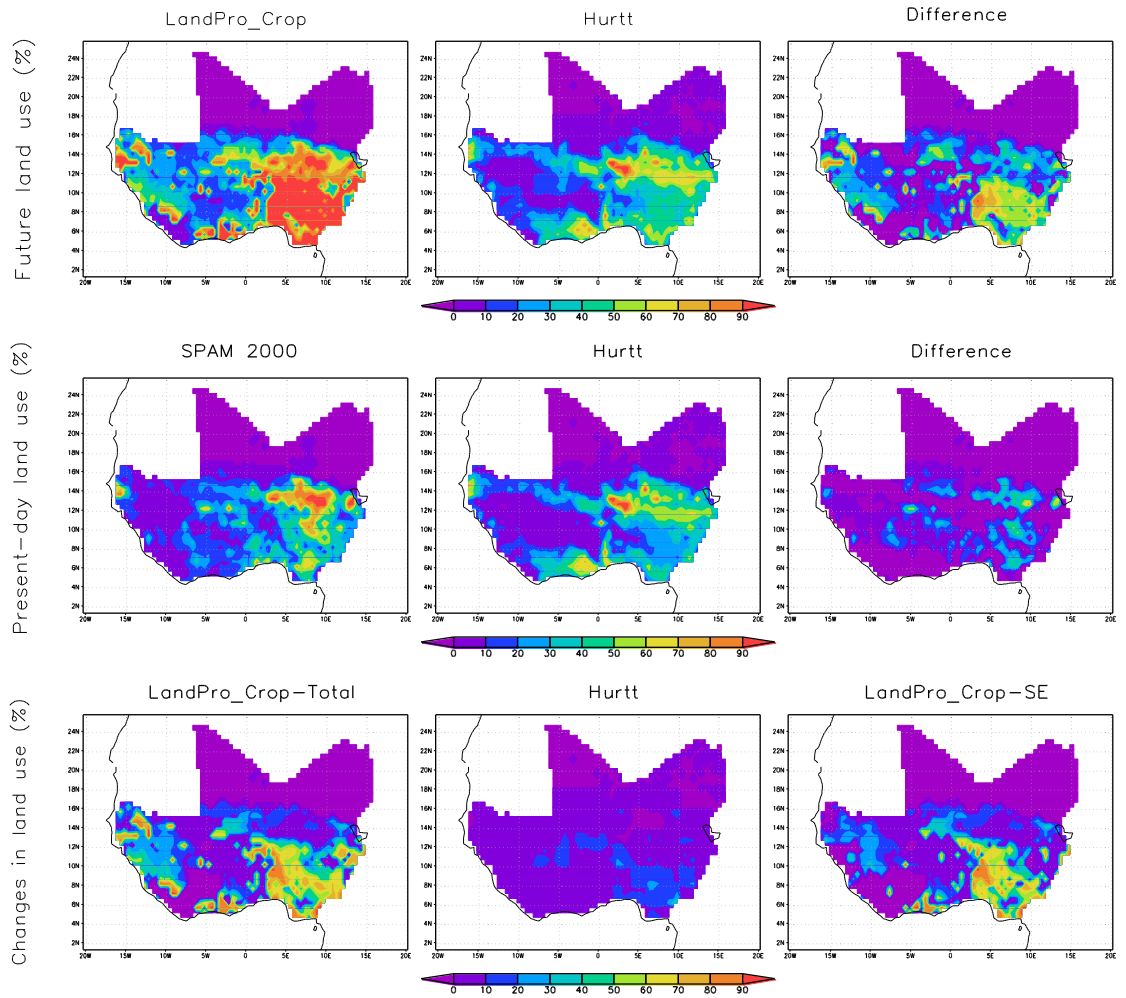


Figure 3.10: Future changes in crop area distribution according to the LandPro_Crop projections accounting for only socioeconomic changes (LandPro_Crop-SE) and Hurtt et al. (2011) data (top row). Comparison of the SPAM present-day (2005) crop area with respective Hurtt et al. (2011) data (bottom row).

Chapter 4

Feedback of land use changes to regional climate projection

4.1 Introduction

Land use and land cover changes can alter different components of land-atmosphere interactions, and thus impact local or regional climate. Anthropogenic modifications of Earth's surface cause changes in surface albedo and roughness length, heat flux partitioning, and other major variables of surface energy and water balance. Land use and land cover changes constitute an important driver for future climate changes (Feddema et al. 2005). Therefore, it is of great importance to evaluate the role of land use and land cover changes in altering the existing patterns of temperature, precipitation and climate variables in a region. However, it is challenging to understand and quantify the climate response to anthropogenic land use and land cover changes in the context of climate projections because of two primary reasons. First, because of the inherent variability in anthropogenic land use, projection of future land use patterns involves large uncertainties. Second, response of climate variables to a specific type of land use change can largely vary from one region to another because of opposing effects of two or more processes linking land use with climate. Therefore, critical assessments of land use-climate interactions should be integrated in a comprehensive future climate projection study.

Agricultural land use represents one of the main factors responsible for anthropogenic LULCC. Before the invention of modern technologies, crop area expansion, usually replacing forest or grasslands, was the most common response to the increase in demand

of food and other agricultural commodities. Although intensive farming adopted by farmers in last few decades has slowed down the rate of crop area expansion, fraction of agricultural land use has still been increasing (Burney 2010, Hurtt 2011). This is especially the case in regions with poor socioeconomic infrastructure, expansion of crop area at the expense of natural vegetation is a common practice. Therefore, with constantly increasing food demand across the globe, the trend of agricultural land use should be carefully considered in analyzing and projecting regional climate change. Despite the crucial link between climate and LULCC in a region, the mechanisms of anthropogenic land use, instead of being directly incorporated, are usually represented as an external forcing in climate models (Pielke 2011, Rounsevell 2014), and biogeophysical impacts the land use change dynamics are often ignored in future climate projection studies.

Agricultural yield, which is strongly influenced by climatic variables, represents a strong link between climate and anthropogenic land use. The climate-induced crop yield loss, in addition to rapidly increasing food demand in many regions, will be an important driver for future LULCC under future climate scenarios. Projection of future yield under changed climate scenario needs to be incorporated explicitly in modeling future land use and land cover changes. Since different crops could respond differently to the changing climate, spatial variability of crop yield also needs to be examined to better understand the land use dynamics. Therefore, comprehensive analysis of crop response to regional climate changes should be included in investigating future land use changes, and the resulting feedback to regional climate. However, to our knowledge, no previous studies projecting regional climate change in West Africa directly addressed the climate change impact on crop yield in evaluating land use-climate interaction in the region.

Land-atmosphere coupling has a major influence on the climate in West Africa (Koster et al. 2004). The West Africa climate is associated with significant inter-annual and inter-decadal variability, especially characterized by strong fluctuation in precipitation. Many studies investigating the Sahel drought, which was persistent for three decades in the second half of the last century, suggested that natural and anthropogenic land use and land cover changes played a critical role (Zeng et al. 1999, Wang and Eltahir 2000, Xue et al. 2010). Land surface characteristics dominate the regional climate in West Africa through albedo, Bowen ratio and surface roughness (Taylor et al. 2002, Hagos et al. 2014, Wang et al. 2015). Therefore, potential impacts of changes in land cover, both natural and anthropogenic, on the regional climate in West Africa have been a topic of extensive research. In this study, to assess the interaction between regional climate and agricultural land use, we designed a comprehensive modeling framework that incorporated a regional climate model (RCM), a process-based crop model, a socioeconomic model and a prototype cropland projection model. We employed the asynchronously coupled models to evaluate the implication of land use-climate coupling in projecting future climate in West Africa. We also investigated the trend of crop area expansion in the region considering climate-induced crop yield changes as one of the key drivers for agricultural land use change in addition to the increase in future food demand.

4.2 Models and Methodology

4.2.1 Modeling approach with asynchronous coupling

To study potential impact of climate change on land use and the resulting feedback to the regional climate in West Africa, we employed an asynchronous coupling between the cropland projection model LandPro_Crop (Ahmed et al. 2015) and the regional climate model RegCM4.3.4 (Giorgi et al. 2012) coupled with the Community Land Model version 4.5 (CLM4.5) (Oleson et al. 2010). Asynchronous coupling has been adopted by previous studies to investigate vegetation-climate feedback (Alo and Wang 2010, Cook and Vizy 2008, Diffenbaugh 2005). In this study, the asynchronously coupled modeling framework also include the crop model Decision Support System for Agrotechnology Transfer (DSSAT) (Jones et al. 2003) and the socioeconomic model International Model for Policy Analysis of Agricultural Commodities and Trade (IMPACT) model (Rosegrant et al. 2012), and an iterative time period of five years is used. In the experiment (FUTURE_TR_LUC) with asynchronous coupling starting from 2005, which represents the starting point of the Representative Concentration Pathways (RCPs) according to the Fifth Assessment Report (AR5) of the Intergovernmental panel on Climate Change (IPCC), LandPro_Crop projected the transient land use patterns at the end of each five-year period using the socioeconomic and crop yield data under the climate scenario simulated by the RCM. RegCM4.3.4-CLM4.5 (Wang et al. 2015) was used to dynamically downscale outputs from the National Center for Atmospheric Research (NCAR) Community Earth System Model (CESM). The CESM outputs were downscaled to 50 km, which is then resampled to a 0.5° grid, to derive the climate data required to drive. The RCM-simulated climate was first corrected for biases and then used to run

DSSAT to simulate the yearly crop yield for each of the years during a five-year period. Using the crop yield data (averaged over five years) from DSSAT, in addition to other inputs, LandPro_Crop projected the land use change at the end of the respective time period, and thus, the land use land cover map required to run the RCM were updated every five years. The updated land use map was then used to run the RCM for the next five-year time period followed by each step repeated. Bias correction of the dynamically downscaled climates follows the Statistical Downscaling and Bias Correction (SDBC) method (Ahmed et al. 2013) using the Sheffield et al. (2006) present-day climate data as reference in the bias-correction algorithm.

Two other future-climate experiments, one (FUTURE_NO_LUC) with the present-day land use map and the other (FUTURE_EQ_LUC) with the future land use map projected by LandPro_Crop in equilibrium mode (Ahmed et al. 2015), were also performed. In the FUTURE_NO_LUC experiment, RegCM4.3.4-CLM4.5 was driven with the present-day vegetation distribution to project future climate for 2040-2050 in West Africa. Comparisons between the FUTURE_NO_LUC outputs and present-day climate provide a measure of the impact of increasing greenhouse gas (GHG) concentration without accounting for land use changes and the resulting feedback to the regional climate. In the FUTURE_EQ_LUC experiment, the RCM-projected future climate from the FUTURE_NO_LUC experiment was used to drive the crop model DSSAT to project the future crop yield for 2040-2049. Using the DSSAT-projected crop yield as one of the inputs, LandPro_Crop was then used to project the future land use by middle of the century without employing the asynchronous coupling. Similar to the FUTURE_TR_LUC experiment, future climate scenarios from the FUTURE_EQ_LUC

experiment also highlight the significance of incorporating information on future LULCC in projecting future climate. However, in the latter, the transient trends in agricultural land use in the region were not captured. Comparison between these two experiments would indicate how and to what extent accounting for the transient processes of land use-climate coupling may influence the outcome of the projections. The Representative Concentration Pathway 8.5 (RCP8.5), which corresponds to a high level of greenhouse gas emission, was chosen for the future-climate experiments.

To evaluate future changes in climate variables, we compared the outputs from the future-climate experiments to the present-day control simulation. RegCM4.3.4–CLM4.5 (without the prognostic carbon-nitrogen dynamics of biogeochemistry (CN) model and the dynamic vegetation (DV) model) was driven for 1981-2000 for the control simulation following the methodology in Yu et al. (2015). Comparisons between the control climate and the University of Delaware observed datasets showed that the control simulation captures spatial patterns and seasonal variations of precipitation and near-surface temperature in general (Figure 4.1).

4.2.2 Description of the climate model

The International Center for Theoretical Physics (ICTP) RegCM4.3.4 coupled with CLM4.5 (Wang et al. 2015) is used in this study. RegCM4.3.4 is a primitive equation, limited area climate model based on hydrostatic balance in a terrain-following sigma vertical coordinate system and an Arakawa B-grid (Giorgi et al. 2012). Atmospheric dynamics component of the model is based on the National Center for Atmospheric Research/Pennsylvania State University's Mesoscale Meteorological Model version 5

(NCAR/PSU's MM5; Grell et al. 1994). The radiation scheme in the model is derived from the NCAR Community Climate Model version 3 (Kiehl et al. 1996). The planetary boundary layer scheme (Grenier and Bretherton 2001; Bretherton et al. 2004) followed by the model is relatively new. The MIT-Emanuel cumulus convection scheme (Emanuel and Živkovic-Rothman 1999) was used for this study with a resolved scale precipitation scheme (Pal et al. 2000).

4.3 Results

Results from the coupled modeling framework demonstrate the transient changes in agricultural land use in West Africa. The FUTURE_TR_LUC experiment projects large increases in crop area at the expense of natural vegetation in many parts of the region. The substantial crop area expansion is due to climate-induced loss in crop yield projected by the DSSAT runs and the IMPACT-projected increase in demand of food in the region (Figure 4.2). According to the present-day crop area distribution, agricultural land use is more dominant in the eastern part of the region. Extensive presence of grassland is noticeable in the central and the western parts of the region, whereas forest area largely dominates the coastal region in the South. According to the model projection, future changes in climate and socio-economic factors would lead to almost complete exhaustion of natural vegetation in the eastern part. More than 90% of land area is projected to be occupied by cropland in Nigeria, Benin and Togo. In the eastern part of the region, fraction of cropland in Gambia would also comprise 95.7% of total land. In comparison with results from the LandPro_Crop equilibrium mode (Ahmed et al. 2015), country-total

crop area expansion by middle of the century projected by the transient runs is substantially higher in most of the countries (Table 4.1). In Guinea and Sierra Leone, however, the projected increase in crop area is smaller in the transient mode, while in Niger and Ivory Coast, the projected increase is similar in both runs. Comparison between the spatial distributions of fraction of crop area according to the two different simulations indicates that the larger increase in agricultural land use projected by the transient run is more evident in the central part of the region. Differences in future projections by two different modes emphasizes the potential significance of running LandPro_Crop in transient mode by employing asynchronous coupling between the cropland projection model and the regional climate model in evaluating the climate-land use feedback in the region.

We also looked into the individual time-series of changes in fraction of crop area in each of the West African countries. The trend of crop area expansion in different countries follows different patterns (Figure 4.3). Moreover, the rate of increase in crop area from one five-year period to another in a particular country can largely vary over the entire simulation period (2005-2050). A sharp increase in the rate of crop area expansion during a particular five-year window is common for many of the countries, which eventually leads to the overall larger increase in the country-average crop area by the middle of the century as projected by LandPro_Crop in the transient approach. The spikes in the rate of crop area expansion cannot be fully explained by the trend of the IMPACT-projected food demands which usually follow a smooth increasing trend for most of the crops in the West African countries (Figure 4.4). Although socioeconomic factors (characterized by changes in food demand) are projected to dominate future changes in agricultural land

use for the most part of West Africa (Ahmed et al. 2015b), they cannot account for the temporal dynamics of the future changes in agricultural land use. However, productivity of the major crops, which is the pathway for climatic factors to affect the agricultural land use, often influences the trend of crop area expansion. The DSSAT-projected annual country-average crop yields show a larger inter-annual variability caused by climate inter-annual variability (Ahmed et al. 2015a). The climate-induced variability in crop yield can also lead to a substantial decrease in average yield over a five-year period, which would result in a sharp increase in the rate of crop area expansion during the time period. For example, the LandPro_Crop-projected country-average crop fraction in Ghana increases by 13.7% between 2030 and 2035. This increase is noticeably higher than the percentages of crop area expansion during the previous five-year periods from 2005 to 2030. Similar increase (13.5%) in crop fraction would also occur from 2040 to 2045. Time-series of the IMPACT-projected food demand in Ghana tend to follow a smooth rate of increase for all the crops throughout the whole study period (2005-2050) (Figure 4.4). However, in the case of yield, although the overall country-average value is projected to decrease for all five crops in Ghana, the trends do not follow a consistent pattern. For example, the country-average maize yield in 2035 is less than in 2030 Ghana by almost 8.9%, which could lead to a higher deficit during that period resulting in the higher rate of crop area expansion. Similarly, the country-average cassava yield in Ghana is projected to decrease by 16.6% from 2040 to 2045, which coincides with the larger crop area expansion during the five-year period.

To evaluate the effect of land use feedback on future climate in West Africa, we compared results from the three future-climate experiments to the control climate. The

difference between the FUTURE_NO_LUC and the control climate indicates future changes in climate variables because of increasing concentration in atmospheric greenhouse gases without considering potential LULCC in the region. In comparison with the control experiment, the FUTURE_EQ_LUC experiment provides a measure of land use feedback to future climate, while the FUTURE_TR_LUC experiment serves the same purpose while accounting for transient trends in the dynamics of land use changes and regional climate changes.

Without future changes in land use, the model generally projects a drier summer precipitation over West Africa (Figure 4.5, top row). Average summer precipitation in all countries in the region would decrease by more than 1 mm/day in many parts. The simulation, however, produces increased precipitation mainly in the northern part of Nigeria and the southern part of Niger. Incorporating the land use feedback with both equilibrium and transient approaches enhances the dry signal in the central and western part of the region. Although the projected increase in precipitation in Nigeria becomes more noticeable in both experiments, they largely differ in projecting the future changes in precipitation in Niger. The transient experiment simulates substantially larger increase in precipitation which extends approximately to 22°N. On the contrary, the equilibrium run projects large increase in precipitation in Burkina Faso contrasting the transient run which project no noticeable changes. Overall, the land use feedback mostly enhances the dry signal while producing strong wet signals over some parts of the region in projecting future summer precipitation.

The projected future change in precipitation is mostly dominated by changes in evapotranspiration (ET) among all three experiments. ET is generally projected to

decrease across the region (Figure 4.5, middle row). The decrease in ET is accompanied by less moisture transport to the atmosphere, leads to the decrease in summer average precipitation. The larger decrease in ET near the western Sahel, which can be attributed to the replacement of forest as result of crop area expansion, contributes to the stronger dry signal. All three future experiments project ET to increase in the north-east part of West Africa which is accompanied by an increase in summer precipitation. The larger ET in future climate can be explained by the cropland expansion replacing bare ground as projected by the cropland projection model. The increase is greater in both magnitude and spatial extent with the land use feedback. The FUTURE_TR_LUC run, in particular, projects average ET during the summer to increase by 0.25 mm/day across northern Nigeria and southern Niger, which coincides with the strongest wet signal. Although the increased ET in the south-west part of West Africa does not lead to a considerable increase in precipitation, it tends to weaken the projected dry signal which would occur in the surrounding region.

The model-projected increase in average summer temperature is generally similar in magnitudes and spatial patterns among all future climate experiments (Figure 4.5, bottom row). Land use feedback does not particularly influence the projection of future warming across the region. Apart from coastal regions, the warming signal follows a more or less similar spatial pattern which indicates a stronger warming in the north than in the south. The conversion of forest into cropland, which generally enhances the reduction of ET across the region, does not necessarily lead to a larger degree of warming. This might be due to the dampening effect of summer monsoon precipitation which tends to offset the additional warming which could be caused by the land use changes (Sylla et al. 2015).

However, there are a few exceptions where changes in ET tend to control future warming across the region. For example, with the land use feedback, especially in the FUTURE_TR_LUC experiment, the warming signal tends to weaken in some parts of the region, which can be attributed to the larger increase in ET leading to an enhanced evaporative cooling and a wetter condition. Also the larger decrease in ET also induces a warmer signal in the western Sahel (near the southwest part of Mali) as compared to other areas across the same latitudes.

The future changes in temperature, precipitation and ET are accompanied by changes in other state and flux variables at land surface. Changes would occur in both incident and absorbed solar radiation at surface, which can be noticeably influenced by land use feedback (Figures 4.6). Without land use feedback, incident solar radiation would generally increase under future climate resulting in more absorbed radiation. This increase can be attributed to the decrease in cloudiness in the drier condition. However, with land use feedback, signal of the change could be reversed in the western part of the region, mainly in Nigeria. The projected decrease in incident solar radiation is particularly noticeable in the FUTURE_TR_LUC experiment, which projects the largest increase in precipitation, is caused by the increased cloudiness. Although the FUTURE_EQ_LUC experiment projects a decrease in incident solar radiation only in southern Nigeria, the absorbed radiation would substantially decrease over the areas where the incident radiation is projected to increase. This opposite signal of changes in incident and absorbed radiation is due to the changes in surface albedo because of agricultural land use changes in the region (Figure 4.7, top row). In the central part of Nigeria, the albedo would substantially increase because of conversion of natural

vegetation into crop area. The higher albedo leads to the reduction in absorbed energy at the surface despite the increase in incident radiation. The increased albedo is responsible for the decreased precipitation in the southern part of Nigeria. The reduction in absorbed solar radiation because of the higher albedo leads to a decrease in available heat fluxes at the surface. Consequently, transfer of sensible and latent heat from the surface into atmosphere reduces, which causes a decrease in the formation of convective clouds and precipitation. The large degree crop area expansion naturally would decrease the LAI with a few exceptions (Figure 4.7, bottom row). The most noticeable increase in LAI in the northern part of Nigeria, which can be attributed to the conversion of bare ground to the cropland, explains the signal of changes in ET and precipitation in the region. The FUTURE_EQ_LUC and the FUTURE_TR_LUC experiments do not considerably differ in projecting both magnitudes and spatial patterns of changes in albedo and LAI, although the degree of changes in a few cases tends to be larger in the transient approaches.

4.4 Summary

The LandPro_Crop model was driven in transient mode employing an asynchronous coupling with the regional climate model RegCM4.3.4-CLM4.5 to investigate potential impacts of climate change on land use and the resulting feedback to the regional climate in West Africa. The model, without accounting for future advancements in agricultural technologies, projects substantial crop area expansion because of climate-induced losses in crop yield associated with increases in food demand. Results from the transient runs

were compared against future land use changes projected by the model driven in equilibrium mode as described in Ahmed et al. (2015). The future land use scenarios from the different runs considerably differ. In simulating agricultural land use, the transient run projects larger crop area expansion for most of the West African countries than the equilibrium run. Spatiotemporal patterns of agricultural land use, depending on the future trends of crop yield and food demand, would largely vary from one country to another. An assessment of trends in country-average crop area expansion indicates that the temporal dynamics of climate-induced yield loss dominates the projected the land use change dynamics.

To understand the feedback from the future land use changes to the regional climate, projections from three different future climate experiments were compared. The future climate experiments based on different land cover distributions were designed to capture the implication of incorporating information on future land use changes in regional climate projections. The comparison indicates that the land use feedback could change the signal of the projected future changes of some climate variables in West Africa. While summer precipitation is mainly projected to decrease across the region in response to increasing atmospheric GHG concentrations, future crop area expansion could result in a wetter condition especially in the western part. The wet signal, which tends to be stronger when the transient processes are accounted for, is primarily caused by the projected increase in ET because of agricultural land use changes. At the same time, the dry signal in the western part of the region would be amplified through the land use change feedback because of the decrease in ET resulting from deforestation. The warming signal resulting from climatic changes, however, is weakened by the feedback

of the projected land use because of the increased evaporative cooling in some parts of the region. The difference in magnitudes and direction of future changes in various climate variables, which resulted from the differences in approaches to include future land use information in projecting future climate in West Africa, indicate a strong land use-climate interaction in the region. The difference between the FUTURE_TR_LUC and the FUTURE_EQ_LUC projections is generally smaller than the difference between the FUTURE_EQ_LUC and the FUTURE_NO_LUC projections, which implies that the equilibrium approach captures the first order impact and the transient approach accounts for additional changes. A comprehensive analysis of land use–climate feedback, which can be devised by incorporating more robust projections of climate change impact on crop yield and agricultural land use in the integrated modeling framework, should be integrated in regional climate projection.

Table 4.1: Present-day (SPAM 2005) and the LandPro_Crop-projected future (mid-21st century) average crop area coverage in the West African countries.

Country	Present-day crop area (%)	Future crop area projected by FUTURE_EQ_L UC (%)	Future crop area projected by FUTURE_TR_LUC(%)	Differen ce (%)
Benin	19.17	60.08	96.25	36.17
Burkina Faso	20.38	37.05	80.46	43.41
Gambia	31.34	70.57	95.72	25.15
Ghana	19.12	52.03	82.14	30.11
Guinea	6.83	42.92	36.49	-6.43
Guinea-Bissau	9.42	41.25	68.32	27.07
Ivory Coast	13.27	37.62	37.83	0.21
Mali	4.97	10.88	15.40	4.52
Niger	13.07	17.63	17.78	0.15
Nigeria	39.44	80.87	92.88	12.01
Senegal	14.58	42.28	81.33	39.05
Sierra Leone	8.7	39.35	25.64	-13.71
Togo	31.62	60.85	99.69	38.84

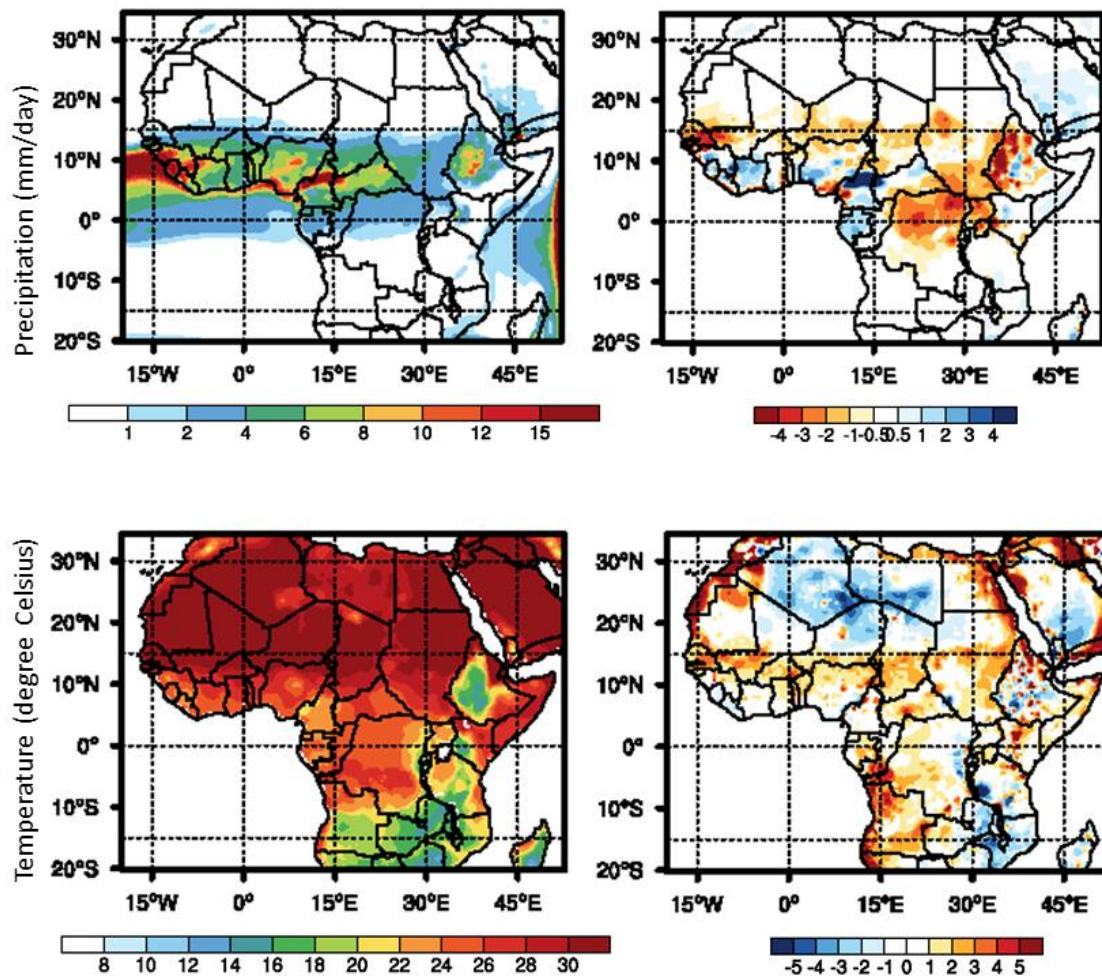


Figure 4.1: Present-day (mean over 1981-2000) average summer (JJA) precipitation and temperature (left column) simulated by the CESM-driven RegCM4.3.4-CLM4.5 and its comparison (right column) with the University of Delaware observed datasets.

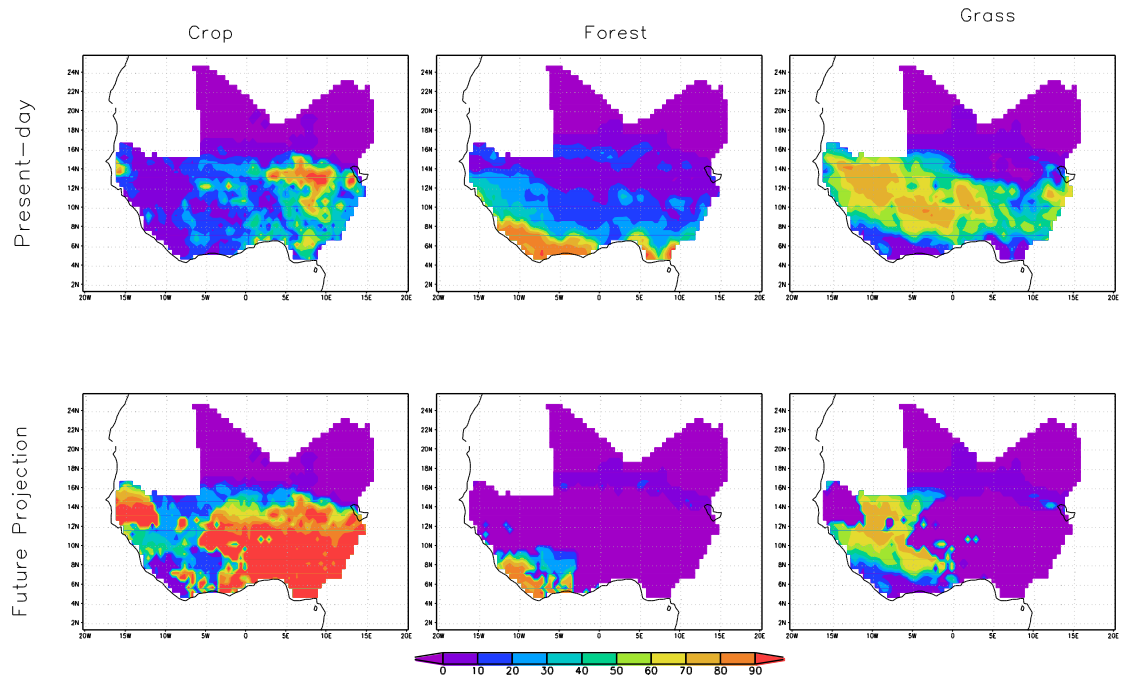


Figure 4.2: Spatial distribution of crop, forest and grass coverage (%) in 14 West African countries from present-day (year 2005) observation (top row) and future projection by the LandPro_Crop algorithm driven in the transient mode for mid-21-st century under two GCM climate - MIROC (middle row) and CESM (bottom row).

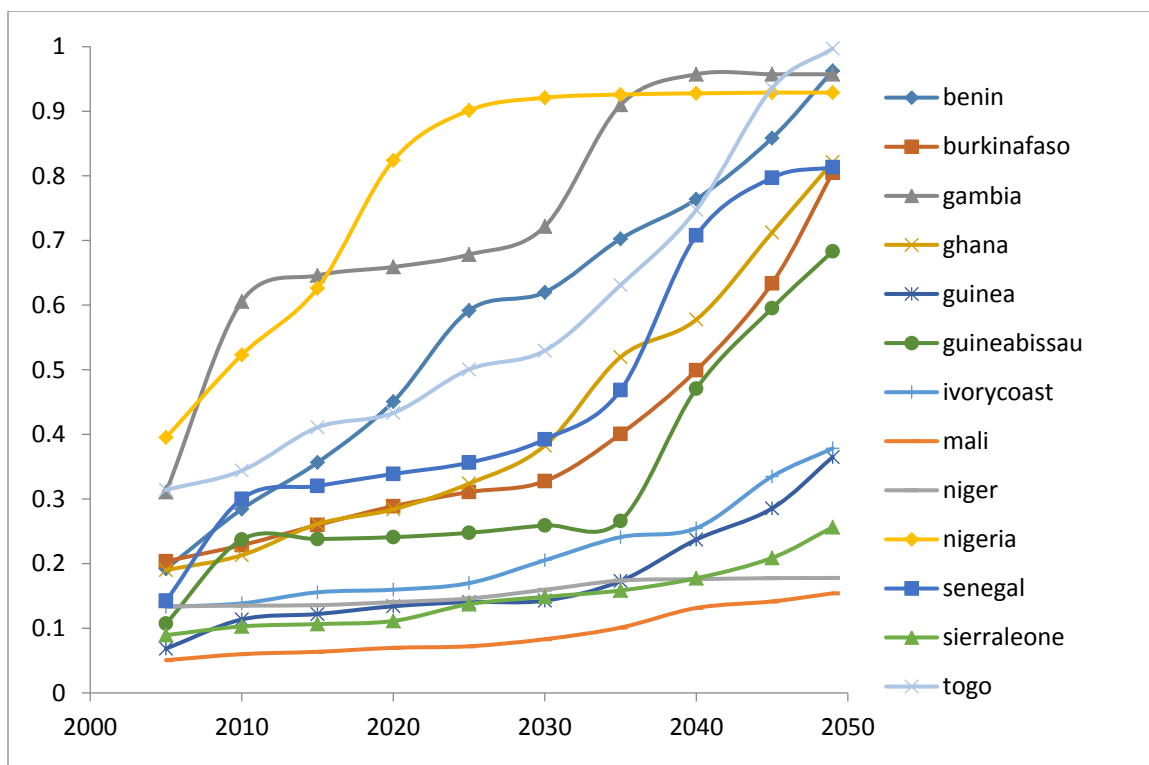


Figure 4.3: Time-series (2005-2050) of changes in fraction of crop area in each of the West African countries.

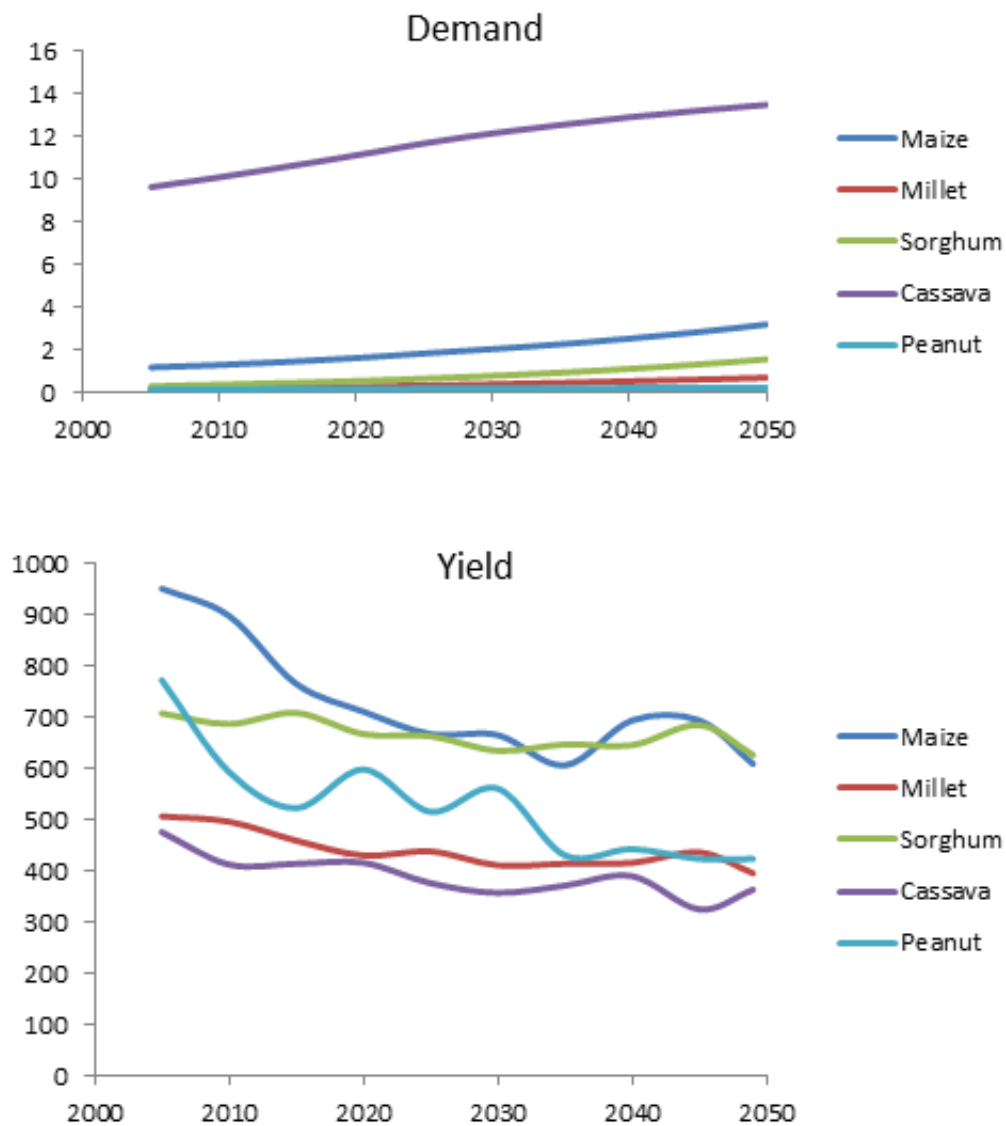


Figure 4.4: Time-series (2005-2050) of the IMPACT-projected food demand and the DSSAT-Projected yield for five major crops in Ghana

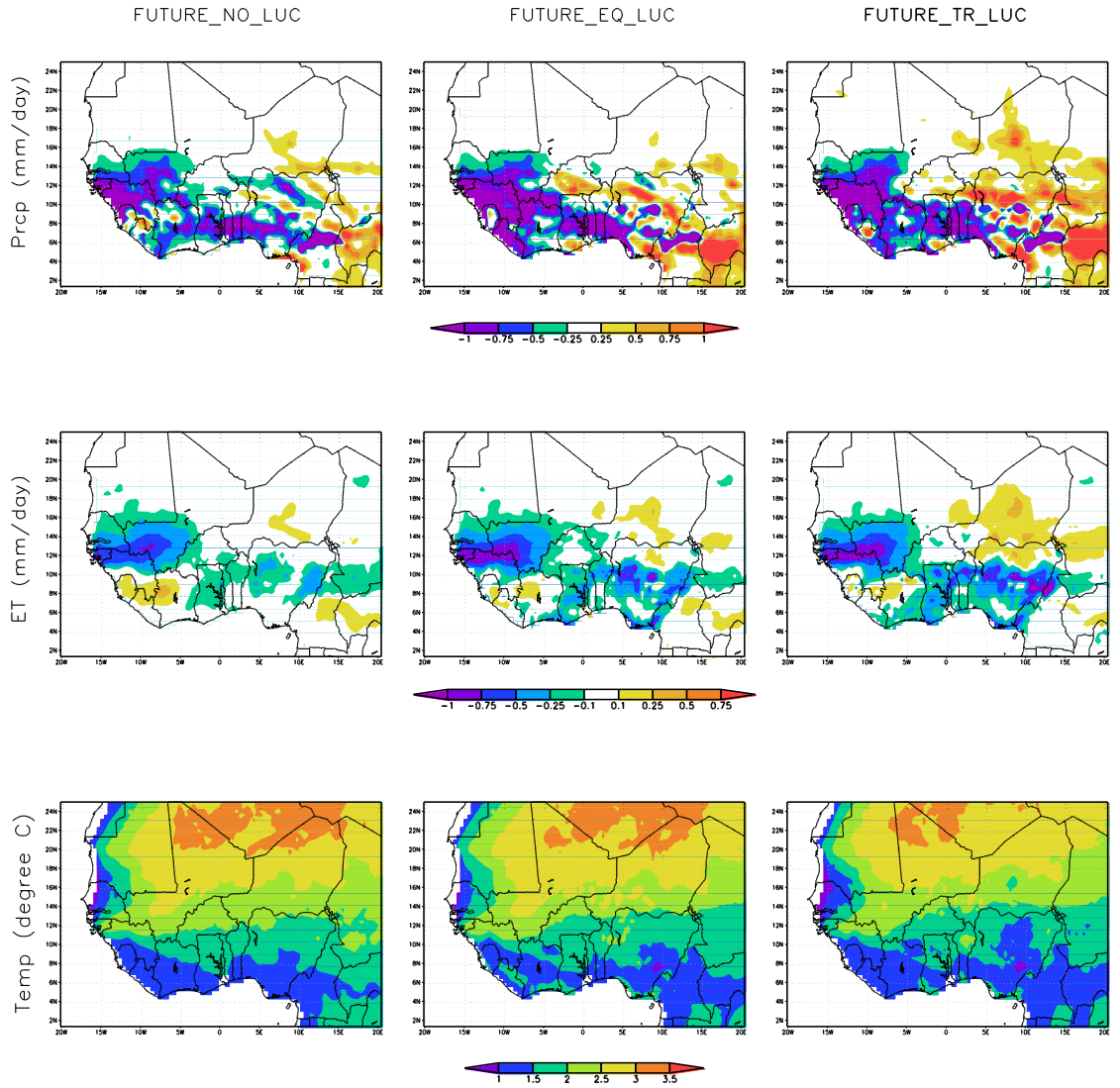


Figure 4.5: Future changes in average summer (JJA) precipitation (mm/day), ET and temperature projected by future-climate runs using three different land use scenarios in West Africa.

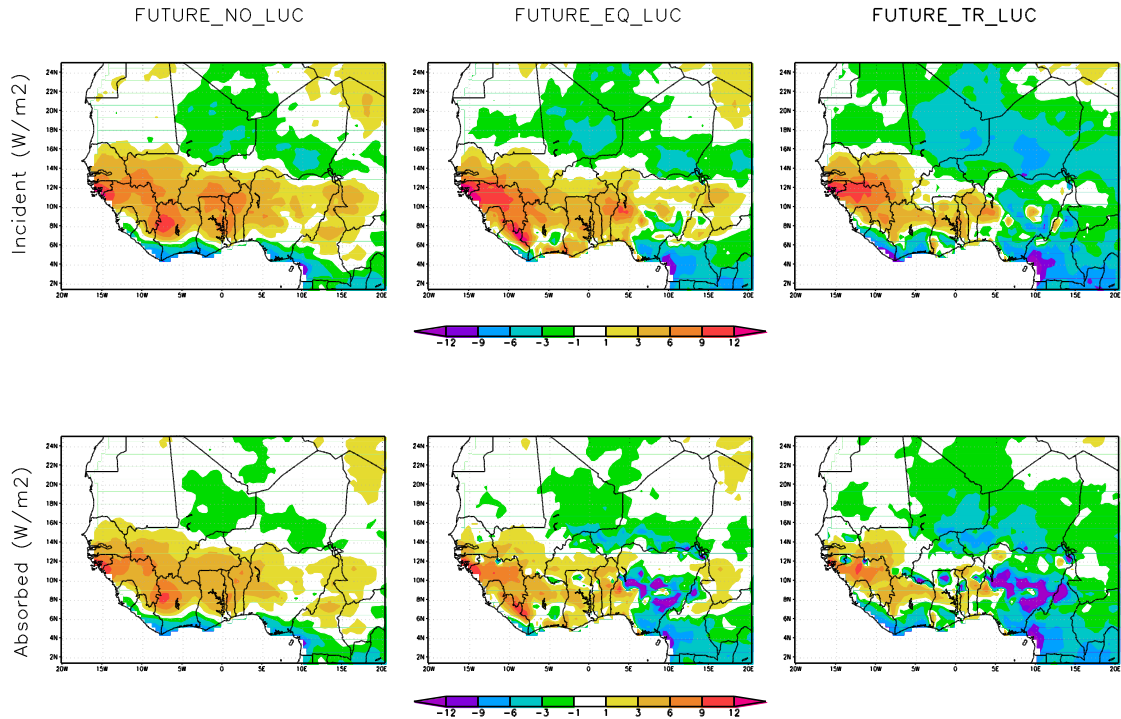


Figure 4.6: Future changes in average summer (JJA) daily incident and absorbed solar radiation (W/m^2) projected by future-climate runs using three different land use scenarios in West Africa.

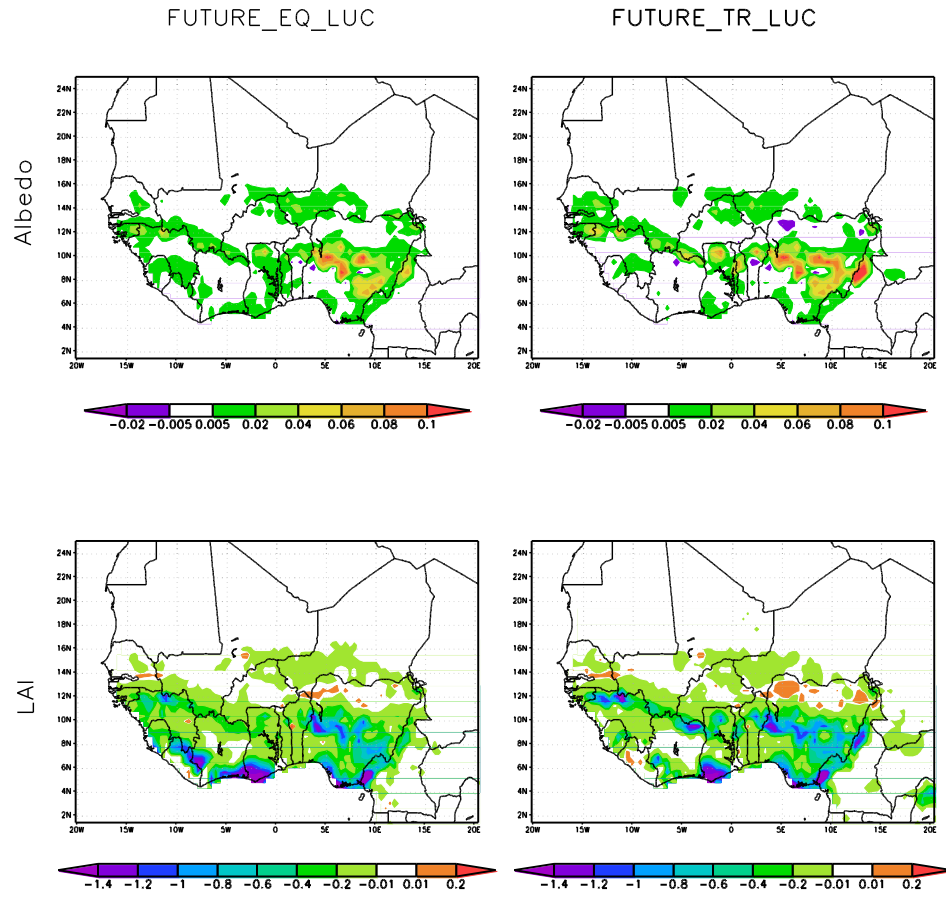


Figure 4.7: Future changes in LAI and surface albedo averaged over summer (JJA) projected by future-climate runs using two different land use change scenarios in West Africa.

Chapter 5

Summary and Conclusion

5.1 Summary of the Study and Concluding Remarks

This research focuses on understanding land-atmosphere interaction in the context of human-induced land use and land cover changes in West Africa. While agricultural land use can influence regional climate, changes in climatic variables can impact crop productivity significantly and play an important role in local and regional agricultural practices. Assessments of climate change impact on crop yield and agricultural land use, and the resulting feedback form the core of this study.

The process-based crop model DSSAT was calibrated by adjusting the grid-level fertilizer data and planting time to reproduce the observed country-average yield of major cereal crops in 13 countries of West Africa. The calibration increased the inter-country variance of crop yield accounted for by the model. The calibrated model was used to evaluate the sensitivity of crops to growing season temperature and precipitation in the region. Both temperature and precipitation variability can significantly influence the productivity in the region. While yield tends to decrease with increase in temperature, a positive correlation exists between present-day yield and growing season precipitation. However, correlation between present-day yield and climate variables follows different spatial patterns for different crops. In addition to the decrease in mean yield, larger climate variability in future decades would increase the year-to-year variations of future crop yield. The lower mean yield and larger inter-annual variability together would make the regional food security extremely volatile. This study effectively employs the process-

based crop model DSSAT to provide grid-level projections of climate-induced changes in crop yield over a large region, and thus provides a framework for assessing the future trend in crop yields in a changing climate to facilitate policymaking and strategic management.

In the second part of this study, a land use and land cover change algorithm (LandPro_Crop) was developed to study the future expansion of agricultural land and the resulting loss of naturally vegetated land. The model was applied to West Africa as a case study. LandPro_Crop integrates the impact of climate change on crop yield and future socioeconomic scenarios to construct a spatially gridded land cover map at a spatial scale of 0.5° . The model projections indicate spatial heterogeneity of land use change dynamics which can be dominated by different controlling factors in different parts of West Africa. Climate change impact on crop yield would considerably vary across the region resulting in large variability in the spatial pattern of future yield loss. While the agricultural land use could be dominated by the projected yield loss in some parts of the region, the projected increase in food demand would be of greater importance in the land use change dynamics in other regions. However, future projections from LandPro_Crop imply that farmers' decision-making can alter the relative importance of different factors in driving future land use changes.

The LandPro_Crop algorithm provides a preliminary framework for the projection and analysis of future agricultural land use. LandPro_Crop offers two clear advantages. It provides spatially distributed land use information needed by climate models as the lower boundary condition; also it can be conveniently used for future land use information at

the individual crop level that is needed for national and regional land use and food security policy analysis.

Following the development of LandPro_Crop, an asynchronous coupling has been employed between the cropland projection model and the regional climate model RegCM4.3.4-CLM4.5. The asynchronously coupled models were employed in equilibrium and transient modes to assess the land use-climate feedback West Africa. In the equilibrium mode, we employed the cropland projection model to evaluate the changes in agricultural land use between two time slices, which are several decades apart, without considering the transient processes in land use dynamics. In the transient application, which necessitates performing the crop modeling and the regional climate modeling in a transient mode as well, the land use-climate interaction were modeled for the period of 2005-2050 using multiple five-year simulation periods. Results based on the climate model outputs from these two experiments were compared with a future projection that does not consider anthropogenic land use and land cover changes. Comparisons among the projections indicate that anthropogenic land use characterized by future crop area expansion replacing natural vegetation could have considerable impacts on future climate scenarios. The signals and the magnitudes of these impacts could vary across the region mainly depending on the form of land use changes. The projected decrease in summer precipitation because of the elevated GHG concentration could be amplified because of crop area expansion in the west part of the region, although it could induce a wetter condition in the eastern part. The effect of land use changes is less dominant on the summer temperature which is projected to follow more or less similar

patterns of future changes in all three experiments. Changes in both temperature and precipitation would be controlled by changes in ET and albedo across the region.

As a whole, this study offers insight into potential vulnerabilities of the agricultural system in specific countries or West Africa as a whole because of regional climate change. It integrates climate and socioeconomic changes to construct a spatially gridded land cover map while facilitating policymaking and strategic management. The integrated modeling framework developed here provides a basis for future research efforts for comprehensive assessments and robust projections of regional climate change.

5.2 Future Research

The first limitation of using a process-based crop model without incorporating information on possible adaptation is that it ignores the adaptive potential of the farmers to address environmental and socio-economic changes (Mendelsohn et al. 1994). While we included the change in planting time as one of the adaptation strategies, it is not sufficient because it is hard to predict what the future farming system would look like under usually long term climate change scenarios. Future crop yield would largely depend on the evolution of local agricultural practices and the farmers' adaption techniques (such as irrigation, shift in planting time, use of drought-tolerant and heat-tolerant cultivars, and so on). To investigate the effectiveness of farmers' adaptive potential to offset the potential climate-induced yield loss under changed climate scenarios is one of our future research plans. Another limitation of this study is related to the model calibration and verification. A more rigorous approach could include additional

data for verification purpose, and the calibration can be conducted at sub-national level with a better representation of local agricultural dynamics over a large region.

Uncertainties in projecting future yield loss resulting from sensitivity of the crop model to future climate data emphasize the importance of more comprehensive assessment of crop-climate interaction. Analyzing the sensitivity of crop yield to sub-seasonal distribution of temperature and precipitation over different growth stages in addition to their distributions over the entire growing season presents another scope of future research. The knowledge of level of crop sensitivity to the climate variables across growth stages will lead to better understanding of future yield projections from a crop model driven with multiple future climate scenarios.

Although LandPro_Crop demonstrated robustness to multiple future climate scenarios, the projection from the model is more sensitive to alternative future scenarios of supply and demand for food. Despite the fact that the IMPACT was run for multiple climate and socioeconomic scenarios in projecting the future demand, the uncertainties involved in the IMPACT projection is a limitation of this study. While incorporating local, national or regional socio-economic policies related to agricultural expansion in the modeling framework of LandPro_Crop is also critical for more robust projections of future land use scenarios, it also involves a great deal of uncertainties. Future research efforts should address these uncertainties in modeling future land use and land cover changes.

The extent to which land use-climate interaction influences regional climate projection depends on the experimental design. Both magnitudes and directions of the changes projected by the transient experiment employing the asynchronous coupling often differ

from the projections by the equilibrium experiment. The difference implies the need for synchronous coupling between land use and climate models in projecting future climate. While results for this study demonstrate the importance of incorporating land use feedback in projecting future climate scenarios, the quantification of additional values added by a more complex synchronously coupled modeling framework would require major model development effort, and represents a scope for future research.

References

- Ackerman, F., DeCanio, S. J., Howarth, R. B., and Sheeran, K. (2009) Limitations of integrated assessment models of climate change. *Climatic Change*, 95(3-4), 297–315. doi:10.1007/s10584-009-9570-x.
- Agarwal, C., Green, G.M., Grove, J.M., Evans, T.P., and Schweik, C.M. (2002) A Review and Assessment of Land-Use Change Models: Dynamics of Space, Time, and Human Choice. GTR NE-297. Newton Square, PA: U.S.D.A., Forest Service, Northeastern Research Station. 61 p.
- Ahmed KF et al. (2013) Statistical downscaling and bias correction of climate model outputs for climate change impact assessment in the U.S. northeast, *Global and Planetary Change*, 100(1), 320-333.
- Ahmed KF, Wang GL, Yu M, Koo J, You LZ (2015a). Potential Impact of Climate Change on Cereal Crop Yield in West Africa. *Climatic Change*, 1-14, doi: 10.1007/s10584-015-1462-7.
- Ahmed KF, Wang GL, Yu M, You LZ (2015b) Potential Impact of Changes in Climate and Socioeconomic Factors on Future Agricultural Land Use in West Africa. *Earth System Dynamics*, conditionally accepted (available online in *Earth System Dynamics Discussion*).
- Allen, L.H., Baker, J.T., Boote, K. (1996) The CO₂ fertilization effect: higher carbohydrate production and retention as biomass and seed yield. In: *Global Climate Change and Agricultural Production. Direct and Indirect Effects of Changing Hydrological, Pedological and Plant Physiological Processes*, John

Wiley & Sons Ltd./FAO, Baffins Lane, Chichester, West Sussex PO19 1UD, England/Rome, Italy.

- Barnabás B, Jäger K, Fehér A (2008) The effect of drought and heat stress on reproductive processes in cereals. *Plant, Cell and Environment*, 31: 11-38.
- Batjes NH (2002) A Homogenized Soil Profile Data Set For Global and Regional Environmental Research. (WISE, Version 1.1). Report 2002/01. International Soil Reference and Information Centre (ISRIC), Wageningen, The Netherlands.
- Berg A, Sultan B, Noblet-Ducoudré N (2011) Including tropical croplands in a terrestrial biosphere model: application to West Africa. *Climatic change*, 104(3-4), 755-782.
- Boé J, Terray L, Habets F, Martin E (2006) A simple statistical-dynamical downscaling scheme based on weather types and conditional resampling. *Journal of Geophysical Research*, 111.
- Boysen, L. R., Brovkin, V., Arora, V. K., Cadule, P., de Noblet-Ducoudré, N., Kato, E., and Gayler, V (2014): Global and regional effects of land-use change on climate in 21st century simulations with interactive carbon cycle. *Earth System Dynamics Discussions*, 5(1), 443–472.
- Burney, J. A., Davis, S. J., and Lobell, D. B. (2010) Greenhouse gas mitigation by agricultural intensification, 1–6. doi:10.1073/pnas.0914216107.
- Deng, X., Zhao, C., and Yan, H. (2013) Systematic Modeling of Impacts of Land Use and Land Cover Changes on Regional Climate: A Review. *Advances in Meteorology*, 2013, 1–11. doi:10.1155/2013/317678.

- Ellis, E. C (2011): Anthropogenic transformation of the terrestrial biosphere. Philosophical Transactions. Series A, Mathematical, Physical, and Engineering Sciences, 369(1938), 1010–35. doi:10.1098/r.
- Ewers, RM, Scharlemann JPW, Balmford A, Green RE (2009) Do increases in agricultural yield spare land for nature? Glob Change Biol, 15 , pp. 1716–1726.
- FAOSTAT Database on Agriculture, Food and Agriculture Organization of the United Nations, Rome, Italy (2010) Available at: <http://faostat.fao.org/>
- Ferris R, Ellis RH, Wheeler TR, Hadley P (1998) Effect of high temperature stress at anthesis on grain yield and biomass of field-grown crops of wheat. Annals of Botany 82, 631–639.
- Foley, A.: Estimating historical changes in global land cover (1999) : Croplands historical have converted areas, 13(4), 997–1027.
- Foley, J.A., DeFries, R., Asner, G.P., Barford, C., Bonan, G., Carpenter, S.R., Chapin, F.S., Coe, M.T., Daily, G.C., Gibbs, H.K., Helkowski, J.H., Holloway, T., Howard, E.A., Kucharik, C.J., Monfreda, C., Patz, J.A., Prentice, I.C., Ramankutty, N. and Snyder, P.K. (2005): Global consequences of land use. Science, 309, 570–574
- Giorgi F et al. (2012) RegCM4: model description and preliminary tests over multiple CORDEX domains. Climate Research 52:7–29.
- Giorgi, F., Coppola, E., Solomon, F., Mariotti, L., Sylla, M.B., Bi, X., Elguindi, N., Diro, G.T., Nair, V., Giuliani, G., Cozzini, S., Guttler, I., O'Brien, T.A., Tawfik, A.B., Shalaby, A., Zakey, A.S., Steiner, A.L., Stordal, F., Sloan, L.C., Brankovic,

C.: RegCM4 (2012): model description and preliminary tests over multiple CORDEX domains. *Clim Res* 52:7–29.

- Hagos et al. (2014): Assessment of uncertainties in the response of the African monsoon precipitation to land use change simulated by a regional model. *Clim Dyn* 43:2765–2775.
- Havlik, P., Schneider, U.A., Schmid, E., Böttcher, H., Fritz, S., Skalský, R., Aoki, K., Cara, S.D., Kindermann, G., Kraxner, F., Leduc, S., McCallum, I., Mosnier, A., Sauer, T., Obersteiner, M. (2011): Global land-use implications of first and second generation biofuel targets. *Energy Pol.* 39, 5690–5702.
- Havlik, P., Valin, H., Mosnier, A., Obersteiner, M., Baker, J.S., Herrero, M., Rufino, M.C., Schmid, E. (2013) : Crop productivity and the global livestock sector: Implications for land use change and greenhouse gas emissions. *Am.J. Agric. Econ.* 95, 442–448.
- Hayhoe K et al. (2006) Past and future changes in climate and hydrological indicators in the US Northeast. *Climate Dynamics* 28 (4), 381–407.
- Houghton, B. R. A., Woods, T., Box, P. O., and Hole, W. (2003): Revised estimates of the annual net flux of carbon to the atmosphere from changes in land use and land management 1850 – 2000, 378–390.
- Hurtt, G. C., Chini, L. P., Frolking, S., Betts, R. a., Feddema, J., Fischer, G., Wang, Y. P. (2011): Harmonization of land-use scenarios for the period 1500–2100: 600 years of global gridded annual land-use transitions, wood harvest, and resulting secondary lands. *Climatic Change*, 109(1-2), 117–161. doi:10.1007/s10584-011-0153-2.

- IIASA/FAO (2012) Global Agro-ecological Zones (GAEZ v3.0). IIASA, Laxenburg, Austria and FAO, Rome, Italy.
- Jones CA, Kiniry JR (1986) CERES-Maize: A Simulation Model of Maize Growth and Development. Texas A,M University Press, College Station, Texas.
- Jones JW et al. (2003) DSSAT Cropping System Model. *European Journal of Agronomy*, 18, 235–265.
- Jones PG, Thornton PK (2003) The potential impacts of climate change on maize production in Africa and Latin America in 2055. *Global environmental change*, 13(1), 51-59.
- Kim SH et al. (2007) Temperature dependence of growth, development, and photosynthesis in maize under elevated CO₂. *Environ. Exp. Bot.* 61, 224–236.
- Knox J, Hess T, Daccache A, Wheeler T (2012) Climate change impacts on crop productivity in Africa and South Asia. *Environ. Res. Lett.* 7, 034032.
- Lambin EF, Geist HJ, Lepers E (2003) Dynamics of land-use and land-cover change in tropical regions. Lambin EF, Geist HJ, Lepers E.
- Lawrence, P. J., and Chase, T. N. (2007): Representing a new MODIS consistent land surface in the Community Land Model (CLM 3.0). *Journal of Geophysical Research*, 112(G1), G01023. doi:10.1029/2006JG000168.
- Leakey, A. D., Uribeharrea, M., Ainsworth, E. A., Naidu, S. L., Rogers, A., Ort, D. R., & Long, S. P. (2006). Photosynthesis, productivity, and yield of maize are not affected by open-air elevation of CO₂ concentration in the absence of drought. *Plant Physiology*, 140(2), 779-790.

- Leclère, D., Havlík, P., Fuss, S., Schmid, E., Mosnier, A., Walsh, B. and Obersteiner, M. (2014): Climate change induced transformations of agricultural systems: insights from a global model. *Environmental Research Letters*, 9(12), 124018.
- Lobell DB, Bänziger M, Magorokosho C, Vivek B (2011) Nonlinear heat effects on African maize as evidenced by historical yield trials. *Nature Climate Change*, 1(4), 42-45.
- Lobell DB, Burke MB (2008) Why are agricultural impacts of climate change so uncertain? The importance of temperature relative to precipitation. *Environ. Res. Lett.* 3, 034007.
- Lobell DB, Burke MB (2010) On the use of statistical models to predict crop yield responses to climate change. *Agric. Forest Meteorol.* 150, 1443–1452.
- Lobell DB, Field CB (2007) Global scale climate-crop yield relationships and the impacts of recent warming. *Environ. Res. Lett.* 2, 004000.
- Lobell DB, Hammer GL, McLean G, Messina C, Roberts MJ, Schlenker W (2013) The critical role of extreme heat for maize production in the United States. *Nature Climate Change*, 3(5), 497-501.
- Lotze-Campen, H., Müller, C., Bondeau, A., Rost, S., Popp, A., and Lucht, W. (2008): Global food demand, productivity growth, and the scarcity of land and water resources: a spatially explicit mathematical programming approach. *Agricultural Economics*, 39(3), 325-338.
- Mahmood, R., Quintanar, A. I., Conner, G., Leeper, R., Dobler, S., Pielke, R. A., Syktus, J. (2010): Impacts of Land Use/Land Cover Change on Climate and

Future Research Priorities. *Bulletin of the American Meteorological Society*, 91(1), 37–46. doi:10.1175/2009BAMS2769.1.

- Mei, R., and Wang, G. (2009): Rain follows logging in the Amazon? Results from CAM3–CLM3. *Climate Dynamics*, 34(7-8), 983–996. doi:10.1007/s00382-009-0592-x.
- Mendelsohn R, Nordhaus W, Shaw D (1994) The impact of global warming on agriculture: a Ricardian analysis. *The American Economic Review*, 84(4), 753–771.
- Meza FJ, Silva D (2009) Dynamic adaptation of maize and wheat production to climate change. *Climatic change*, 94(1-2), 143-156.
- Middelmeier, C. (2003): Impact of urbanization and land-use change on climate, 423(May), 528–532. doi:10.1038/nature01649.1.
- Monfreda C, Ramankutty N, Foley JA (2008) Farming the planet: 2. Geographic distribution of crop areas, yields, physiological types, and net primary production in the year 2000. *Glob. Biogeochem. Cycles* 22, GB1022.
- Monteith JL, Moss CJ (1977) Climate and the efficiency of crop production in Britain. *Phil. Trans. R. Soc. B*, 281, 277-294.
- Murray-Rust, D., Dendoncker, N., Dawson, T. P., Acosta-Michlik, L., Karali, E., Guillem, E., and Rounsevell, M. (2011): Conceptualizing the analysis of socioecological systems through ecosystem services and agent-based modelling. *Journal of Land Use Science*, 6(2-3), 83–99. doi:10.1080/1747423X.2011.558600.

- Olesen, J. E., and Bindi, M.(2002) Consequences of climate change for European agricultural productivity, land use and policy. *European Journal of Agronomy*, 16(4), 239–262. doi:10.1016/S1161-0301(02)00004-7.
- Oleson KW et al. (2010) Technical Description of version 4.0 of the Community Land Model (CLM). NCAR Technical Note NCAR/TN-478+STR, National Center for Atmospheric Research, Boulder, CO, 257 pp.
- Organization for Economic Co-Operation and Development (OECD) (2008) Environmental Performance of Agriculture in OECD Countries since 1990. Available at http://www.oecd.org/document/48/0,3343,en_2649_33793_40374392_1_1_1_1,0_0.html].
- Osborne TM, Wheeler TR (2013). Evidence for a climate signal in trends of global crop yield variability over the past 50 years. *Environmental Research Letters*, 8(2), 024001.
- Parker, D. C., Manson, S. M., Janssen, M. A., Hoffmann, M. J., Deadman, P., Manson, S. M., Hall, S. (2002): Multi-Agent Systems for the Simulation of Land-Use and Land-Cover Change : A Review *Annals of the Association of American Geographers*..
- Pielke, R.A., Pitman, A., Niyogi, D., Mahmood, R., McAlpine, C., Hossain, F., Klein Goldewijk K., Nair, U., Betts, R., Fall, S., Reichstein, M., Kabat, P., de Noblet-Ducoudre, N. (2011): Land use/land cover changes and climate: modeling analysis and observational evidence. *WIREs Climate Change* 2: 828–850.

- Pongratz, J., Reick, C. H., Raddatz, T., and Claussen, M. (2010): Biogeophysical versus biogeochemical climate response to historical anthropogenic land cover change. *Geophysical Research Letters*, 37(8), n/a–n/a. doi:10.1029/2010GL043010.
- Porter JR, Semenov MA (2005) Crop responses to climatic variation. *Philos Trans R Soc London B* 360:2021–2035.
- Potter P, Ramankutty N, Bennett EM, Donner SD (2010) Characterizing the spatial patterns of global fertilizer application and manure production. *Earth Interact.* 14, 1–22.
- Ritchie JT, Otter S (1985) Description and performance of CERES-Wheat: a user-oriented wheat yield model. ARS Wheat Yield Project. USDA-ARS-38. Natl Tech Info Serv, Springfield, Missouri, pp. 159/175.
- Robinson, S., van Meijl, H., Willenbockel, D., Valin, H., Fujimori, S., Masui, T., Sands, R., Wise, M., Calvin, K., Havlik, P., Mason d’Croz, D., Tabeau, A., Kavallari, A., Schmitz, C., Dietrich, J.D., von Lampe, M. (2014): Comparing supply-side specifications in models of global agriculture and the food system. *AgricEcon* 45(1):21–35.
- Romero CC et al. (2012) Reanalysis of a global soil database for crop and environmental modeling. *Environmental Modelling and Software* 35, 163–170.
- Ronneberger, K. E. (2006): The global agricultural land-use model KLUM – A coupling tool for integrated assessment, PhD dissertation, University of Hamburg.

- Rosegrant, M. W. (2012): International Model for Policy Analysis of Agricultural Commodities and Trade (IMPACT) Model Description International Food Policy Research Institute, (July).
- Roudier P, Sultan B, Quirion P, Berg A (2011) The impact of future climate change on West African crop yields: What does the recent literature say?. *Global Environmental Change*, 21(3), 1073-1083.
- Rounsevell, M. D. A., Arneth, A., Alexander, P., Brown, D. G., de Noblet-Ducoudré, N., Ellis, E., Young, O. (2014): Towards decision-based global land use models for improved understanding of the Earth system. *Earth System Dynamics*, 5(1), 117–137. doi:10.5194/esd-5-117.
- Rounsevell, M. D., Annetts, J., Audsley, E., Mayr, T., and Reginster, I. (2003): Modelling the spatial distribution of agricultural land use at the regional scale. *Agriculture, Ecosystems and Environment*, 95(2-3), 465–479. doi:10.1016/S0167-8809(02)00217-7.
- Rowhani P, Lobell DB, Linderman M, Ramankutty N (2011) Climate variability and crop production in Tanzania. *Agric. For. Meteorol.* 151, 449–460.
- Ruane et al. (2013) Multi-factor impact analysis of agricultural production in Bangladesh with climate change. *Global Environmental Change*, 23(1), 338-350.
- Saxton KE, Rawls WJ, Romberger JS, Papendick RI (1985) Estimating generalized soil-water characteristics from texture. *Soil. Sci. Soc. Am. J.* 50, 1031-1036.
- Schlenker W, Lobell DB (2010) Robust negative impacts of climate change on African agriculture. *Environ. Res. Lett.* 5, 014010.

- Schmitz, C., van Meijl, H., Kyle, P., Nelson, G. C., Fujimori, S., Gurgel, A., Alin, H. (2014) Land-use change trajectories up to 2050 : insights from a global agro-economic model comparison. *Agricultural Economics*, 45(1), 69–84. doi:10.1111/agec.12090.
- Schröter, D., Cramer, W., Leemans, R., Prentice, I.C., Araújo, M.B., Arnell, N.W., Bondeau, A., Bugmann, H., Carter, T.R., Gracia, C.A., de la Vega-Leinert, A.C., Erhard, M., Ewert, F., Glendining, M., House, J.I., Kankaanpää, S., Klein, R.J.T., Lavorel, S., Lindner, M., Metzger, M.J., Meyer, J., Mitchell T.D., Reginster, I., Rounsevell, M., Sabaté, S., Sitch, S., Smith, B., Smith, J., Smith, P., Sykes, M.T., Thonicke, K., Thuiller, W., Tuck, G., Zaehle, S. and Zierl, B. (2005): Ecosystem service supply and vulnerability to global change in Europe. *Science*, 310, 1333–1337.
- Sheffield J, Goteti G, Wood EF (2006) Development of a 50-yr, high resolution global dataset of meteorological forcings for land surface modeling. *J. Climate*(13), 3088-3111.
- Smith, P., Haberl, H., Popp, A., Erb, K.-H., Lauk, C., Harper, R., Rose, S. (2013): How much land-based greenhouse gas mitigation can be achieved without compromising food security and environmental goals? *Global Change Biology*, 19(8), 2285–302. doi:10.1111/gcb.12160.
- Stéphenne, N., and Lambin, E. F. (2001): A dynamic simulation model of land-use changes in Sudano-sahelian countries of Africa (SALU). *Agriculture, Ecosystems and Environment*, 85(1-3), 145–161. doi:10.1016/S0167-8809(01)00181-5.

- Sultan B et al. (2013) Assessing climate change impacts on sorghum and millet yields in the Sudanian and Sahelian savannas of West Africa. *Environmental Research Letters*, 8(1), 014040.
- Taylor KE, Stouffer RJ, Meehl GA (2012) An Overview of CMIP5 and the experiment design.” *Bull. Amer. Meteor. Soc*, 93, 485-498, doi:10.1175/BAMS-D-11-00094.1.
- Thornton PK, Jones PG, Alagarwamy G, Andresen J (2009) Spatial variation of crop yield response to climate change in East Africa. *Global Environmental Change*, 19, 54-65.
- Tubiello, F. N., Salvatore, M., Rossi, S., Ferrara, A., Fitton, N., and Smith, P. (2001): The FAOSTAT database of greenhouse gas emissions from agriculture. *Environmental Research Letters*, 8(1), 015009. doi:10.1088/1748-9326/8/1/015009.
- Valbuena, D., Verburg, P. H., Bregt, A. K., and Ligtenberg, A. (2010): An agent-based approach to model land-use change at a regional scale. *Landscape Ecology*, 25(2), 185–199. doi:10.1007/s10980-009-9380-6.
- Valin, H., Havlík, P., Mosnier, A., Herrero, M., Schmid, E., and Obersteiner, M. (2013): Agricultural productivity and greenhouse gas emissions: trade-offs or synergies between mitigation and food security?. *Environmental Research Letters*, 8(3), 035019.
- Veldkamp, A, and Lambin, E. (2011): Predicting land-use change. *Agriculture, Ecosystems and Environment*, 85(1-3), 1–6. doi:10.1016/S0167-8809(01)00199-2.

- Verburg, P. H., Kok, K., Pontius Jr, R. G., and Veldkamp, A. (2006): Modeling land-use and land-cover change. In *Land-use and Land-cover Change* (pp. 117-135). Springer Berlin Heidelberg.
- Verburg, P. H., Neumann, K., and Nol, L. (2011): Challenges in using land use and land cover data for global change studies. *Global Change Biology*, 17(2), 974–989. doi:10.1111/j.1365-2486.
- Verburg, P. H. (2006): Simulating feedbacks in land use and land cover change models. *Landscape Ecology*, 21(8), 1171–1183. doi:10.1007/s10980-006-0029-4
- Waha, K., Müller, C., & Rolinski, S. (2013). Separate and combined effects of temperature and precipitation change on maize yields in sub-Saharan Africa for mid-to late-21st century. *Global and Planetary Change*, 106, 1-12.
- Wang G, Eltahir EA (2000): Ecosystem dynamics and the Sahel drought. *Geophys Res Lett* 27:795–798
- Wang GL, Yu M, Xue Y-K, (2015): Modeling the potential contribution of land cover changes to the late 20th Century Sahel drought using a regional climate model: Sensitivity to lateral boundary conditions. *Climate Dynamics*, DOI: 10.1007/s00382-015-2812-x
- Wang, G. L., Miao, Y., Pal, J. S., Rui, M., Bonan, G., Levis, S., Thornton, P. (2015): On the development of a coupled RegCM-CLM-CN-DV model and its validation in West Africa. *Climate Dynamics*, DOI 10.1007/s00382-015-2596-z, 2015.
- Wilby RL (1998) Statistical downscaling of general circulation model output: a comparison of methods. *Water Resources Research*, 34, pp. 2995–3008.

- Wint GR, Robinson TP (2007) Gridded livestock of the world. FAO, 132 pp.
- World Bank (2008): Investment in Agricultural Water for Poverty Reduction and Economic Growth in Sub-Saharan Africa. A collaborative programme of ADB, FAO, IFAD, IWMI and World Bank. Synthesis Report, 2008.
- Xue YK, De Sales F, Vasic R, Mechoso CR, Prince SD, Arakawa A (2010): Global and temporal characteristics of seasonal climate/vegetation biophysical process (VBP) interactions. J Clim 23:1411–1433
- You LS, Wood S, Wood-Sichra U, Wu W (2014) Generating global crop distribution maps: From census to grid. Agricultural Systems 127 (2014) 53–60
- You, L. S., and Wood, S. (2006): An entropy approach to spatial disaggregation of agricultural production. Agricultural Systems, 90(1-3), 329–347. doi:10.1016/j.agry.2006.01.008.
- Yu M et al. (2014) Future changes of the terrestrial ecosystem based on a dynamic vegetation model driven with RCP8.5 climate projections from 19 GCMs. Climatic Change, 1-15.
- Zeng N, Neelin JD, Lau KW, Tucker CJ (1999): Enhancement of interdecadal climate variability in the Sahel by vegetation interaction. Science 286:1537–1540.